Structure-based design of an *in vivo* active selective BRD9 inhibitor

Laetitia J. Martin,*[,†] Manfred Koegl,[†] Gerd Bader,[†] Xiao-Ling Cockcroft,[†] Oleg Fedorov,[§] Dennis Fiegen,[‡] Thomas Gerstberger,[†] Marco H. Hofmann,[†] Anja F. Hohmann,[∥] Dirk Kessler,[†] Stefan Knapp,[§] Petr Knesl,[†] Stefan Kornigg,[†] Susanne Müller,[§] Herbert Nar,[‡] Catherine Rogers,[§] Klaus Rumpel,[†] Otmar Schaaf,[†] Steffen Steurer,[†] Cynthia Tallant,[§] Christopher R. Vakoc,[∥] Markus Zeeb,[‡] Andreas Zoephel,[†] Mark Pearson,[†] Guido Boehmelt,[†] and Darryl McConnell[†]

[†] Boehringer Ingelheim RCV GmbH & Co KG, Vienna, Austria

[‡] Boehringer Ingelheim Pharma GmbH & Co KG, Biberach, Germany

[§] SGC, University of Oxford, Oxford, UK

[∥] Cold Spring Harbor Laboratory, Cold Spring Harbor, New York, U.S.A

ABSTRACT

Components of the chromatin remodelling SWI/SNF complex are recurrently mutated in tumours, suggesting that altering the activity of the complex plays a role in oncogenesis. However, the role that the individual subunits play in this process is not clear. We set out to develop an inhibitor compound targeting the bromodomain of BRD9 in order to evaluate its function within the SWI/SNF complex. Here, we present the discovery and development of a potent and selective BRD9 bromodomain inhibitor series based on a new pyridinone-like scaffold arising from two parallel screening approaches consisting of a fragment based screening and a virtual screening of proprietary libraries. Crystallographic information of the inhibitors bound to BRD9 guided their development with respect to potency for BRD9 and selectivity against BRD4. These compounds modulate BRD9 bromodomain cellular function and display anti-tumour activity in an AML xenograft model. Two chemical probes, **BI-9564** and **BI-7273**, were identified that should prove useful in further exploring BRD9 bromodomain biology in both *in vitro* and *in vivo* settings, not only in oncology but potentially also in neurology, immunology and inflammation.

Chromatin remodelling complexes regulate nucleosome positioning along DNA.[1] These complexes are required for a variety of processes including chromatin organisation, transcriptional regulation, decatenation of chromatids during mitosis and DNA repair.[2] The mammalian SWI/SNF (SWItch/Sucrose Non-Fermentable) complex is one of four mammalian chromatin remodelling complexes. Recurrent inactivating mutations in certain subunits of this complex have been identified in different cancers. Despite its known roles in tumor suppression, the mammalian SWI/SNF complex has recently received attention as a potential target for therapeutic inhibition. This stems from the recognition that residual SWI/SNF complexes are critical for the growth of genetically defined cancers, including SWI/SNF mutant and Max mutant tumors as well as acute leukemias.[3,4] In acute leukemias, it was found that the SWI/SNF complex supports an oncogenic transcriptional program. In the absence of the SWI/SNF ATPase Brg1, leukemic cells arrest in G1 and differentiate. A recent study highlighted a role of another SWI/SNF subunit, BRD9, in leukemia growth. The BRD9 bromodomain (BD) was shown to be required for the proliferation of acute myeloid leukemia (AML) cells[5].

Over the last decade, chemical probe compounds have been shown to be invaluable in the elucidation of protein function.[6,7] We set out to develop a probe compound targeting the bromodomain of BRD9 in order to evaluate the function of this domain within the SWI/SNF complex. Bromodomains are protein-binding domains with an affinity to lysine-acetylated target proteins.[8] The acetyl-lysine binding pockets of these domains have been shown to be amenable to inhibition by drug-like small molecules and the activity of several inhibitors directed against Bromodomain and Extra-Terminal motif (BET) containing proteins (BRD2, BRD3, BRD4 and BRD-T) is being clinically assessed in cancer, including hematopoietic malignancies,[9,10] and atherosclerosis (http://www.resverlogix.com/blog/tag/atherosclerosis/). A key selectivity parameter in designing our tool compounds was to avoid activity against

BET family proteins, due to the pleiotropic effects that BET inhibitors exert on various cellular processes.[11]

In this paper, we describe the discovery and development of a potent and selective BRD9 bromodomain inhibitor series based on a new scaffold arising from two parallel screening approaches consisting of a fragment based screening, as well as a virtual screening of proprietary libraries. In particular, we report the structure-based design of the BRD9 inhibitor **BI-7273**, which was previously demonstrated to mimic genetic perturbation of BRD9.[5] We further describe a second BRD9 inhibitor, **BI-9564**, which displays enhanced selectivity against the BRD7 bromodomain as well as improved pharmacokinetic properties when compared to **BI-7273**. These two chemical probes, **BI-9564** and **BI-7273**, should prove useful in further probing BRD9 bromodomain biology in both *in vitro* and *in vivo* settings.

RESULTS

Binding the BRD9 bromodomain with an isoquinolinone or a pyridinone scaffold

Two parallel screening approaches were followed to identify BRD9 bromodomain binders. Three parallel biophysical assays, a differential scanning fluorimetry (DSF) assay, a surface plasmon resonance (SPR) assay and a microscale thermophoresis (MST) assay, were used to screen our proprietary fragment library of around 1700 compounds against the BRD9 bromodomain (Supporting Information Figure 1, Supporting Information Figure 2 & Supporting Information Table 1). Of note, this is one of the first fragment screening applications described for the MST technology.[12] The hits coming from these three screening methods were validated in an orthogonal binding assay using ^{15}N HSQC NMR (Heteronuclear Single Quantum Coherence Nuclear Magnetic Resonance) (Supporting Information Figure 3).

77 hits showed significant cross peak shifts in the 2D $^{1}H/\ ^{15}N$ HSQC NMR spectra and 55 of these compounds were successfully soaked into the crystals of the BRD9 bromodomain. After quantification of the binding affinity of the 77 compounds by SPR, 12 compounds displayed a dissociation constant (K_D) below 100 µM. Additionally, a proprietary high concentration screening (HiCoS) library of ~ 74,500 compounds was screened by Glide docking,[13] followed by BRD9 bromodomain pharmacophore mapping and finally filtering based on molecular weight (MW < 280) and lipophilicity (clogP < 2) (Supporting Information Figure 4). This virtual screening led to the selection of 208 available compounds, which were measured in DSF and SPR (% ctrl) assays. The binding affinity (K_D) of the hits was quantified using SPR (Supporting Information Figure 1) leading to the discovery of 23 additional candidates of which 11 compounds had their binding mode elucidated by X-ray co-crystal structure determination. All 23 compounds were resynthesized and had their binding affinity confirmed by SPR. Eleven compounds had a K_D below 100 µM by SPR (Supporting Information Figure 1). Structure based medicinal chemistry was then initiated using the X-ray co-crystal structures of the fragments obtained in the BRD9 bromodomain (Supporting Information Figures 5-8 & Supporting Information Table 2).

The compound series containing the methylpyridopyrimidinone or the dimethylpyridinone scaffold were selected as promising starting points [K_D(**1**, SPR) = 37.5 µM, K_D(**2**, SPR) = 9.1 µM] (Figure 1a with the scaffold highlighted). The binding mode of the two compounds showed similar binding in the BRD9 anchor region (Figures 1b-c & Supporting Information Figures 5-8). The carbonyl of the pyridinone functionality makes two hydrogen bonds with the protein: a direct H-bond with the $N^{\delta 2}H_2$ side chain of Asn100 and an H-bond to Tyr57 *via* a conserved water molecule. A methyl group (either from the *N*-methyl or from the methyl alpha to the carbonyl) occupies a small lipophilic pocket surrounded by four conserved water molecules. The binding mode of these small acetylated lysine mimic binders is typical of

those reported for other bromodomains.[8] Indeed, similar binding activity was observed towards BET family members [*eg.* IC_{50} (**1**, BRD4-BD1) = 80.2 µM and IC_{50} (**2**, BRD4-BD1) = 3.7 µM] for both fragments, highlighting the challenge of achieving high selectivity against BRD4. Additionally, the aromatic pyridinone core in compounds **1** and **2** makes a π-stacking interaction with the Tyr106 in the BRD9 bromodomain. The distance between the aromatic core and Tyr106 was measured at 3.4 Å and 3.7 Å for **1** and **2**, respectively (optimal aromatic C-aromatic C parallel offset stacking is 3.4-3.6 Å).[14] Finally, in the specific case of compound **2**, we observe a C-H π-interaction between Ile53 and the phenyl moiety (distance CH_3-phenyl 3.6 Å) which could be beneficial for improving potency towards BRD9 (Figure 1c).

In parallel to the biophysical SPR assay, we developed a biochemical assay measuring the inhibitory effect of our compounds on the binding between acetylated histone H3 and BRD9 bromodomain. This assay showed good correlation with the data obtained by SPR [K_D(**1**, SPR) = 37.5 µM *vs.* IC_{50}(**1**) = 48.9 µM; K_D(**2**, SPR) = 9.1 µM *vs.* IC_{50}(**2**) = 9.4 µM]. As the aim of the project was to develop a potent and selective inhibitor, we developed *in vitro* peptide displacement assays to routinely monitor the inhibitory effect of our compounds on the binding between BRD9, BRD7, BRD4-BD1, BRD4-BD2 or BRD2-BD1 bromodomains and acetylated histone H3 or H4.

Structure-based design of BRD9 bromodomain inhibitors

Acetylated histones bind to their bromodomain partners via their *N*-acetylated lysine tails, in particular interacting with a conserved asparagine (BRD9 bromodomain is Asn100) in the anchor region and along a region previously referred to as the "N-side"[15] (Figures 1b-c). Considering that this binding mode is conserved among all bromodomains, we decided to concentrate on improving potency by growing the initial fragment towards the less conserved

"ZA channel" area (Figures 1b-c), as we anticipated that this approach would give us a greater chance of successfully achieving selectivity against BET family members.

In order to optimise the ZA channel linker, we used the dimethylpyridinone scaffold as an anchor binder. Both methyl and carbonyl functions on this scaffold are essential for effective binding to the BRD9 bromodomain; indeed removal of one of the methyl groups [position 1 (*N*-Me) or 3] or removal of the carbonyl moiety (*eg.* replacement of anchor binder by 2,6-dimethylpyridine) led to a loss of binding. In the ZA channel of the BRD9 bromodomain, we identified Phe44 (Figures 1b-c) as an amino acid of interest and hypothesised that addressing this interaction could improve potency. Compound **2** showed a sub-optimal edge to face interaction (referred also as T-stacking) with Phe44 [distance Phe44-phenyl (**2**) = 4.67 Å *vs.* optimal aromatic C-aromatic C edge to face distance: 3.6-3.9 Å[14]]. It is reported that introduction of electron donating groups on the facially substituted phenyl improves T-stacking.[16] Following this principle, we replaced the amide functional group by a methylene dimethylamine (compound **3**, Table 1), which led to an 8-fold increase in potency. Introduction of additional electron donating groups onto the phenyl ring further enhanced potency by improving T-stacking with Phe44 (compounds 4 to 8, Table 1). Using 4-(dimethylamino)methyl-3,5-dimethoxyphenyl as a ZA channel linker (compound **5**) increased the potency ~170-fold compared to the initial starting hit **2** [IC_{50}(**5**, BRD9) = 54 nM *vs.* IC_{50}(**2,** BRD9) = 9338 nM]. It was possible to further boost potency by addressing the backbone carbonyl of His42 with either a hydroxyl moiety or an amine moiety (compounds **9** and **10**, Table 1). The azetidine substituent provided the best vector to the His42 carbonyl without interfering with the optimal T-stacking of the dimethoxyphenyl ZA channel linker with Phe44. 4-(3-Aminoazedinylmethyl)-3,5-dimethoxyphenyl dimethylpyridinone (**10**) exhibited low nanomolar activity [IC_{50}(**10**, BRD9) = 9 nM]. Binding of the structurally closely related compound **9** was confirmed by X-ray co-crystal structure determination (Figure 2a,

Supporting Information Figures 9-10 & Supporting Information Table 2). The anchor region binding is similar to the one observed with fragment 2: the pyridinone core binds through its carbonyl to Asn100 and to the conserved water molecule bound to Tyr57, a methyl group occupies the small lipophilic pocket and the pyridinone makes a π-stacking interaction with Tyr106. In the ZA channel, the dimethoxyphenyl linker adopts a conformation that permits optimal T-stacking with Phe44, the distance between the aromatic core and Phe44 now being the ideal 3.9 Å, while keeping the C-H π-interaction with Ile53, the distance between aromatic core and Ile53 being 3.6 Å. The azedin-3-ol forms an H-bond to His42 and additionally for this molecule we observe an induced fit with Phe47 closing onto the molecule due to a C-H π-interaction with the methoxy group of compound **9**.[17]

While improving the potency towards BRD9, we also observed an enhancement of the selectivity against the first bromodomain of BRD4 (BRD4-BD1) compared to starting hit **2**, which showed higher potency for the off-target BRD4-BD1 than for BRD9. Encouraged by these results, we investigated modifications in the anchor region in order to further improve selectivity. As stated previously, we considered essential that our final BRD9 chemical probes were inactive against BRD4-BD1 and other BET family members to avoid any misinterpretation of biological results [*i.e.* IC_{50}(BET family members) > 100μM]. After comparing the surface of BRD9 and BRD4-BD1, we hypothesised that enhanced selectivity could be achieved by forcing a clash with key amino acids in the anchor region or the ZA channel of BRD4-BD1. This could be done by introducing substituents at the 4 or 6 position on the pyridine-2-one core of our inhibitors to force the torsion angle between the anchor binder ring and the ZA channel linker ring (Table 2). A methyl group at position 4 (or 6) forced a twist between the 2 aryl moieties "anchor binder" pyridine-2-one and "ZA channel linker" (measured torsion angle ~ -60° vs. -27° to -44° when hydrogen is present) and indeed translated to an improvement of selectivity against the BET family (compounds **11** and **12**,

Table 2). Based on the same principle, an aromatic ring merged to the pyridinone scaffold gave an improved selectivity against the BET family, and concomitantly improved the π-stacking interaction with Tyr106 in the BRD9 anchor region (compounds **13** to **18**, Table 2). The most efficient inhibitor was 2-methyl-2,7-naphthyridin-1-one compound **15** (**BI-7273**) with a three-fold increase in affinity for BRD9 and 50-fold increase in selectivity against BRD4-BD1 over compound **5** (selectivity BRD9 vs. BRD4-BD1: ~ 100-fold for compound **5**; > 5200-fold for **BI-7273**). **BI-7273** forms an additional positive interaction with the carbonyl of Asn100 in BRD9; indeed the presence of a nitrogen atom at position 7 on the naphthyridinone ring acidifies the CH bond at position 8 permitting the interaction with the carbonyl side chain of Asn100 (Figure 2b, Supporting Information Figures 11-12 & Supporting Information Table 2). This translates into an improved potency for the BRD9 bromodomain. **BI-7273** displays no measureable activity towards BET family bromodomains up to a concentration of 100 µM, in our biochemical Alpha assay which can be explained by a potential clash of the anchor part of the molecule with Leu92 in BRD4-BD1 and a clash of the tri-substituted phenyl linker of the molecule with Glu85 and Trp81 in BRD4-BD1 (**Figures 3a-b**, superimposition of **BI-7273** with BRD4-BD1 surface).

Finally, while investigating modifications on the ZA linker part, we discovered that para-substituted dimethoxy groups resulted in an enhanced selectivity for BRD9 over its closest homologue BRD7 (Table 3). We believe that this selectivity might stem from differences in flexibility between the two proteins. Based on the protein melting properties shown in the thermal shift assay, we hypothesised that the BRD7 bromodomain was more flexible and dynamic in solution than BRD9. Compound **21** (**BI-9564**) was slightly less potent towards BRD9 compared to **BI-7273** in the Alpha assay, but showed an improved selectivity against BRD7 (45-fold more potent for BRD9 *vs.* BRD7) and most importantly it remained inactive towards the BET family members (Scheme 1). The binding mode of **BI-9564** in the BRD9

bromodomain was confirmed by X-ray co-crystal structure determination (Figure 2c, Supporting Information Figures 13-14 & Supporting Information Table 2). **BI-9564** bound with an induced fit of Phe47 in the ZA channel, similar to compound **9**. Synthesis of para-substituted dimethoxy analogues of **BI-9564**, which could directly address the carbonyl of His42 with either a benzyl amine linker or sulphonamide linker at the 4 position of the ZA linker, yielded compounds with an improved BRD9 potency and similar selectivity profile compared to **BI-9564**. However, these compounds later presented less attractive pharmacokinetic properties (*eg.* low permeability or high efflux ratio), which made them unsuitable for *in-vivo* testing.

Finally, **BI-9564** and **BI-7273** binding affinities towards BRD9 were measured by isothermal titration calorimetry (ITC) and bromoKdELECT® (Figure 4, Table 4 & Supporting Information Figures 17-18). High affinity binding to the BRD9 bromodomain was confirmed for both compounds [K_D(**BI-7273**, ITC) = 15.4 nM and K_D(**BI-9564**, ITC) = 14.1 nM]. **BI-7273** and **BI-9564** were selected as BRD9 bromodomain chemical probes for further *in vitro* and *in vivo* profiling.

BI-9564 and BI-7273 are potent, selective and cell permeable BRD9 bromodomain inhibitors

Target engagement in the cell was demonstrated in a semi-quantitative FRAP assay[18] using a green fluorescent protein-BRD9 fusion protein expressed in U2OS cells. **BI-9564** showed inhibition of BRD9 in cells at 100 nM, while **BI-7273** was active in the cell at 1µM (1µM being the lowest concentration tested) (Figures 5a-d, Table 4). No compound related toxicity was observed in U2OS cell lines after 24 hours.

To assess selectivity, the compounds were profiled against a variety of other bromodomains. Bromodomain selectivity was checked by differential scanning fluorimetry for 48 bromodomains followed by ITC K_D determination (Table 4 & Supporting Information Figures 15-16 & 19-20). The same selectivity pattern was observed using the bromoMAX® / bromodKdMAX® technology (32 bromodomains screened, Supporting Information Figures 17-18). High selectivity against BET family members was confirmed, with K_D values exceeding 10 µM. Aside from BRD9, the only two bromodomains identified as additional targets belonged to the highly homologous BRD7 and CECR2 (Table 4 & Supporting Information Figures 19-20). Although **BI-9564** showed potency at 1µM in a BRD7 FRAP assay (Table 4 and & Supporting Information Figure 22), no cellular inhibition of the CECR2 bromodomain was observed at this concentration (CECR2 FRAP assay: Table 4 & Supporting Information Figure 23).

Further profiling was conducted to assess the selectivity over a range of targets, in particular kinases and G-protein coupled receptors (GPCRs). Concentrations of **BI-9564** of less than 5 µM showed no activity against 324 kinases and at 10µM an inhibition > 40% was observed for only 2 out of 55 GPCRs (Table 4 & Supporting Information Figure 24). **BI-7273** showed an inhibition below 40% against 31 kinases at 10 µM concentration.

Inhibition of cellular proliferation by BI-9564 and BI-7273

The cellular response to BRD9 inhibition was assessed in a broad cancer cell line panel. Treatment of the panel with **BI-9564** resulted in selective growth inhibition of a significant proportion of AML cell lines tested (Supporting Information Figure 31). This result was in agreement with evidence of **BI-7273** activity in the murine AML RN2 cell line.[5]

Additionally to the lack of cellular activity of **BI-9564** in the CECR2 FRAP assay (Supporting Information Figure 23), CECR2 mRNA expression was hardly detectable in any of the 8 sensitive cell lines, suggesting that the anti-proliferative effect was not due to the effects of the compound on this bromodomain. The most sensitive cell line was the human acute myeloid eosinophilic leukemia cell line EOL-1 [EC_{50}(**BI-9564**, EOL-1)=800 nM; EC_{50}(**BI-7273**, EOL-1)=1400 nM] (Figure 6, Supporting Information Figure 31)

As observed from the phenotype of murine cells exposed to **BI-7273**[5], BRD9 inhibition translated into a potent but only partial inhibition of MYC expression in AML cell lines (Supporting Information Figures 32 a-d). The rationale behind the inhibition of MYC expression is currently not understood. Complete suppression of MYC expression, observed at higher concentrations with some of the less selective compounds, was likely due to the effects of the compounds on BET family members [*eg.* IC_{50}(**BI-7189**, BRD4-BD1) = 78 µM, IC_{50}(**BI-7271**, BRD4-BD1) = 22 µM] (Supporting Information Figures 32 a-b).

BRD9 can fulfil its cellular function in murine leukemia cells when its bromodomain is exchanged with the BRD4 bromodomain.[5] These domain-swap experiments were used to demonstrate that the antiproliferative activities of **BI-7273** in this cell line are due to its effect on the BRD9 bromodomain. Using a similar domain-swap strategy, we also found that BRD9 is a relevant target underlying the anti-proliferative effects of **BI-9564**, suggesting on-target effects at concentrations below 5 µM. However, we also noted a degree of off-target effects of **BI-9564** in this murine leukemia cell line, when used at higher compound concentrations. Nonetheless, these findings suggested that **BI-9574** is a suitable chemical probe for probing the function of BRD9 *in vitro* and *in vivo* settings.

Pharmacokinetic profiling of BI-9564 and BI-7273

Both compounds, **BI-7273** and **BI-9564**, showed attractive ADME/PK profiles for *in vivo* proof-of-concept studies, namely high solubility at pH 6.8, moderate to high *in vitro* metabolic stability, low plasma protein binding, no cytochrome P450 inhibition together with moderate to high absorptive permeability and moderate *in vivo* plasma clearances upon *i.v.* dosing (Table 4, Supporting Information Figure 25 & Supporting Information Figure 28). Despite elevated efflux ratios in the Caco-2 transporter assay, both compounds displayed high oral bioavailability (Table 4, Supporting Information Figures 25-30). In order to explore the potential of **BI-9564** and **BI-7273** as *in vivo* chemical probes, female BomTac:NMRI-Foxn1nu mice were given two doses orally (20 and 180 mg/kg *p.o.*) and the compound concentration in plasma over time was measured. Dose-dependent, but non-linear AUCs were obtained for both compounds, achieving exposures that were higher compared to the EC_{50} levels determined for both compounds in proliferation assays with EOL-1 cells (Figure 6). **BI-9564** presented twice as high compound exposure over time than **BI-7273** and a higher oral bioavailability (Table 4). This justified *in vivo* efficacy experiments in mice at the highest dose of **BI-9564** (180 mg/kg *p.o.*) in the disseminated EOL-1 AML mouse model (summary of properties: Table 4, Supporting Information Figures 26-27 & Supporting Information Figures 29-30).

BI-9564 showed efficacy in a disseminated mouse model of AML

Prior to performing efficacy studies, one week tolerability studies were carried out using 180 mg/kg of **BI-9564** in non-tumour bearing female CIEA-NOG mice. Continuous daily dosing of the selected dose was well tolerated with a medium weight change on day 7 of -3.8% (n=4).

The human acute myeloid eosinophilic leukemia cell line EOL-1 was chosen for *in vivo* experiments as it was the most sensitive cell line *in vitro* to BRD9 inhibition. A disseminated

model, that more closely reflects the clinical situation compared to a subcutaneous xenograft, was chosen to assess the efficacy of **BI-9564**. 10^7 EOL-1 cells, stably transduced with a luciferase-expressing vector to allow continuous assessment of tumour load by bioluminescence, were injected in the tail vein of CIEA-NOG mice. Oral treatment with 180 mg/kg of **BI-9564** was initiated on day 5 and applied daily (*q.d.*) with an interruption at day 18 and 19. A significant (p=0.0086) reduction in tumour growth (measured in average Radiance [p/s/cm^2/sr]) compared to controls was observed on day 18 resulting in a median tumour growth inhibition (TGI) value of 52% (Figure 7a). Imaging data on day 18 provided evidence of a significantly reduced disease burden (Figure 7b) in **BI-9564**-treated mice. The animals were closely monitored for clinical signs and were sacrificed when the disease burden exceeded a pre-specified grade, as a surrogate endpoint for survival. Increase of tumour burden in the control mice resulted in body weight loss at the end of the study. On day 18, dosing with **BI-9564** was interrupted for 2 days, as continuous body weight loss was observed and a body loss of 15% was observed in one mouse. The body weight loss might be explainable by an increased tumor burden, as on this day the control group showed a median body weight loss of -11 compared to -8 in the treated group, however tolerability issues with the compound cannot be ruled out (Figure 7c). In the disseminated EOL-1 mouse model, the median survival of the vehicle (Natrosol 0.5%) treated control animals was 20 days. Median survival of the animals treated with 180 mg/kg **BI-9564** resulted in a modest but significant additional survival benefit of 2 days, compared to the control group (Figure 7d). Pharmacokinetic analysis of plasma samples taken on the last day of treatment showed that systemic exposure had been reached, with an AUC(0-last) of 119,000 nM·h, as expected from single dose PK experiments in mice (Table 4). While the anti-leukemia effects of **BI-9564** in this model are modest, these experiments demonstrate that **BI-9564** is a suitable probe to evaluate the effects of *in vivo* modulation of BRD9 bromodomain activity.

DISCUSSION

Epigenetic modifications have been linked to many diseases, in particular cancer and immune/inflammatory disorders. The molecular machinery required to read and modify chromatin has been shown to comprise large protein complexes where the activities of multiple domains is coordinated. The need to identify the activities that drive disease pathology has spurred the development of high quality inhibitors to probe the function of individual domains in the context of the native cellular complexes.

In this paper, we have focused on the bromodomain of BRD9, a subunit of the SWI/SNF chromatin remodeling complex. Our study describes how a combination of FBS and virtual screening of proprietary libraries allowed us to identify a new scaffold class of BRD9 bromodomain inhibitors. **BI-9564** and **BI-7273** are the first cellular potent BRD9 bromodomain inhibitors which are inactive on the BET family. This was principally achieved following a structure guided chemical optimization leading to introduction of 2-methyl-2,7-naphthyridin-1-one as an anchor region binder. Optimization of the compounds focused on addressing all key interactions as efficiently as possible, keeping the overall size of the final molecule small and the ligand efficiency high [MW(**BI-7273**) = MW(**BI-9564**) = 353.4 Da, ligand efficiency(**BI-7273**) = 0.41 & LE(**BI-9564)** = 0.38, lipophilic ligand efficiency(**BI-7273**) = 5.7 & LLE(**BI-9564**) = 5.7]. The overall ADME properties of the 2 compounds permit them to be used in *in vivo* experiments. Early work in a disseminated mouse model of AML showed efficacy for **BI-9564** (dose: 180mg/kg) with a median TGI value of 52% on day 18, which translated into an additional survival benefit compared to the control group.

Three structurally unrelated BRD9 inhibitors have been recently published in the literature: **LP99**[19], **I-BRD9**[20] and ketone "compound 28"[21] (Supporting Information Figure 33), prone to

make important contributions to further understanding BRD9 biology. However a combination of high potency and high selectivity (in particular versus the BET family) has so far not been achieved.[22] **BI-7273** and **BI-9564** combine both sufficiently high potency and selectivity (see Table 4). The ADME parameters of these 2 inhibitors will in addition allow the scientific community to elucidate the role of BRD9, either as a single agent or in combination with other inhibitors in *in vitro* as well as in *in vivo* settings. **BI-9564** is available to the scientific community *via* the SGC consortium as a BRD9/BRD7 potent, selective, cell permeable and non-cytotoxic probe compound (http://www.thesgc.org/chemical-probes/BI-9564). We believe that this molecular probe will provide a useful tool to broaden the study of chromatin regulators not only in oncology but potentially also in additional therapeutic areas such as neurology, immunology[20,23] and inflammation.[19]

a

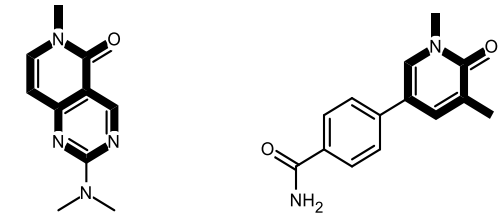

1

K_D(1, SPR, BRD9)=37.5 µM
IC_{50}(1, BRD9)= 48.9 µM

2

K_D(2, SPR, BRD9)=9.1 µM
IC_{50}(2, BRD9)= 9.4 µM

b

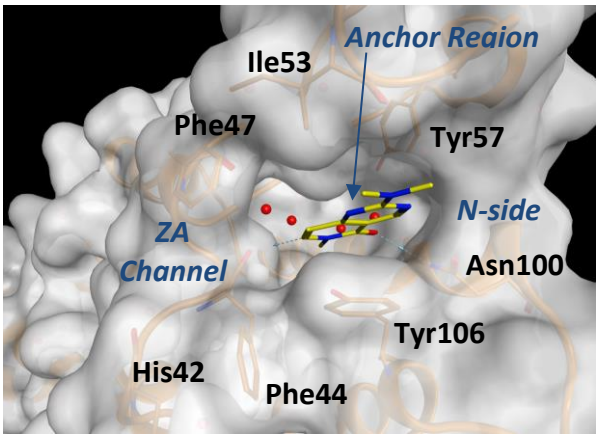

c

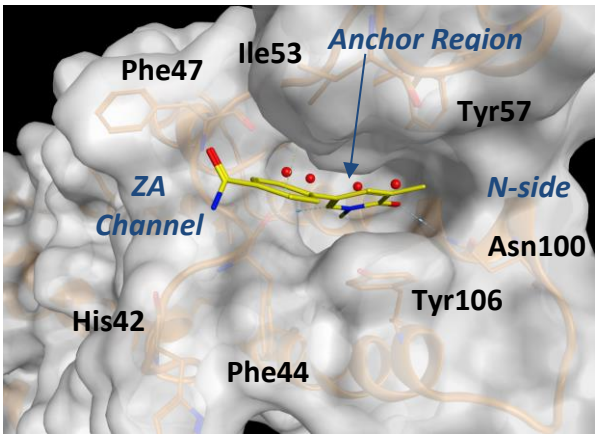

Figure 1. Binding mode of methylpyridopyrimidinone 1 or the dimethylpyridinone 2 scaffold in BRD9 bromodomain

(a) Structures and binding affinities of compounds **1** and **2** identified by FBS screening and virtual screening of HiCos library respectively

(b) and **(c)** Binding mode of **1** and **2** in the BRD9 bromodomain respectively: H-bond to Asn100, water bridged interaction with Tyr57, π-stacking with Tyr106, C-H π-interaction with Ile53. The protein is shown as a surface representation colored in grey. Important amino acids for binding to the BRD9 bromodomain are indicated. ZA channel, anchor region and N-side are indicated in blue.

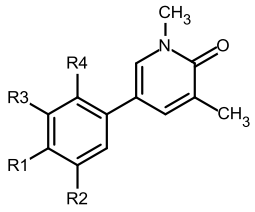

Compound	R1	R2	R3	R4	IC_{50} (BRD9) [nM]*	IC_{50} (BRD4-BD1) [nM]*
2	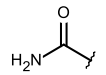	-H	-H	-H	9338	3681
3	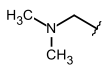	-H	-H	-H	1147	31421
4	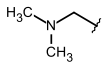	-OMe	-H	-H	470	81300
5	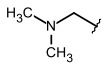	-OMe	-OMe	-H	54	5861
6	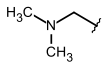	-OMe	-Me	-H	656	32430
7	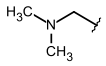	-OMe	-Et	-H	195	19165
8	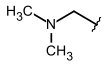	-OMe	-H	-OMe	468	3778
9	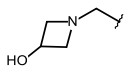	-OMe	-OMe	-H	21	1121
10	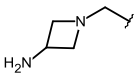	-OMe	-OMe	-H	9	1147

Table 1. SAR for BRD9 activity in the ZA channel (*Alpha format, mean value; number of measurements: 2 to 5)

a

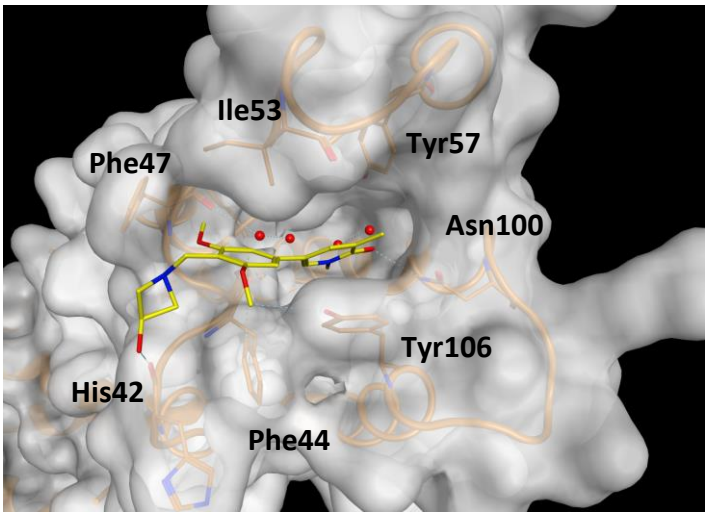

b

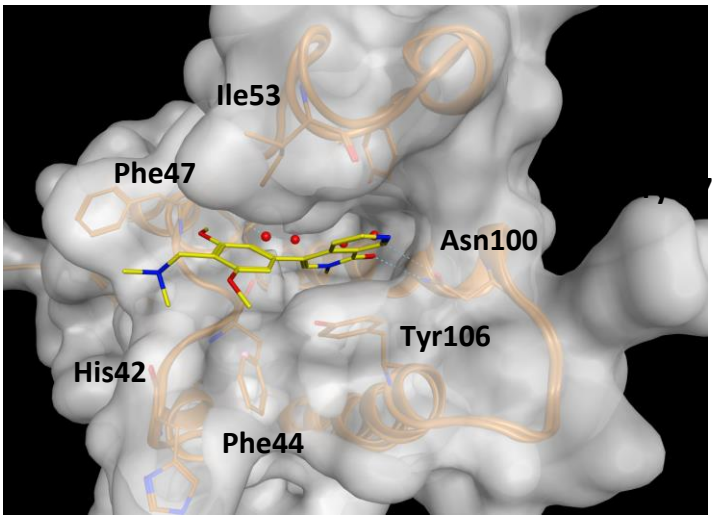

c

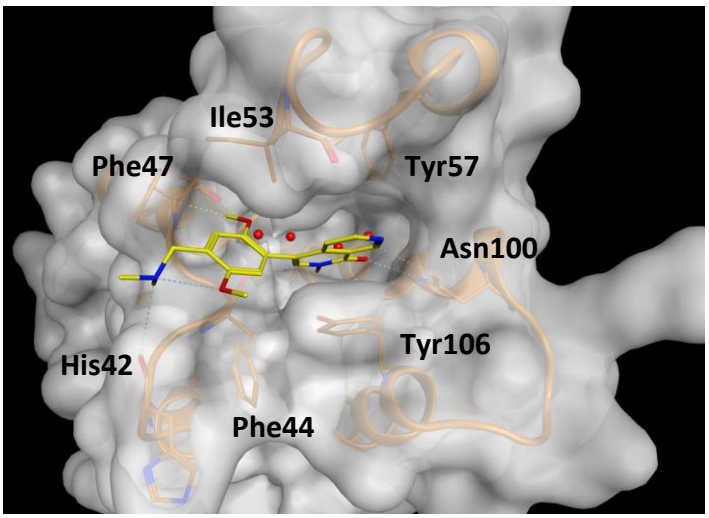

Figure 2. Binding mode of BRD9 bromodomain inhibitors.

a) Binding mode of compound **9** in the BRD9 bromodomain**:** H-bond to Asn100, water-bridged interaction with Tyr57, π-stacking with Tyr106, C-H π-interaction with Ile53, T-stacking with Phe44, H-bond to His42, induced fit Phe47/ C-H π-interaction. b) Binding mode of compound **15** (**BI-7273**) in the BRD9 bromodomain[5]: two H-bonds to Asn100, water-mediated hydrogen bond with Tyr57, π-stacking with Tyr106, C-H π-interaction with Ile53, T-stacking with Phe44. c) Binding mode of compound **21** (**BI-9564**) in BRD9 bromodomain: two H-bonds to Asn100, water-bridged interaction with Tyr57, π-stacking with Tyr106, C-H π-interaction with Ile53, T-stacking with Phe44, induced fit Phe47/ C-H π-interaction.

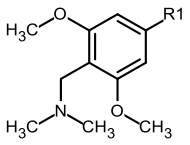

Compound	R1	IC_{50} (BRD9) [nM]*	IC_{50} (BRD4-BD1) [nM]*	IC_{50} (BRD4-BD2) [nM]*	IC_{50} (BRD2-BD1) [nM]*	IC_{50} (BRD7) [nM]*	Lit. Name
5	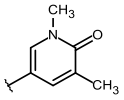	54	5861	14256	5876	230	
11	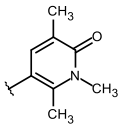	57	30652	>100000	33234	240	**BI-7189**[5]
12	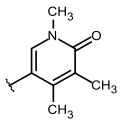	37	23005	42281	16654	41	
13	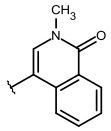	30	23576	32432	50857	108	**BI-7271**[5]
14	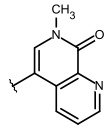	250	47359	>100000	>100000	3725	
15	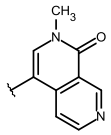	19	>100000	>100000	>100000	117	**BI-7273**[5]
16	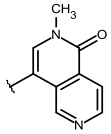	128	>100000	>100000	>100000	1565	
17	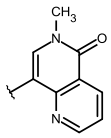	134	>100000	>100000	>100000	2475	
18	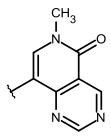	37	>100000	>100000	>100000	188	

Table 2. SAR for BRD9, BRD4-BD1, BRD4-BD2, BRD2-BD1 and BRD7 activity (*Alpha format, mean value; number of measurements: 2 to 5)

a **b**

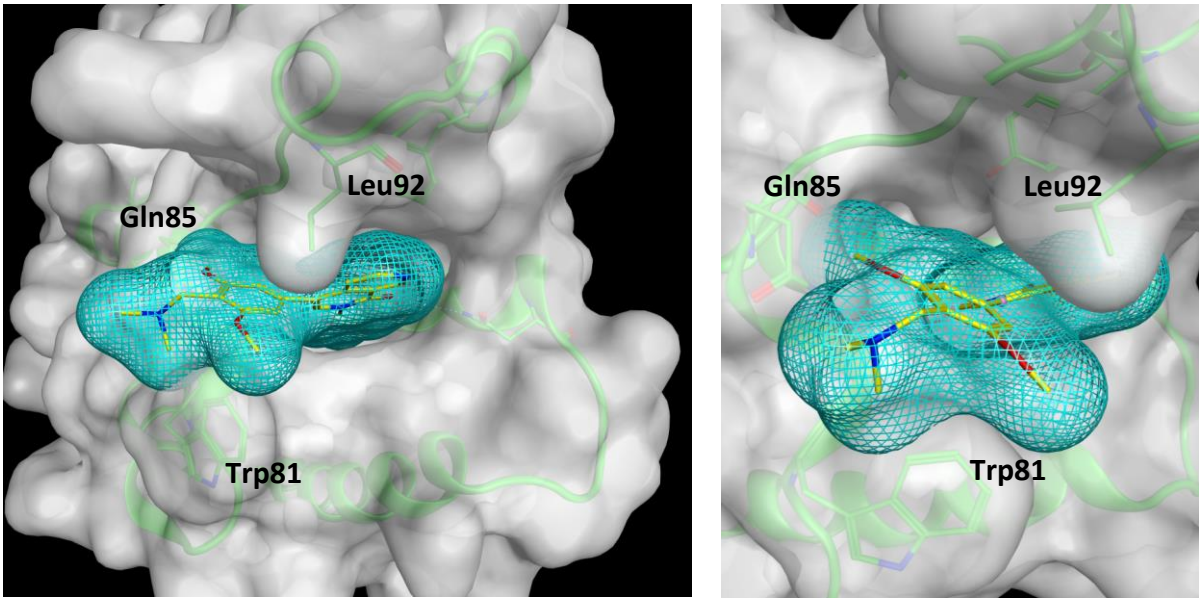

Figure 3. X-ray co-crystal structure of BI-7273 (yellow) in BRD9 (not shown) & aligned with BRD4-BD1 (green)

a) & b) Clash between **BI-7273** and BRD4-BD1 bromodomain amino acids (Trp81, Glu 85 & Leu 92) is shown.

BI-7273 (compound **17**) is shown as a surface representation colored in blue (mesh). The BRD4-BD1 protein is shown as a surface representation colored in grey

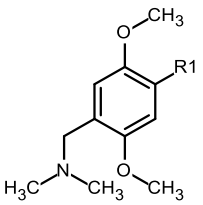

Compound	R1	IC_{50} (BRD9) [nM]*	IC_{50} (BRD4-BD1) [nM]*	IC_{50} (BRD4-BD2) [nM]*	IC_{50} (BRD2-BD1) [nM]*	IC_{50} (BRD7) [nM]*	Litt. Name
19	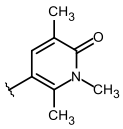	134	61917	>100000	59555	3283	
20	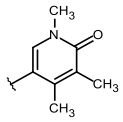	507	43998	67479	30330	2976	
21	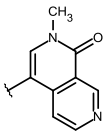	75	>100000	>100000	>100000	3410	**BI-9564**[a]
22	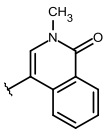	134	47095	86973	21687	4307	

Table 3. SAR for BRD9, BRD4-BD1, BRD4-BD2, BRD2-BD1 and BRD7 activity (*Alpha format, mean value; number of measurements: 2 to 5)

(a) http://www.thesgc.org/chemical-probes/BI-9564

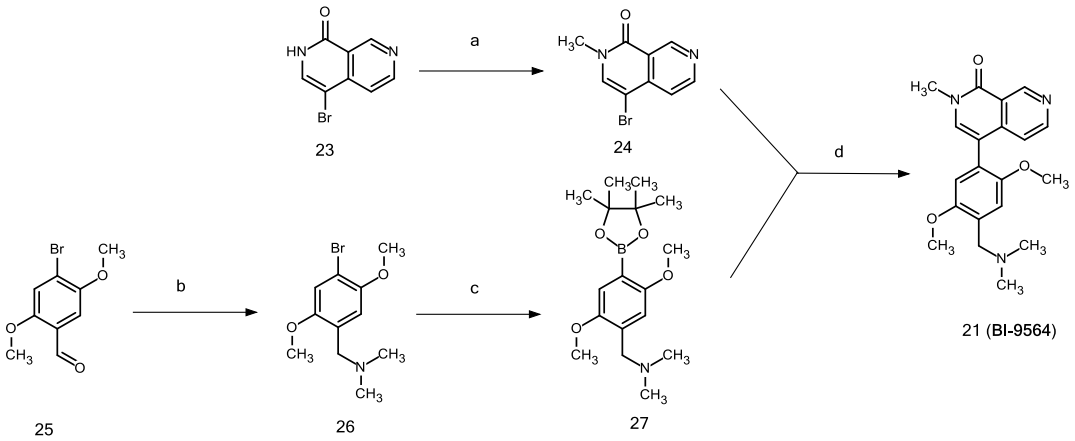

Scheme 1. Synthesis of BI-9564

Reagents and conditions: (a) NaH, MeI, DMF, rt, 71%; (b) $HNMe_2$.HCl, NaOAc, AcOH, DCM, rt, 89%; (c) B_2pin_2, KOAc, $Pd(dppf)Cl_2$, 1,4-dioxane, 90°C, 63%; (d) $Pd(dppf)Cl_2$·DCM, Na_2CO_3 aq, DMF, 100°C, 17%

a

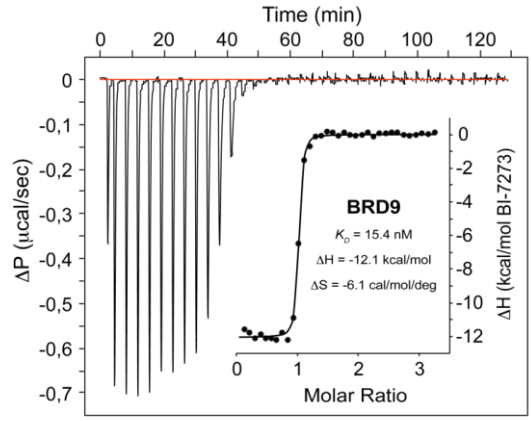

b

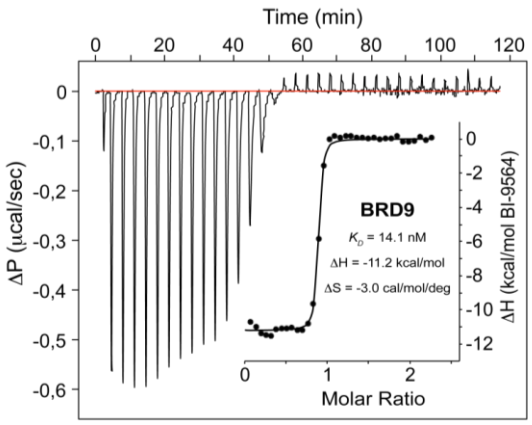

Figure 4. ITC analysis of compounds BI-7273 and BI-9564 (T = 293.15 K)

a) Compound **BI-7273** binds with a K_D value of 15.4 nM (ΔH = -12.1 kcal/mol); b) **BI-9564** with a K_D value of 14.1 nM (ΔH = -11.2 kcal/mol).

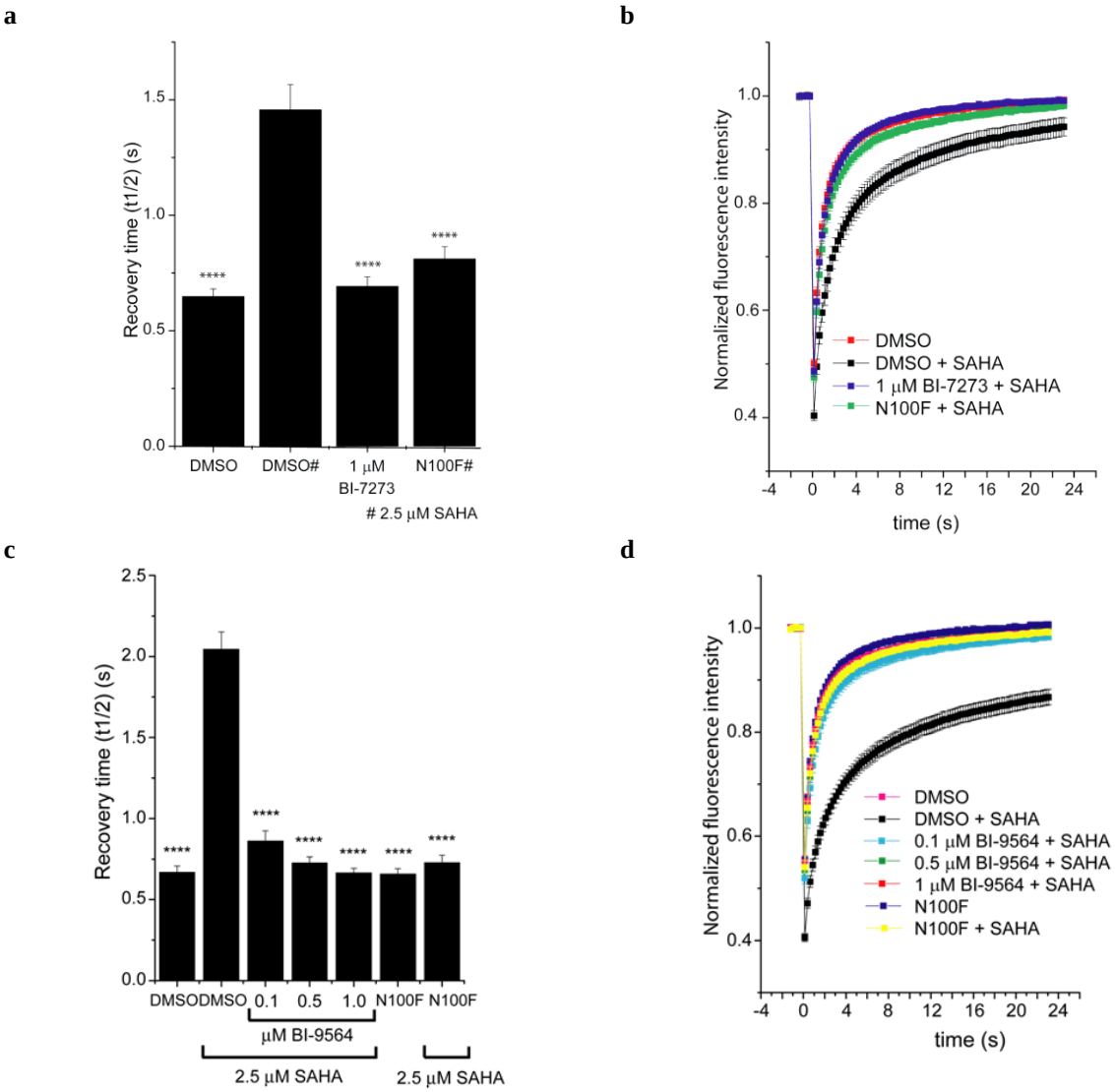

Figure 5. Recovery After Photobleaching (FRAP) assay U2OS cells transfected with GFP-BRD9.

a) Shown are recovery half times of wild type cells treated with DMSO in the absence or presence of 2.5µM SAHA or treated with **BI-7273** at 1 µM and SAHA as indicated. In addition, cells expressing GFP-BRD9 with a bromodomain inactivating mutant (N100F) were analysed. . Significant differences to cells treated with SAHA of p< 0.0001 are shown by ****; b) Time dependence of fluorescence recovery in the bleached area of cells expressing wt or mutant GFP-BRD9 with the corresponding treatment as in (a); c) Shown are recovery half times of cells expressing wt GFP-BRD9 treated with various concentrations of DMSO and **BI-9564** in the presence or absence of SAHA as indicated. Cells expressing GFP-BRD9 mutant (N100F) were treated as indicated. Significant differences to cells treated with SAHA of p< 0.0001 are shown by ****; d) Time dependence of fluorescence recovery in the bleached area of cells expressing wt or mutant GFP-BRD9 with the corresponding treatment as in (c).

Curves represent averaged data of at least 20 replicates.

BI-7273 shows potency (100% inhibition) at 1 µM in the BRD9 FRAP assay.

BI-9564 shows potency (~90% inhibition) at 0.1 µM in the BRD9 FRAP assay. Both compounds showed no toxicity in U2OS cells after 24h.

The N100F construct is a negative control BRD9 mutant in which Asn100 is replaced by Phe100 and therefore acetylated histone cannot bind anymore due to the lack of interaction to the anchor Asn and also steric hindrance. SAHA is added to the mixture to increase the signal to noise ratio by inhibiting the deacetylation of histones.

	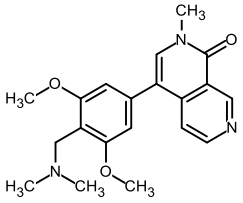	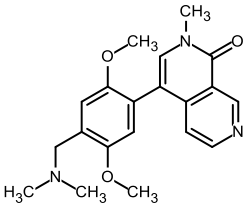
	15 (BI-7273)	**21(BI-9564)**
BRD9-BD Affinity/Activity		
K_D(BRD9, ITC)	15 nM	14 nM
IC_{50}(BRD9, Alpha assay)	19 nM[5]	75 nM
Bromodomain Selectivity	BRD9 +11.4°C	BRD9 +9.2°C
(48 bromodomains)	BRD7 +9.7°C	BRD7 +6.5°C
T_M shift at 10µM	CECR2 +8.2°C	CECR2 +5.6°C
	BETs < 1°C	BETs < 1°C
	All other bromodomains ≤ 2°C	All other bromodomains ≤ 2°C
K_D(BRD7, ITC)	n.d.	239 nM
IC_{50}(BRD7. Alpha assay)	117 nM[5]	3410 nM
K_D(BRD4-BD1, ITC)	> 20 µM	> 20 µM
K_D(BRD4-BD1, DiscoveRx)	> 10 µM	> 10 µM
IC_{50}(BRD4-BD1, Alpha assay)	> 100 µM	> 100 µM
K_D(CECR2, ITC)	187 nM	200 nM
Kinase Selectivity	All 31 kinases < 43%	ACVR1 76%
% ctrl inhibition at 10µM		TGFBR1 74%
		ACVR2B 72%
		All other 321 kinases < 40%
IC_{50}(ACVR1)	5130 nM	5090 nM
IC_{50}(TGFBR1)	3850 nM	5140 nM
IC_{50}(ACVR2B)	> 20,000 nM	7680 nM
GPCR Selectivity	n.d.	M1(h) 75%
% ctrl inhibition at 10µM		M3(h) 86%
		All other 53 GPCR < 40%
Target Engagement		
BRD9 FRAP assay	Full inhibition at 1µM	~90% inhibition at 100 nM
EC_{50}(BRD9 BD, RN2)	275 nM[5]	n.a.
BRD7 FRAP assay	Full inhibition at 1µM	Full inhibition at 1µM
CECR2 FRAP assay	n.d.	No Inhibition at 1µM
***In vitro* ADME Properties**		
Aqueous solubility (pH 6.8)	> 91 µg/mL	> 90 µg/mL
Hepatocytes pred. CL mouse/rat/human (% Q_H)	58% / <7% / 17%	56% / 17% / 17%
Plasma protein binding mousre/rat/human (% bound)	44% / 33% / 31%	35% / 23% / 42%
CytochromeP450 inhibition IC_{50}	All > 50 µM	> 50µM (2C8, 2C9, 2C19, 3A4), 49 µM (2D6)
Caco-2 permeability P_{appA-B} / efflux ratio	$11 \cdot 10^{-6}$ cm/s / 26	$11 \cdot 10^{-6}$ cm/s / 4.5
PK profile		
Mouse 5 mg/kg *i.v.* bolus plasma CL (% Q_H)	57%	65%
Mouse 5 mg/kg *i.v.* bolus plasma Vss	1.6 L/kg	2.1 L/kg
Mouse 20mg/kg *p.o.* AUC(0-last) / c_{max} / F_{oral}	7,500 nM·h / 3.0 µM / 39%	15,000 nM·h / 5.4 µM / 88%
Mouse 180mg/kg *p.o.* AUC(0-last) / c_{max} / F_{oral}	108,000 nM·h / 25 µM / 64%	226,000 nM·h / 35 µM / 151%
Cellular Effect		
EC_{50} (EOL-1)	1400 nM	800 nM

Table 4. Summary of properties of BI-7273 and BI-9564

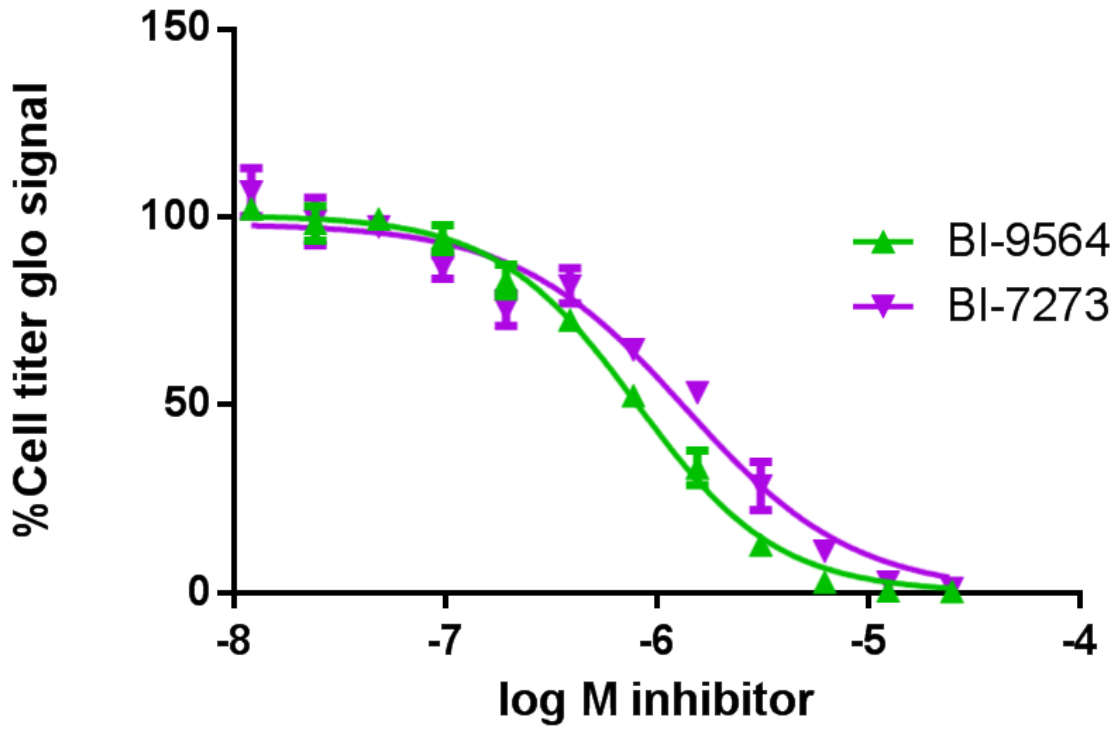

Figure 6. BI-7273 and BI-9564 block EOL-1 cell proliferation with EC_{50}s of 1400 nM and 800 nM, respectively.

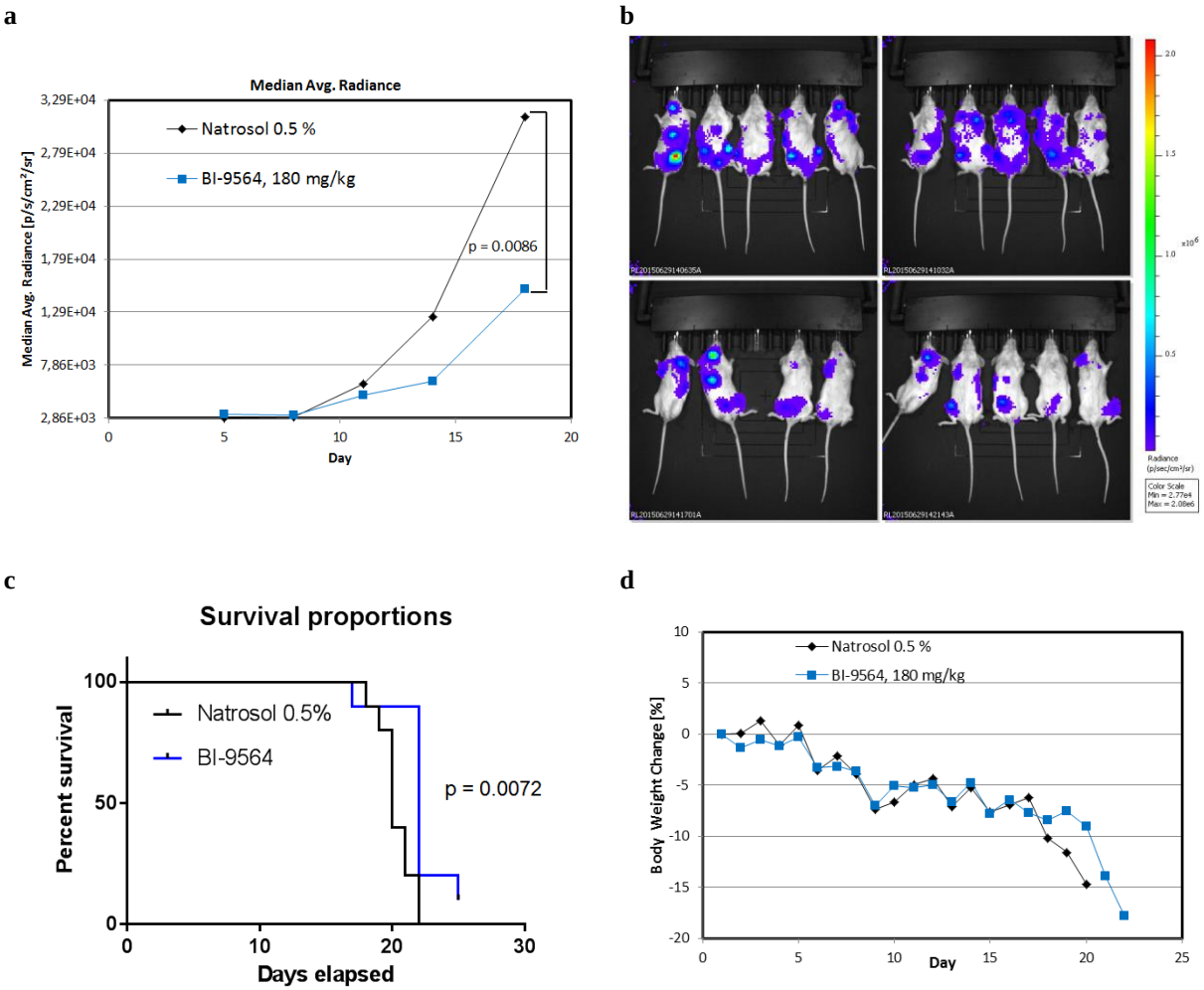

Figure 7. Efficacy and tolerability of the BRD9 inhibitor BI-9564 in a xenograft model of human AML.
Data for Figure a-d was collected in the same *in vivo* experiment.

a) CIEA-NOG mice were injected intravenously with 1 × 10^7 EOL-1 AML cells. Starting on day 5 after cell injection, mice were orally treated with vehicle (daily) or with 180 mg/kg **BI-9564** (qd5-17 and qd20-22). With the help of bioluminescence imaging the tumor burden was assessed in each animal on day 5, 8, 11, 14 and 18 and calculated as median average radiance [p/s/cm²/sr]. One-sided decreasing Mann-Whitney tests were used to compare tumor volumes.
b) Bioluminescence imaging on day 18: (upper) vehicle control, (lower) 180 mg/kg **BI-9564**.
c) The Kaplan-Meier curve shows prolonged survival of animals treated with 180 mg/kg **BI-9564** (vehicle = black line, 180 mg/kg **BI-9564** = blue line). The P-value was calculated by Mann-Whitney test.
d) The average body weight changes in percentage of initial weight.

EXPERIMENTAL SECTION

Unless otherwise indicated all reactions were carried out in standard commercially available glassware using standard synthetic chemistry methods. Air-sensitive and moisture-sensitive reactions were performed under an atmosphere of dry nitrogen or argon with dried glassware. Commercial starting materials were used without further purification. Solvents used for reactions were of commercial "dry"- or "extra-dry" or "analytical" grade. All other solvents used were reagent grade.

Preparative RP-HPLC was carried out on Agilent or Gilson systems using columns from Waters (Sunfire C18 OBD, 5 or 10 µm, 20x50 mm, 30x50 mm or 50x150 mm; X-Bridge C18 OBD, 5 or 10 µm, 20x50, 30x50, or 50x150 mm) or YMC (Triart C18, 5 or 10 µm, 20x50 mm, or 30x50 mm). Unless otherwise indicated compounds were eluted with MeCN/water gradients using either acidic (0.2 % HCOOH or TFA) or basic water (5 mL 2 M NH_4HCO_3 + 2 mL NH_3 (32 %) made up to 1 L with water).

NMR experiments were recorded on Bruker Avance 400 MHz and 500 MHz spectrometers at 298K. Samples were dissolved in 600µL DMSO-d6 or $CDCl_3$ and TMS was added as an internal standard. 1D 1H spectra were acquired with 30° excitation pulses and an interpulse delay of 4.2 sec with 64k datapoints and 20 ppm sweep width. 1D 13C spectra were acquired with broadband composite pulse decoupling (WALTZ16) and an interpulse delay of 3.3 sec with 64k datapoints and a sweep width of 240 ppm. Processing and analysis of 1D spectra was performed with Bruker Topspin 2.0 software. No zero filling was performed and spectra were manually integrated after automatic baseline correction. Chemical shifts are reported in ppm on the δ scale.

Analytical LC/MS data [**LC/MS(BAS1)**] were measured on an Agilent HPLC 1100 Series with Agilent LC/MSD SL detector using a Waters X-Bridge C18, 2.5 µm, 2.1x20mm column

(Part.No. 186003201) and solvent A [20mM aqueous NH_4HCO_3/ NH_3 (pH 9)] and solvent B [acetonitrile HPLC grade] as eluent (additional settings: flow 1mL/min; injection volume 5 µl; column temp. 60 °C). Standard gradient: 0.00 min:10 % B; 0.00 – 1.50 min: 10 % -> 95 % B; 1.50 – 2.00 min: 95 % B; 2.00 – 2.10 min: 95 % -> 10 % B. For some intermediates analytical LC/MS data was measured using different methods: **LC/MS(INT1)** was measured on a Shamadzu HPLC LC-20AB, SPD-M20A 190-370 nm system using a Luna C18(2), 5 µm, 50x2 mm column and solvent A [H_2O containing 0.0375 % TFA] and solvent B [acetonitrile HPLC grade containing 0.018 % TFA] as eluent (additional settings: flow 0.8 mL/min, column temp. 40 °C). Standard gradient: 0.00 min:10 % B; 0.00 – 4.00 min: 10 % -> 80 % B; 4.00 – 4.90 min: 80 % B; 4.90 – 4.92 min: 80 % B -> 10 % B; 4.92 – 5.50 min: 10 % B. **LC/MS(INT2)** was measured on an Agilent HPLC 1200 Series (DAD 200-400 nm) with an Agilent 6120 MS system using a Luna C18(2), 3 µm, 30x2mm column and solvent A [H_2O containing 0.0375 % TFA] and solvent B [acetonitrile HPLC grade containing 0.018 % TFA] as eluent (additional settings: flow 1.0 mL/min, column temp. 50 °C). Standard gradient: 0.00 min:10 % B; 0.00 – 1.15 min: 10 % -> 80 % B; 1.15 – 1.55 min: 80 % B; 1.55 – 1.56 min: 80 % B -> 10 % B; 1.56 – 2.99 min: 10 % B.

HRMS data were recorded using a Thermo Scientific Orbitrap Elite Hybrid Ion Trap/Orbitrap Spectrometer system with an Ultimate 3000 Series LPG-3400XRS Pump system. The mass calibration was performed using the Pierce LTQ Velos ESI positive ion calibration solution from Thermo Scientific (Lot PF200011, Product Nr. 88323)

Compound **1** is commercially available from *e.g.* ChemDiv.

Selected Experimental Procedures:

4-bromo-2-methyl-1,2-dihydro-2,7-naphthyridin-1-one **(24)**

Sodium hydride (3.41 g; 142 mmol) is added slowly to a cooled solution (0 °C) of 4-bromo-1,2-dihydro-2,7-naphthyridin-1-one (**23**) (16.0 g; 71.1 mmol; commercial from Activate) in DMF (300 mL) and the resulting mixture is stirred for 0.5 h. Methyl iodide (40.4 g; 285 mmol) is added slowly and stirring is continued for 2 h. The reaction mixture is quenched with ice water whereupon the product precipitates. The solid is collected by filtration, washed and dried *in vacuo* to give pure 4-bromo-2-methyl-1,2-dihydro-2,7-naphthyridin-1-one (**24**) (12.0 g; 50.2 mmol; 71 %). ^{1}H-NMR (400 MHz, DMSO-d_6) δ 9.36 (s, 1H), 8.87 (d, J = 5.6 Hz, 1H), 8.26 (s, 1H), 7.62 (d, J = 5.6 Hz, 1H), 3.53 (s, 3H); LC/MS (BAS1): $[M+H]^+$ = 239/241; t_R = 0.92.

[(4-Bromo-2,5-dimethoxyphenyl)methyl]dimethylamine **(26)**

A solution of NaOAc (6.10 g; 44.9 mmol), AcOH (2.45 g; 40.8mmol) and dimethylamine hydrochloride (6.98 g; 85.7 mmol) in DCM (160 mL) is stirred for 10 min at rt. 4-Bromo-2,5-dimethoxybenzaldehyde (**25**) (10.0 g; 40.8 mmol) is added and stirring is continued. After 30 min sodium triacetoxyborohydride (17.2 g; 81.6 mmol) is added in one portion and the reaction mixture is stirred at rt for 16 h. Saturated $NaHCO_3$ solution is added and the layers are separated. The aqueous layer is extracted three times with DCM. The combined organic layer is dried over $MgSO_4$, filtered and evaporated to give [(4-bromo-2,5-dimethoxyphenyl)-methyl]dimethylamine (10.0 g; 36.5 mmol; 89 %). ^{1}H NMR (500 MHz, DMSO-d6) δ 7.17 (d, J = 1.4 Hz, 1H), 7.06 (s, 1H), 3.78 (d, J = 1.5 Hz, 3H), 3.74 (d, J = 1.4 Hz, 3H), 3.35 (s, 2H), 2.16 (s, 6H); LC/MS (BAS1): [M+H]+ = 274/276; tR = 1.11 min.

{[2,5-dimethoxy-4-(tetramethyl-1,3,2-dioxaborolan-2-yl)phenyl]methyl}dimethylamine **(27)**

[(4-bromo-2,6-dimethoxyphenyl)methyl]dimethylamine (**26**) (7.80 g; 28.5 mmol) and bis(pinacolato)diboron (21.7 g; 85.5 mol) are dissolved/suspended in 1,4-dioxane (150 mL) under N_2. Potassium acetate (8.43 g; 49.6 mmol) and Pd(dppf)Cl_2 (1.00 g; 1.37 mmol) is added and the mixture is stirred at 90° C for 8 h. After cooling to rt, the mixture is concentrated and the residue is taken-up in DCM. Water is added, the layers are separated and the aqueous phase is extracted three times with DCM. The combined organic layer is dried over Na_2SO_4, filtered and evaporated. The crude product is purified by preparative RP-HPLC using a MeCN/water (0.2 % TFA added to the water) gradient as eluent to give the TFA salt of {[2,6-dimethoxy-4-(tetramethyl-1,3,2-dioxaborolan-2-yl)phenyl]methyl}-dimethylamine (**27**) which is transferred into the corresponding hydrochloride by dissolving and stirring in HCl/MeOH for 30 min (5.80 g; 18.1 mmol; 63 %). ^{1}H NMR (500 MHz, DMSO-d6) δ 10.15 (s, 1H, prot. amine), 7.24 (s, 1H), 7.16 (s, 1H), 4.24 (d, J = 5.4 Hz, 2H), 3.80 (s, 3H), 3.74 (s, 3H), 2.70 (d, J = 4.9 Hz, 6H), 1.29 (s, 12H); LC/MS (BAS1): $[M+H]^+$ = 240 (Ester cleaved); t_R = 0.70 min.

4-{4-[(dimethylamino)methyl]-2,5-dimethoxyphenyl}-2-methyl-1,2-dihydro-2,7-naphthyridin-1-one **(21, BI-9564)**

4-bromo-2-methyl-1,2-dihydro-2,7-naphthyridin-1-one (**24**) (7.44 g; 31.1 mmol), **27** (10.0 g; 31.1 mmol) and Pd(dppf)Cl_2·DCM (2.54 g; 3.11 mmol) are suspended in DMF (100 mL) under argon. A degassed Na_2CO_3-solution (2N; 38.9 mL; 77.8 mmol) is subsequently added and the resulting mixture is heated at 100 °C for 2 h. After cooling to rt, DMF is evaporated and a mixture of MeOH/DCM is added. All solids are filtered off and the filtrate is evaporated again to give the crude material which is purified by flash chromatography on SiO_2 using a MeOH/DCM gradient as eluent to give 4-{4-[(dimethylamino)methyl]-2,5-dimethoxy-

phenyl}-2-methyl-1,2-dihydro-2,7-naphthyridin-1-one (**21**) (3.40g; 9.62 mmol; 31 %). Further purification is achieved by preparative RP-HPLC (X-Bridge C 18 50x100 mm; 10 µm) using a MeCN/water gradient as eluent to give highly pure material (1.90 g; 5.38 mmol; 17 %). ^{1}H NMR (500 MHz, DMSO-d_6) δ 9.41 (s, 1H), 8.64 (d, J = 5.6 Hz, 1H), 7.74 (s, 1H), 7.12 (s, 1H), 7.03 (d, J = 5.6 Hz, 1H), 6.93 (s, 1H), 3.75 (s, 3H), 3.63 (s, 3H), 3.58 (s, 3H), 3.48 – 3.44 (m, 2H), 2.22 (s, 6H); ^{13}C NMR (125 MHz, DMSO-d6) δ 161.1, 151.7, 151.4, 150.8, 150.6, 142.0, 138.5, 128.4, 122.2, 120.0, 118.6, 115.1, 113.6, 113.5, 57.1, 56.5, 56.2, 45.8 (2C), 36.8. HRMS (CI+): calculated for $C_{20}H_{24}N_3O_3$ (MH+) 354.18122, found 354.18091, Δ -0.88 ppm; LC/MS (BAS1): $[M+H]^+$ = 354; t_R = 0.91 min.

ASSOCIATED CONTENT

Supporting Information.

Additional text describing all biophysical and biological methods and results, FBS screening and virtual screening, X-ray co-crystal structure, selectivity data (Bromoscan, TM shift, ITC, GPCR, kinase data for **BI-7273** and **BI-9564**), Recovery After Photobleaching (FRAP) assay data , PK profile *i.v.* and *p.o.* for **BI-7273** and **BI-9564** experiments, cell results, chemistry experimental procedures for compound **2-20** and compound **22**.

This material is available free of charge via the Internet at http://pubs.acs.org.

Accession Codes

Atomic coordinate of BRD9 BD bound to compounds **1** (PDB code #), **2** (PDB code #), **1** (PDB code #), **9** (PDB code #), **BI-7273** (5EU1)[5], **BI-9564** (PDB code #) have been deposited with the Protein Data Bank

AUTHOR INFORMATION

* corresponding author, email: laetitia_janine.martin@boehringer-ingelheim.com

Phone: : +43 (1) 80 105-2584

ACKNOWLEDGMENTS

The authors thank Thomas Arnhold, Alexandra Beran, Helmut Berger, Adrian Carter, Sonia-Lucia Cesana, Yunhai Cui, Wolfgang Egermann, Norbert Eidkum, Andreas Fischer, Gerlinde Flotzinger, Michael Galant, Gerhard Gmaschitz, Eric Haaksma, Eva-Marie Haupt, Wolfgang

Hela, Hans Hoffmann, Gudrun Illibauer, Matthias Klemencic, Martina Kohla, Roland Kousek, Rebecca Langlois, Moriz Mayer, Jürgen Moll, Oliver Petermann, Franziska Popp*, Nikolai Pototschnig, Carlos Roberto Ramirez-Santa Cruz, Heidi Roth*, Samira Selman, Bernadette Sharps, Gabriella Siszler, Christian Smethurst, Michaela Streicher, Diane Thompson, Anika Weiss, Alexander Weiss-Puxbaum

(*BI Global Skill Center Alternative Lead Identification)

AUTHOR CONTRIBUTION

L.J.M supervised the chemistry team. L.J.M, M.K. and M.H.H. wrote the manuscript. L.J.M and S.S. designed synthetic strategies. M.K. designed biological experiments and supervised the biology team. G.Ba., D.F., D.K. and H.N. determined and analysed crystal structures. X-L.C. performed the virtual screening of HiCoS library. O.F. supervised ITC and FRAP assay. D.F. designed and supervised the crystal soaking experiments. T.G. designed and supervised the biochemical Alpha assays. A.F.H. carried out the bromodomain-swap allele experiments. M.H.H. designed and supervised the animal experiments. D.K. and H.N. supervised the FBS screening. S.Kn., S.M. & G.Bo. supervised the collaboration with SGC. P.K. and S.Ko. synthesised the compounds and developed chemistry routes. C.R. performed all the FRAP assays. K.R. supervised the SPR assays. O.S. supervised PK studies. S.S. wrote the synthesis supporting information. C.T. supervised protein production and performed ITC experiments and K_D determination. C.R.V. designed the bromodomain-swap allele experiments. M.Z. performed the NMR experiments and supervised the DSF, MST and NMR measurements of the FBS screening. A.Z. supervised the production of protein and DSF assays. M.P. was responsible for the biology strategy. D.McC was responsible for the medicinal chemistry strategy

REFERENCES

[1] Whitehouse, I.; Flaus, A.; Cairns, B. R.; White, M. F.; Workman, J. L.; Owen-Hughes, T. Nucleosome mobilization catalysed by the yeast SWI/SNF complex *Nature* **1999**, *400*, 784-787.

[2] Liu, B., Yip, R. K. H. & Zhou, Z. Chromatine remodeling, DNA damage repair and aging *Current Genomics* **2012**, *13*, 533-547.

[3] Hohmann, A. F.; Vakoc, C. R. A rationale to target the SWI/SNF complex for cancer therapy *Trends Genet.* 2014, *30*, 356-361.

[4] Kadoch, C.; Hargreaves, D. C.; Hodges, C.; Elias, L.; Ho, L.; Ranish J.; Crabtree G. R. Proteomic and bioinformatic analysis of mammalian SWI/SNF complexes identifies extensive roles in human malignancy *Nat. Genet.* **2013**, *45*, 592−601.

[5] Hohmann, A. F.; Martin, L. J.; Minder, J.; Roe, J-S.; Shi, J.; Steurer, S.; Bader; G., McConnell, D.; Pearson, M.; Gerstberger, T.; Gottschamel, T.; Thompson, D.; Suzuki, Y.; Koegl, M.; Vakoc, C. R A bromodomain-swap allele demonstrates that on-target chemical inhibition of BRD9 limits the proliferation of acute myeloid leukemia cells, *unpublished results.*

[6] Bunnage, M. E., Piatnitski Chekler, E. L., Jones, L. H. Target validation using chemical probes *Nat. Chem. Biol.* **2013**, *9*, 195-199.

[7] Arrowsmith, C. H.; Audia, J. E.; Austin, C.; Baell, J.; Bennett, J.; Blagg, J.; Bountra, C.; Brennan, P. E.; Brown, P. J.; Bunnage, M. E.; Buser-Doepner, C.; Campbell, R. M.; Carter, A. J.; Cohen, P.; Copeland, R. A.; Cravatt, B.; Dahlin, J. L.; Dhanak, D.; Edwards, A. M.; Frederiksen, M.; Frye, S. V.; Gray, N.; Grimshaw, C. E.; Hepworth, D.; Howe, T.; Huber, K. V. M.; Jin, J.; Knapp, S.; Kotz, J. D.; Kruger, R. G.; Lowe, D.; Mader, M. M.; Marsden, B.; Mueller-Fahrnow, A.; Müller, S.; O'Hagan, R. C.; Overington, J. P.; Owen, D. R.; Rosenberg, S. H.; Ross, R.; Roth, B.; Schapira, M.; Schreiber, S. L.; Shoichet, B.; Sundström, M.; Superti-Furga, G.; Taunton, J.; Toledo-Sherman, L.; Walpole, C.; Walters, M. A.; Willson, T. M.; Workman, P.; Young, R. N.; Zuercher, W. J. The promise and peril of chemical probes *Nat. Chem. Biol*. **2015**, *11*, 536-541.

[8] Hewings, D. S.; Rooney, T. P. C.; Jennings, L. E.; Hay, D. A.; Schofield, C. J.; Brennan, P. E.; Knapp, S.; Conway, S. J. Progress in the development and application of small molecule inhibitors of bromodomain-acetyl-lysine interactions. *J. Med. Chem.* **2012**, *55*, 9393-9413.

[9] Herait, P.; Dombret, H.; Thieblemont, C.; Facon, T.; Stathis, A.; Cunningham, D.; Palumbo, A.; Vey, N.; Michallet, M.; Recher, C.; Rezai, K.; Preudhomme, C. O7.3 BET-bromodomain (BRD) inhibitor OTX015: Final

results of the dose-finding part of a phase I study in hematologic malignancies *Annals of Oncology*. **2015**, *26* (Supplement 2) ii10-ii11.

[10] Moros, A.; Rodríguez, V.; Saborit-Villarroya, I.; Montraveta, A.; Balsas, P.; Sandy, P.; Martínez, A.; Wiestner, A.; Normant, E.; Campo, E.; Pérez-Galán, P.; Colomer, D.; Roué, G. Synergistic antitumor activity of lenalidomide with the BET bromodomain inhibitor CPI203 in bortezomib-resistant mantle cell lymphoma *Leukemia* **2014**, *28*, 2049–2059.

[11] Garnier, J-M., Sharp, P. P. & Burns, C. J. BET bromodomain inhibitors: a patent review *Expert Opin. Ther. Pat.* **2014**, *24*, 185-199.

[12] Seidel, S. A.; Wienken, C. J.; Geissler, S.; Jerabek-Willemsen, M.; Duhr, S.; Reiter, A.; Trauner, D.; Braun, D.; Baaske, P. Label-Free Microscale Thermophoresis Discriminates Sites and Affinity of Protein–Ligand Binding *Angew. Chem., Int. Ed.* **2012**, *51*, 10656-10659.

[13] Friesner, R. A.; Banks, J. L.; Murphy, R.B.; Halgren, T. A.; Klicic, J. J.; Mainz, D. T.; Repasky, M. P.; Knoll, E. H.; Shelley, M.; Perry, J. K.; Shaw, D. E.; Francis, P.; Shenkin, P.S. Glide: A New Approach for Rapid, Accurate Docking and Scoring. 1. Method and Assessment of Docking Accuracy *J. Med. Chem.* **2004**, *47*, 1739-1749.

[14] Meyer, E. A., Castellano, R. K. & Diederich F. Interactions with Aromatic Rings in Chemical and Biological Recognition *Angew. Chem., Int. Ed.* **2003**, *42*, 1210-1250.

[15] Lawton, G.; Witty, D. R. *Progress in Medicinal Chemistry* Volume 51 (Elsevier B.V., Amsterdam, 2012)

[16] Lee, E. C.; Hong, B. H.; Lee, J. Y.; Kim, J. C.; Kim, D.; Kim, Y.; Tarakeshwar, P.; Kim, K. S. Substituent Effects on the Edge-to-Face Aromatic Interactions *J. Am. Chem. Soc.* **2005**, *127*, 4530–4537.

[17] Picaud, S. 9H-purine scaffold reveals induced-fit pocket plasticity of the BRD9 bromodomain. *J. Med. Chem.* **2015**, *58*, 2718-2736.

[18] Philpott, M.; Rogers, C. M.; Yapp, C.; Wells, C.; Lambert, J. P.; Strain-Damerell, C.; Burgess-Brown, N. A.; Gingras, A. C.; Knapp, S.; Müller, S. Assessing cellular efficacy of bromodomain inhibitors using fluorescence recovery after photobleaching *Epigenetics Chromatin* **2014**, *7*, 1-12.

[19] Clark, P. G. K.; Vieira, L. C. C.; Tallant, C.; Fedorov, O.; Singleton, D. C.; Rogers, C. M.; Monteiro, O. P.; Bennett, J. M.; Baronio, R.; Müller, S.; Daniels, D. L.; Mendez, J.; Knapp, S.; Brennan, P.; Dixon, D. J. LP99: Discovery and Synthesis of the First Selective BRD7/9 Bromodomain Inhibitor *Angew. Chem. Int. Ed.* **2015**, *54*, 6217-6221.

[20] Theodoulou, N. H.; Bamborough, P.; Bannister, A. J.; Becher, I.; Bit, R. A.; Che, K. H.; Chung, C.-W.; Dittmann, A.; Drewes, G.; Drewry, D. H.; Gordon, L.; Grandi, P.; Leveridge, M.; Lindon, M.; Michon, A.-M.; Molnar, J.; Robson, S. C.; Tomkinson, N. C. O.; Kouzarides, T.; Prinjha, R. K.; Humphreys, P. G. Discovery of I-BRD9, a Selective Cell Active Chemical Probe for Bromodomain Containing Protein 9 Inhibition *J. Med. Chem.* [Online early access]. DOI: 10.1021/acs.jmedchem.5b00256. Published Online: April 9, 2015.

[21] Hay, D. A.; Rogers, C. M.; Fedorov, O.; Tallant, C.; Martin, S.; Monteiro, O. P.; Muller, S.; Knapp, S.; Schofield, C. J.; Brennan, P. E. Design and synthesis of potent and selective inhibitors of BRD7 and BRD9 bromodomains *Med. Chem. Commun.* **2015**, *6*, 1381-1386.

[22] Romero, F. A.; Taylor, A. M.; Crawford, T. D.; Tsui, V.; Cote, A.; Magnuson, S. Disrupting Acetyl-Lysine Recognition: Progress in the Development of Bromodomain Inhibitors *J. Med. Chem.* [Online early access]. DOI: 10.1021/acs.jmedchem.5b01514. Published Online: November 23, 2015.

[23] Cain, C. Chromatin´s rising tide *SciBX* **2014**, *7*, 1-7.

SUPPORTING INFORMATION

Structure-based design of an *in vivo* active selective BRD9 inhibitor

Laetitia J. Martin,*[,†] Manfred Koegl,[†] Gerd Bader,[†] Xiao-Ling Cockcroft,[†] Oleg Fedorov,[§] Dennis Fiegen,[‡] Thomas Gerstberger,[†] Marco H. Hofmann,[†] Anja F. Hohmann,[∥] Dirk Kessler,[†] Stefan Knapp,[§] Petr Knesl,[†] Stefan Kornigg,[†] Susanne Müller,[§] Herbert Nar,[‡] Catherine Rogers,[§] Klaus Rumpel,[†] Otmar Schaaf,[†] Steffen Steurer,[†] Cynthia Tallant,[§] Christopher R. Vakoc,[∥] Markus Zeeb,[‡] Andreas Zoephel,[†] Mark Pearson,[†] Guido Boehmelt,[†] and Darryl McConnell[†]

[†] Boehringer Ingelheim RCV GmbH & Co KG, Vienna, Austria

[‡] Boehringer Ingelheim Pharma GmbH & Co KG, Biberach, Germany

[§] SGC, University of Oxford, Oxford, UK

[∥] Cold Spring Harbor Laboratory, Cold Spring Harbor, New York, U.S.A

*Corresponding Author: E-mail address: laetitia_janine.martin@boehringer-ingelheim.com

Table of contents

Synthesis of Compounds

List of abbreviations

AcOH	Acetic acid
MeCN	Acetonitrile
Boc	*tert*.butoxy carbonyl; di-*tert*-butyl dicarbonate
cHex	Cyclohexane
DAD	Diode array detector
DCM	Dichloromethane, CH_2Cl_2
dppf	1,1'-Bis(diphenylphosphino)ferrocene
DIPEA	Diisopropylethyl amine
DME	1,2-Dimethoxyethane
DMF	*N*,*N*-Dimethylformamide
DMSO	Dimethylsulphoxide
EtOAc or EA	Ethyl acetate
EtOH	Ethanol
h	Hour(s)
HPLC	High performance liquid chromatography
HRMS	High resolution mass spectroscopy
INT	Intermediate
KOAc	Potassium acetate
LC	Liquid Chromatography
M	Molar (mol/L)
MeOH	Methanol
µL	Microliter
µm	Micrometer
min	Minute(s)
mL	Milliliter
mm	Millimeter
MS	Mass spectrometry
MsCl	Methanesulfonyl chloride
nm	Nanometer
N	Normal

NMR	Nuclear magnetic resonance
PE	Petrolether
Pd_2dba_3	Tris(dibenzylideneacetone)dipalladium(0)
$Pd(dppf)Cl_2$	[1,1′-Bis(diphenylphosphino)ferrocene]dichloropalladium(II)
ppm	Parts per million
prot.	Protonated
RP	Reversed phase
rt	Room temperature (20 to 25°C)
SM	Starting material
TEA	Triethylamine
TFA	Trifluoroacetic acid
THF	Tetrahydrofuran
t_R	Retention time [min]
XPhos	2-Dicyclohexylphosphino-2′,4′,6′-triisopropylbiphenyl

General Methods

Unless otherwise indicated all reactions were carried out in standard commercially available glassware using standard synthetic chemistry methods. Air-sensitive and moisture-sensitive reactions were performed under an atmosphere of dry nitrogen or argon with dried glassware. Commercial starting materials were used without further purification. Solvents used for reactions were of commercial "dry"- or "extra-dry" or "analytical" grade. All other solvents used were reagent grade.

Preparative RP-HPLC was carried out on Agilent or Gilson systems using columns from Waters (Sunfire C18 OBD, 5 or 10 µm, 20x50 mm, 30x50 mm or 50x150 mm; X-Bridge C18 OBD, 5 or 10 µm, 20x50, 30x50, or 50x150 mm) or YMC (Triart C18, 5 or 10 µm, 20x50 mm, or 30x50 mm). Unless otherwise indicated compounds were eluted with MeCN/water gradients using either acidic (0.2 % HCOOH or TFA) or basic water (5 mL 2 M NH_4HCO_3 + 2 mL NH_3 (32 %) made up to 1 L with water).

NMR experiments were recorded on Bruker Avance 400 MHz and 500 MHz spectrometers at 298K. Samples were dissolved in 600µL DMSO-d6 or $CDCl_3$ and TMS was added as an internal standard. 1D 1H spectra were acquired with 30° excitation pulses and an interpulse delay of 4.2 sec with 64k datapoints and 20 ppm sweep width. 1D 13C spectra were acquired

with broadband composite pulse decoupling (WALTZ16) and an interpulse delay of 3.3 sec with 64k datapoints and a sweep width of 240 ppm. Processing and analysis of 1D spectra was performed with Bruker Topspin 2.0 software. No zero filling was performed and spectra were manually integrated after automatic baseline correction. Chemical shifts are reported in ppm on the δ scale.

Analytical LC/MS data [**LC/MS(BAS1)**] were measured on an Agilent HPLC 1100 Series with Agilent LC/MSD SL detector using a Waters X-Bridge C18, 2.5 µm, 2.1x20mm column (Part.No. 186003201) and solvent A [20mM aqueous NH_4HCO_3/ NH_3 (pH 9)] and solvent B [acetonitrile HPLC grade] as eluent (additional settings: flow 1mL/min; injection volume 5 µl; column temp. 60 °C). Standard gradient: 0.00 min:10 % B; 0.00 – 1.50 min: 10 % -> 95 % B; 1.50 – 2.00 min: 95 % B; 2.00 – 2.10 min: 95 % -> 10 % B. For some intermediates analytical LC/MS data was measured using different methods: **LC/MS(31)** was measured on a Shamadzu HPLC LC-20AB, SPD-M20A 190-370 nm system using a Luna C18(2), 5 µm, 50x2 mm column and solvent A [H_2O containing 0.0375 % TFA] and solvent B [acetonitrile HPLC grade containing 0.018 % TFA] as eluent (additional settings: flow 0.8 mL/min, column temp. 40 °C). Standard gradient: 0.00 min:10 % B; 0.00 – 4.00 min: 10 % -> 80 % B; 4.00 – 4.90 min: 80 % B; 4.90 – 4.92 min: 80 % B -> 10 % B; 4.92 – 5.50 min: 10 % B. **LC/MS(32)** was measured on an Agilent HPLC 1200 Series (DAD 200-400 nm) with an Agilent 6120 MS system using a Luna C18(2), 3 µm, 30x2mm column and solvent A [H_2O containing 0.0375 % TFA] and solvent B [acetonitrile HPLC grade containing 0.018 % TFA] as eluent (additional settings: flow 1.0 mL/min, column temp. 50 °C). Standard gradient: 0.00 min:10 % B; 0.00 – 1.15 min: 10 % -> 80 % B; 1.15 – 1.55 min: 80 % B; 1.55 – 1.56 min: 80 % B -> 10 % B; 1.56 – 2.99 min: 10 % B.

HRMS data were recorded using a Thermo Scientific Orbitrap Elite Hybrid Ion Trap/Orbitrap Spectrometer system with an Ultimate 3000 Series LPG-3400XRS Pump system. The mass calibration was performed using the Pierce LTQ Velos ESI positive ion calibration solution from Thermo Scientific (Lot PF200011, Product Nr. 88323)

Compound **1** is commercially available from e.g. ChemDiv.

Synthesis of compound 2

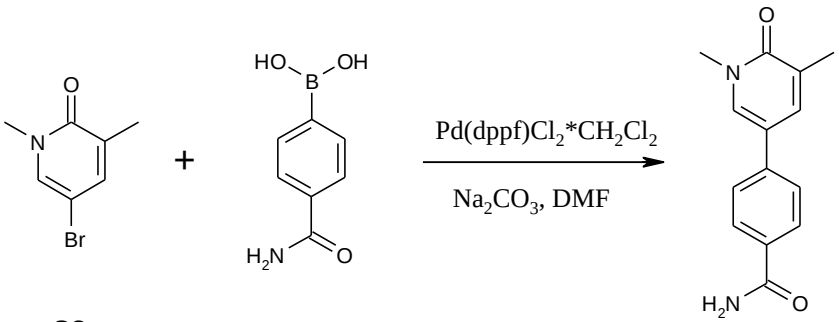

28 **29** **2**

Supplementary Scheme 1: Synthesis of compound (**2**)

4-(1,5-dimethyl-6-oxo-1,6-dihydropyridin-3-yl)benzamide (2)

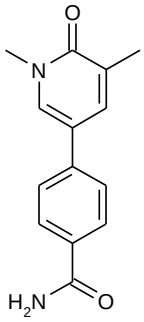

5-bromo-1,3-dimethyl-1,2-dihydropyridin-2-one (**28**) (83.3 mg; 412 µmol; commercial from AlfaAesar) and (4-carbamoylphenyl)boronic acid (**29**) (66.0 mg; 400 µmol; commercial from ABCR) and Pd(dppf)Cl_2·DCM (32.7 mg; 40.0 µmol) are suspended in DMF (800 µL) under argon. A degassed Na_2CO_3-solution (2N; 500 µL; 1.00 mmol) is subsequently added and the resulting mixture is heated at 100 °C for 3 h. After cooling to rt, water is added (several drops) and the mixture is filtered and purified by preparative RP-HPLC (column: Sunfire C-18 30x50 mm) using a MeCN/water gradient under acidic conditions. The product containing fractions are freeze dried. Further purification is achieved by automated silica gel chromatography (Combiflash; column: Redisep RF, 12g) using a DCM/MeOH gradient as eluent (100:0 --> 90:10; MeOH). The product containing fractions are evaporated, dissolved in MeCN/water and freeze dried to give 4-(1,5-dimethyl-6-oxo-1,6-dihydropyridin-3-yl)benzamide (**2**) (38.6 mg; 159 µmol; 40 %). ^{1}H NMR (500 MHz, DMSO-d6) δ 8.11 (s, 1H), 7.99 (s, 1H), 7.92 (d, J = 7.9 Hz, 2H), 7.82 (s, 1H), 7.67 (d, J = 7.9 Hz, 2H), 7.34 (s, 1H), 3.53 (s, 3H), 2.09 (s, 3H); ^{13}C NMR (125 MHz, DMSO) δ 167.9, 162.2, 139.5, 136.0, 135.6, 132.6, 128.6 (2C), 128.3, 125.1 (2C), 116.7, 37.8, 17.5; HRMS (CI+): calculated for $C_{14}H_{15}N_2O_2$ (MH+) 243.11280, found 243.11235, Δ -1.85 ppm; LC/MS (BAS1): $[M+H]^+$ = 243; t_R = 0.39.

Synthesis of compound 3

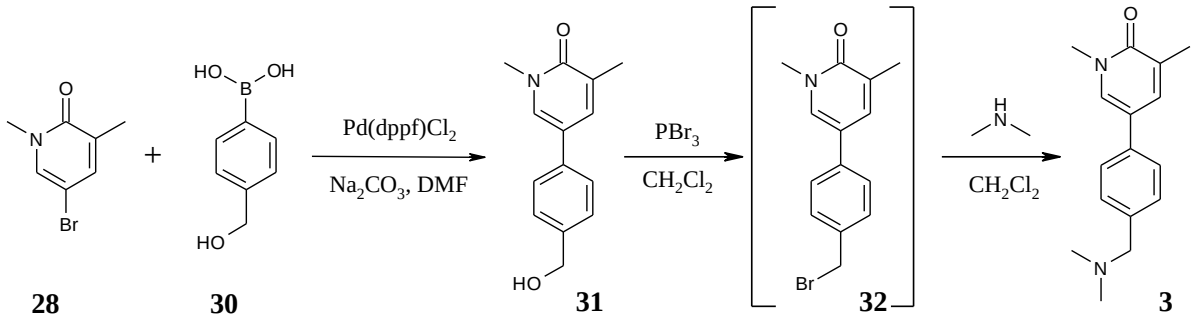

Supplementary Scheme 2: Synthesis of compound (**3**)

5-[4-(hydroxymethyl)phenyl]-1,3-dimethyl-1,2-dihydropyridin-2-one (31)

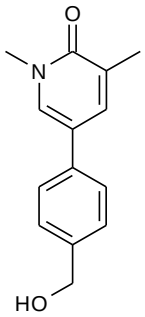

5-bromo-1,3-dimethyl-1,2-dihydropyridin-2-one (**28**) (9.70 g; 48.0 mmol; commercial from AlfaAesar), [4-(hydroxymethyl)phenyl]boronic acid (**30**) (10.9 g; 71.7 mmol; commercial from ABCR) and Cs_2CO_3 (46.9 g; 144 mmol) are dissolved in a 5:1 mixture of 1,4-dioxane and water (200 mL). $Pd(dppf)Cl_2$ (3.84 g; 5.25 mmol) is added under an inert atmosphere (argon) and the mixture is heated at 90 °C for 12 h. After cooling, 1,4-dioxane is removed under reduced pressure, water is added and the mixture is extracted three times with DCM. The combined organic layer is washed with brine, dried over Na_2SO_4, filtered and evaporated. The crude product is purified by flash chromatography on SiO_2 using a PE/EA gradient (5:1 --> 2:1). The product containing fractions are evaporated to give pure 5-[4-(hydroxymethyl)phenyl]-1,3-dimethyl-1,2-dihydropyridin-2-one (**31**) (4.40 g; 19.2 mmol; 40 %). ^{1}H NMR (400 MHz, DMSO-d6) δ 7.99 (s, 1H), 7.74 (s, 1H), 7.53 (d, J = 8.3 Hz, 2H), 7.35 (d, J = 8.0 Hz, 2H), 5.21 (s, 1H), 4.51 (s, 2H), 3.52 (s, 3H), 2.09 (s, 3H); LC/MS (BAS1): $[M+H]^+$ = 230; t_R = 0.69.

5-{4-[(dimethylamino)methyl]phenyl}-1,3-dimethyl-1,2-dihydropyridin-2-one (3)

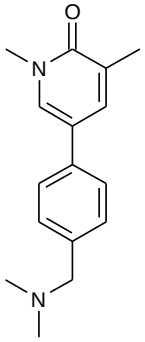

31 (500 mg; 2.18 mmol) is dissolved in DCM (10 mL) and cooled to 0 °C in an ice bath. Phosphorous tribromide (295 mg; 1.09 mmol) is added dropwise and the resulting mixture is stirred for 30 min. at 0 °C. After completion, water is added and the mixture is extracted three times with DCM. The combined aqueous layer is washed with brine, dried over Na_2SO_4, filtered and evaporated to give crude 5-[4-(bromomethyl)phenyl]-1,3-dimethyl-1,2-dihydropyridin-2-one (**32**), which is used without further purification.

Crude **32** is dissolved in DCM (5 mL). Dimethylamine (5.45 mL; 10.9 mmol, 2M solution in MeOH) is added and the resulting mixture is stirred at rt for 12 h. All solvents are removed under reduced pressure and the residue is taken-up in a small amount of MeCN and purified by preparative RP HPLC. The product containing fractions are freeze dried to give 5-{4-[(dimethylamino)methyl]phenyl}-1,3-dimethyl-1,2-dihydropyridin-2-one (**3**) (40.0 mg; 156 µmol; 7.2 %). ^{1}H NMR (500 MHz, DMSO-d6) δ 7.97 (s, 1H), 7.73 (s, 1H), 7.52 (d, J = 7.8 Hz, 2H), 7.31 (d, J = 7.8 Hz, 2H), 3.52 (s, 3H), 3.39 (s, 2H), 2.15 (s, 6H), 2.08 (s, 3H); ^{13}C NMR (125 MHz, DMSO) δ 162.1, 137.9, 136.3, 135.4, 134.7, 129.7 (2C), 128.1, 125.6 (2C), 117.5, 63.5, 45.4 (2C), 37.7, 17.5; HRMS (CI+): calculated for $C_{16}H_{21}N_2O$ (MH+) 257.16483, found 257.16484, Δ – 0.1 ppm; LC/MS (BAS1): $[M+H]^+$ = 257; t_R = 0.93.

Synthesis of compound 4

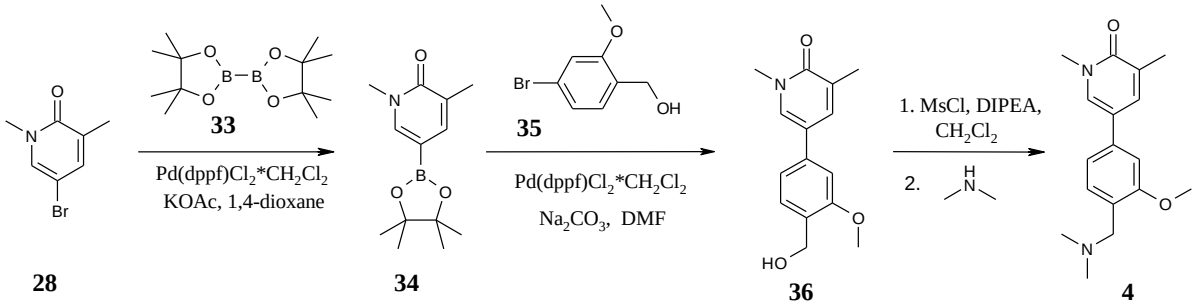

Supplementary Scheme 3: Synthesis of compound (**4**)

1,3-dimethyl-5-(tetramethyl-1,3,2-dioxaborolan-2-yl)-1,2-dihydropyridin-2-one (34)

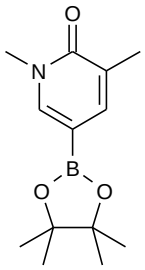

5-bromo-1,3-dimethyl-1,2-dihydropyridin-2-one (**28**) (10.0 g; 49.5 mmol), bis(pinacolato)-diboron (**33**) (17.2 g; 67.7 mmol, commercial from CombiBlocks), Pd(dppf)Cl_2·DCM (2.00 g; 2.45 mmol) and potassium acetate (9.42 g; 96.0 mmol) are suspended in 1,4-dioxane (100 mL) under argon and the resulting mixture is heated at 90 °C for 3 h. After cooling to rt the reaction mixture is filtered through Celite and washed with 1,4-dioxane (2x 100 mL). The filtrate is concentrated under reduced pressure, the residue is taken-up in DCM (200 mL) and washed with water (100 mL). The organic layer is dried over Na_2SO_4, filtered and concentrated *in vacuo*. The crude product is purified by silica gel chromatography (Combiflash; column: Redisep RF, 330g) using a cHex/EA gradient as eluent (100:0 --> 0:100). The product containing fractions are evaporated to give 1,3-dimethyl-5-(tetramethyl-1,3,2-dioxaborolan-2-yl)-1,2-dihydropyridin-2-one (**34**) (8.35 g; 33.5 mmol; 68 %) as a dark yellow oil, which slowly crystallizes. ^{1}H NMR (400 MHz, DMSO-d6) δ 7.87 (s, 1H), 7.39 (s, 1H), 3.46 (s, 3H), 1.98 (s, 3H), 1.26 (s, 12H); LC/MS (BAS1): $[M+H]^+$ = 250; t_R = 0.87.

5-[4-(hydroxymethyl)-3-methoxyphenyl]-1,3-dimethyl-1,2-dihydropyridin-2-one (36)

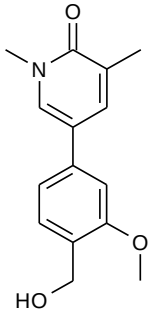

(4-bromo-2-methoxyphenyl)-methanol (**35**) (1.05 g 4.84 mmol; commercial from Aldrich), **34** (1.20 g; 4.82 mmol) and Pd(dppf)Cl_2·DCM (393 mg; 481 µmol) are suspended in DMF (5 mL) under argon. A degassed solution of sodium carbonate (2N; 6.02 mL; 12.0 mmol) is added and the resulting mixture is heated at 100 °C for 1 h. After cooling to rt water is added and the mixture is extracted three times with DCM (30 mL each). The combined organic layer

is dried over Na_2SO_4, filtered and evaporated. The crude product is purified by silica gel chromatography (Combiflash; column: Redisep RF, 40g) using a cHex/EA gradient as eluent (100:0 --> 0:100). The product containing fractions are evaporated to give 5-[4-(hydroxymethyl)-3-methoxyphenyl]-1,3-dimethyl-1,2-dihydropyridin-2-one (**36**) (0.97 g; 3.74 mmol; 77 %). ^{1}H NMR (500 MHz, DMSO-d6) δ 8.00 (d, J = 2.5 Hz, 1H), 7.77 (d, J = 2.6 Hz, 1H), 7.38 (d, J = 7.8 Hz, 1H), 7.14 (dd, J = 7.9, 1.7 Hz, 1H), 7.10 (d, J = 1.7 Hz, 1H), 4.98 (t, J = 5.5 Hz, 1H), 4.50 (d, J = 5.5 Hz, 2H), 3.86 (s, 3H), 3.53 (s, 3H), 2.10 (s, 3H); LC/MS (BAS1): $[M+H]^+$ = 260; t_R = 0.95.

5-{4-[(dimethylamino)methyl]-3-methoxyphenyl}-1,3-dimethyl-1,2-dihydropyridin-2-one (4)

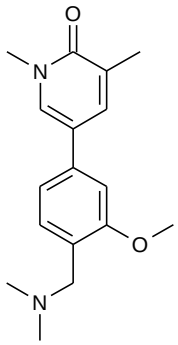

36 (100 mg; 386 µmol) is dissolved in DCM (1.0 mL). DIPEA (149 mg; 1.16 mmol) and methansulfonyl chloride (66.2 mg; 578 µmol) is added drop wise and the mixture is stirred at rt for 16 h. Dimethylamine hydrochloride (94.6 mg; 1.16 mmol) is added and stirring is continued for 8 h. The reaction mixture is concentrated under reduced pressure, dissolved in DMSO (1.0 mL) and purified by preparative RP-HPLC (column: X-Bridge C-18 30x50 mm) using a MeCN/water gradient under basic conditions. The product containing fractions are freeze dried. Further purification is achieved by preparative RP-HPLC (column: Sunfire C-18 30x50 mm) using a MeCN/water gradient under acidic conditions. The product containing fractions are freeze dried to give pure 5-{4-[(dimethylamino)methyl]-3-methoxyphenyl}-1,3-dimethyl-1,2-dihydropyridin-2-one (**4**) (18.1 mg; 63.2 µmol; 16 %). ^{1}H NMR (500 MHz, DMSO-d6) δ 9.32 (s, 1H, ammonium ion), 8.12 (d, J = 2.7 Hz, 1H), 7.86 – 7.81 (m, 1H), 7.44 (d, J = 7.8 Hz, 1H), 7.29 (d, J = 1.8 Hz, 1H), 7.25 (dd, J = 7.9, 1.7 Hz, 1H), 4.25 (s, 2H), 3.95 (s, 3H), 3.54 (s, 3H), 2.74 (s, 6H), 2.10 (s, 3H); ^{13}C NMR (125 MHz, DMSO, 1 C missing) δ 162.2, 158.8, 140.2, 136.2, 135.6, 133.5, 128.2, 117.7, 116.8, 108.6, 56.4, 55.3, 42.7 (2C), 37.8, 17.5; HRMS (CI+): calculated for $C_{17}H_{23}N_2O_2$ (MH+) 287.17540, found 287.17523, Δ -0.60 ppm; LC/MS (BAS1): $[M+H]^+$ = 287; t_R = 0.91.

Synthesis of compound 5

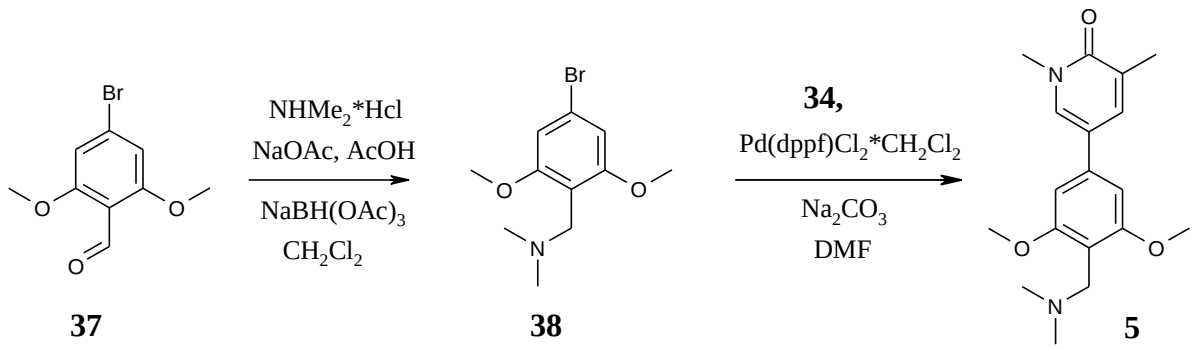

37 **38** **5**

Supplementary Scheme 4: Synthesis of compound (**5**)

[(4-Bromo-2,6-dimethoxyphenyl)methyl]dimethylamine (38)

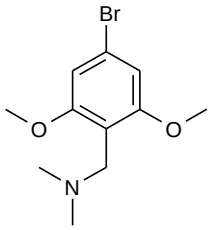

A mixture of NaOAc (17.7 g; 216 mmol), AcOH (8.65 g; 144 mmol) and dimethylamine hydrochloride (17.6 g; 216 mmol) in DCM (600 mL) is stirred for 10 min at rt. 4-Bromo-2,6-dimethoxybenzaldehyde (**37**) (35.3 g; 144 mmol, commercial from Activate) is added and stirring is continued. After 30 min sodium triacetoxyborohydride (63.1 g; 298 mmol) is added in one portion and the reaction mixture is stirred at rt for 16 h. Saturated $NaHCO_3$ solution is added and the layers are separated. The aqueous layer is extracted three times with DCM. The combined organic layer is dried over $MgSO_4$, filtered and evaporated to give pure [(4-bromo-2,6-dimethoxyphenyl)methyl]dimethylamine (**38**) (27.3 g; 99.6 mmol; 69 %). ^{1}H-NMR (400 MHz, $CDCl_3$): δ 6.70 (s, 2H), 3.81 (s, 6H), 3.48 (s, 2H), 2.26 (s, 6H); LC/MS (BAS1): $[M+H]^+$ = 274/276; t_R = 1.11 min.

5-{4-[(dimethylamino)methyl]-3,5-dimethoxyphenyl}-1,3-dimethyl-1,2-dihydropyridin-2-one (5)

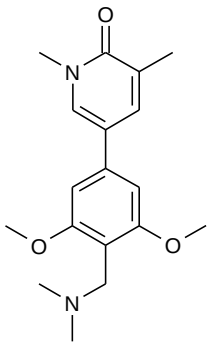

38 (110 mg; 401 µmol), 1,3-dimethyl-5-(tetramethyl-1,3,2-dioxaborolan-2-yl)-1,2-dihydropyridin-2-one (**34**) (100 mg; 401 µmol) and Pd(dppf)Cl_2·DCM (32.7 mg; 40.1 µmol) are suspended in DMF (800 µL) under argon. A degassed solution of sodium carbonate (2N, 500 µL; 1.00 mmol) is added and the resulting mixture is heated at 100 °C for 1 h. After cooling to rt, water is added and the mixture is purified by preparative RP-HPLC (column: X-Bridge C-18 30x50 mm) using a MeCN/water gradient under basic conditions. The product containing fractions are freeze dried to give 5-{4-[(dimethylamino)methyl]-3,5-dimethoxyphenyl}-1,3-dimethyl-1,2-dihydropyridin-2-one (**5**) (48.3 mg; 153 µmol; 38 %). ^{1}H NMR (500 MHz, DMSO-d6) δ 8.04 (d, J = 2.8 Hz, 1H), 7.81 (dd, J = 2.6, 1.3 Hz, 1H), 6.79 (s, 2H), 3.83 (s, 6H), 3.54 (s, 3H), 3.39 (s, 2H), 2.10 (s, 3H), 2.09 (s, 6H); ^{13}C NMR (125 MHz, DMSO) δ 162.2, 159.6 (2C), 137.4, 136.5, 135.1, 127.9, 118.0, 112.9, 101.6 (2C), 56.3 (2C), 49.9, 45.4 (2C), 37.7, 17.5; HRMS (CI+): calculated for $C_{18}H_{25}N_2O_3$ (MH+) 317.18597, found 317.18558, Δ -1.26 ppm; LC/MS (BAS1): $[M+H]^+$ = 317; t_R = 0.88 min.

Synthesis of compound 6

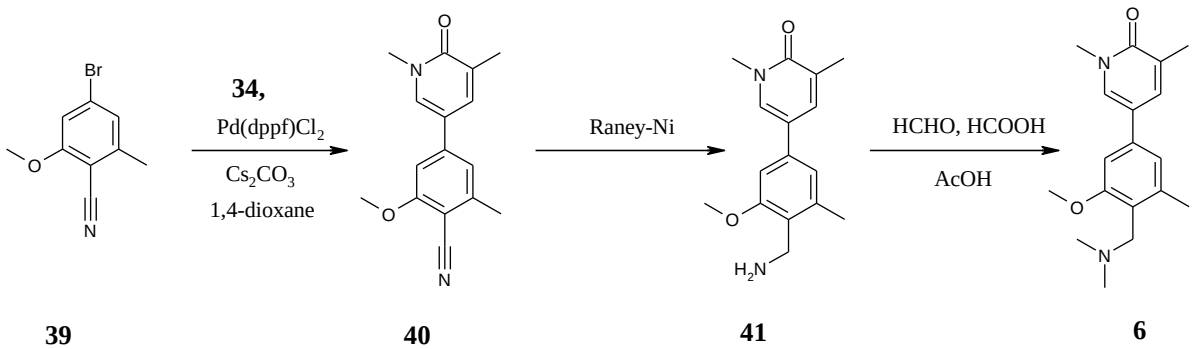

Supplementary Scheme 5: Synthesis of compound (**6**)

5-{4-[(dimethylamino)methyl]-3-methoxy-5-methylphenyl}-1,3-dimethyl-1,2-dihydro-pyridin-2-one (6)

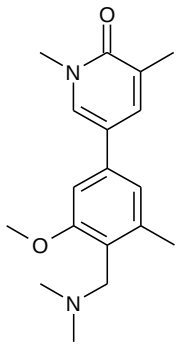

To a solution of 4-bromo-2-methoxy-6-methyl-benzonitrile (**39**) (1.00 g; 4.42 mmol; commercial from ArkPharm) and 1,3-dimethyl-5-(tetramethyl-1,3,2-dioxaborolan-2-yl)-1,2-dihydropyridin-2-one (**34**) (1.10 g; 4.42 mmol) in 1,4-dioxane (50 mL) and water (2 mL) is added cesium carbonate (4.50 g; 13.9 mmol) and Pd(dppf)Cl_2 (200 mg; 0.27 mmol). The reaction mixture is stirred at 90 °C for 2 h. The reaction mixture is then filtered through celite. The filtrate is concentrated, dissolved in EA and washed with brine. The combined organic layer is dried over Na_2SO_4, filtered and concentrated under reduced pressure. The residue is purified by preparative RP-HPLC using a MeCN/water gradient as eluent to give 4-(1,5-dimethyl-6-oxo-1,6-dihydro-pyridin-3-yl)-2-methoxy-6-methylbenzonitrile (**40**) (480 mg; 1.79 mmol; 40 %) which is directly used for the next step. LC/MS(INT1): (M+H)+ =269; t_R = 1.16 min. To a solution of **40** (200 mg; 745 µmol) in MeOH (15 mL) is added aqueous ammonia (500 µL) and Raney-Ni (200 mg). The mixture is degassed and refilled with H_2 twice and stirred at rt under 50 Psi for 16 h. The reaction mixture is filtered and the residue is washed with THF/MeOH. The filtrated is then concentrated to give 5-{4-[(dimethylamino)methyl]-3-methoxy-5-methylphenyl}-1,3-dimethyl-1,2-dihydropyridin-2-one (**41**) (150 mg; 550 µmol; 74 %), which is directly used in the next step. LC/MS(INT2): (M+H)+ =273; t_R = 0.8 min. A mixture of **41** (50.0 mg; 184 µmol), aqueous formaldehyde (50 µL), formic acid (50 µL) and acetic acid (1.0 mL) is heated at reflux for 16 h. After cooling to rt, the reaction mixture is concentrated under reduced pressure and the residue is dissolved in MeOH and purified by preparative RP-HPLC using a McCN/water gradient as eluent. The product containing fractions are freeze dried to give 5-{4-[(dimethylamino)methyl]-3-methoxy-5-methylphenyl}-1,3-dimethyl-1,2-dihydropyridin-2-one (**6**) (28.0 mg; 93.2 µmol; 51 %). ^{1}H NMR (500 MHz, DMSO-d6) δ 9.38 (s, 1H, prot. amine), 8.11 (s, 1H), 7.82 (s, 1H), 7.14 (s, 1H), 7.12 (s, 1H), 4.26 (d, J = 5.6 Hz, 2H), 3.93 (s, 3H), 3.54 (s, 3H), 2.72 – 2.78 (m, 6H), 2.44 (s, 3H), 2.10 (s, 3H); ^{13}C NMR (125 MHz, DMSO) δ 162.2, 159.2, 140.8, 139.2, 136.2, 135.5, 128.1, 120.1, 116.9, 115.9, 106.0, 56.5, 52.5, 42.9 (2C), 37.8, 20.0, 17.5; HRMS

(CI+): calculated for $C_{18}H_{25}N_2O_2$ (MH+) 301.19105, found 301.19069, Δ -1.21 ppm; LC/MS (BAS1): [M+H]+ = 301; t_R = 1.02 min.

Synthesis of compound 7

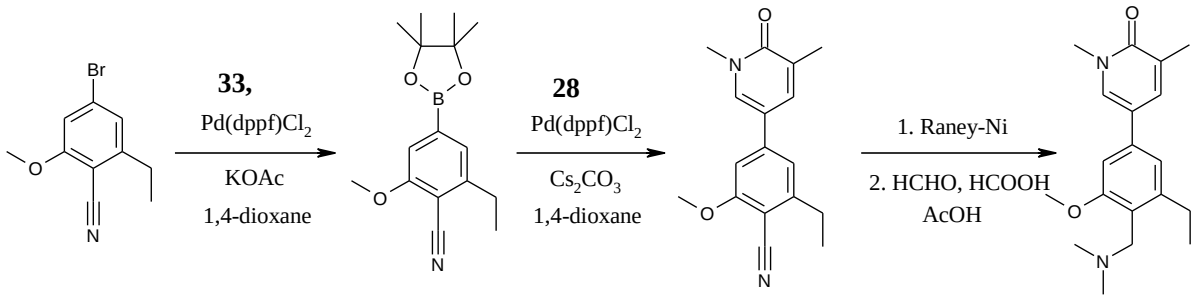

42 **43** **44** **7**

Supplementary Scheme 6: Synthesis of compound (**7**)

5-{4-[(dimethylamino)methyl]-3-ethyl-5-methoxyphenyl}-1,3-dimethyl-1,2-dihydro-pyridin-2-one (7)

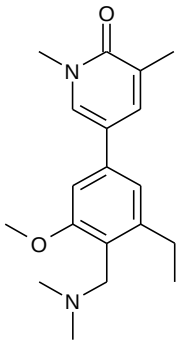

To a solution of 4-bromo-2-ethyl-6-methoxybenzonitrile (**42**) (480 mg; 2.00 mmol; commercial from FCHGroup) and bis(pinacolato)diboron (**33**) (558 mg; 2.20 mmol) in 1,4-dioxane (9.0 mL) is added Pd(dppf)Cl_2 (146 mg; 0.20 mmol) and potassium acetate (588 mg; 6.00 mmol) and the mixture is refluxed for 24 h. After cooling to rt, EA and water is added, the layers are separated and the aqueous layer is extracted three times with EA. The combined organic layer is dried over Na_2SO_4, filtered and evaporated. The crude material is purified by silica gel chromatography to give 2-ethyl-6-methoxy-4-(tetramethyl-1,3,2-dioxaborolan-2-yl)benzonitrile (**43**) (570 mg; 1.98 mmol; 99 %) which is directly used for the next step. LC/MS(INT2): (M+H)+ =288; t_R = 1.86 min. To a solution of **43** (570 mg; 1.99 mmol) and 5-bromo-1,3-dimethyl-1,2-dihydropyridin-2-one (**28**) (440 mg; 2.18 mmol) in 1,4-dioxane (20 mL) and water (1.0 mL) is added Cs_2CO_3 (2.00 g; 6.15 mmol) and Pd(dppf)Cl_2 (100 mg; 137

µmol). The mixture is heated to 90 °C for 2 h. The reaction is filtered over a pad of celite and the filtrate is concentrated. The residue is dissolved in EA, washed with brine. The combined organic layer is dried over Na_2SO_4, filtered and concentrated under reduced pressure. The crude material is purified by preparative RP-HPLC to give 4-(1,5-dimethyl-6-oxo-1,6-dihydropyridin-3-yl)-2-ethyl-6-methoxybenzonitrile (**44**) (350 mg; 1.24 mmol; 62 %), which is directly used for the next step. LC-MS(INT2): $(M+H)^+$ = 283; t_R = 1.36 min. To a solution of **44** (350 mg; 1.24 mmol) in MeOH (20.0 mL) is added aq. NH_3 (1.0 mL) and Raney nickel (300 mg). The mixture is degassed and refilled with H_2 twice and stirred under 50 Psi at rt for 16 h. The reaction mixture is filter, washed with THF/MeOH and concentrated to give 5-[4-(aminomethyl)-3-ethyl-5-methoxyphenyl]-1,3-dimethyl-1,2-dihydropyridin-2-one, which is without further purification dissolved in AcOH (2.0 mL). Aqueous formaldehyde (100 µl) and formic acid (100 µL) is added and the mixture is heated to reflux for 24 h. After cooling to rt the reaction mixture is evaporated, taken-up in MeOH and purified by preparative RP-HPLC to give 5-{4-[(dimethylamino)methyl]-3-ethyl-5-methoxyphenyl}-1,3-dimethyl-1,2-dihydropyridin-2-one (**7**) (32.8 mg; 104 µmol; 8.4 % for last two steps). ^{1}H NMR (500 MHz, DMSO-d6) δ 9.15 (s, 1H; prot. amine), 8.12 (s, 1H), 7.83 (s, 1H), 7.15 (s, 1H), 7.12 (s, 1H), 4.28 (d, J = 5.8 Hz, 2H), 3.93 (s, 3H), 3.54 (s, 3H), 2.73 – 2.79 (m, 8H), 2.10 (s, 3H), 1.18 (t, J = 7.4 Hz, 3H); ^{13}C NMR (125 MHz, DMSO) δ 162.2, 159.1, 146.6, 139.5, 136.2, 135.5, 128.1, 118.4, 117.0, 115.1, 106.0, 56.5, 52.1, 42.9 (2C), 37.7, 25.8, 17.5, 16.3; HRMS (CI+): calculated for $C_{19}H_{27}N_2O_2$ (MH+) 315.20670, found 315.20627, Δ -0.43 ppm; LC/MS (BAS1): [M+H]+ = 315; t_R = 1.09 min.

Synthesis of compound 8

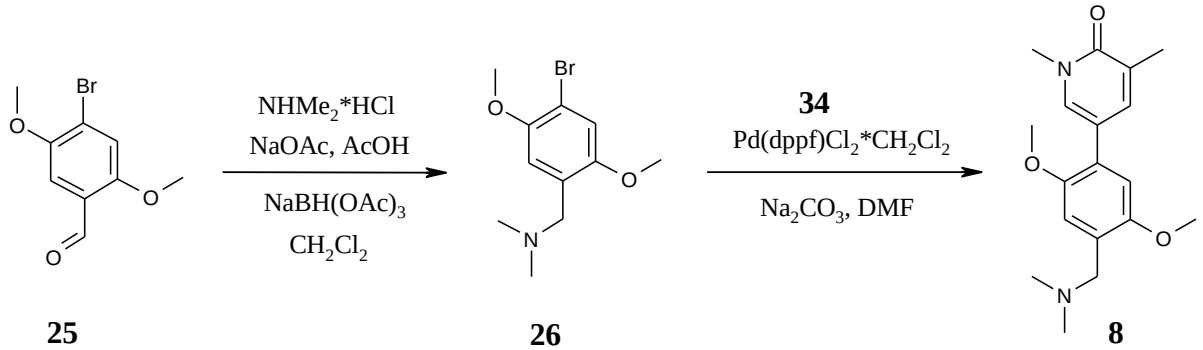

25 **26** **8**

Supplementary Scheme 7: Synthesis of compound (**8**)

5-{4-[(dimethylamino)methyl]-2,5-dimethoxyphenyl}-1,3-dimethyl-1,2-dihydropyridin-2-one (8)

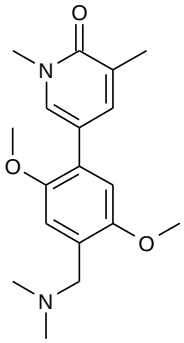

26 (120 mg; 438 µmol), 1,3-dimethyl-5-(tetramethyl-1,3,2-dioxaborolan-2-yl)-1,2-dihydropyridin-2-one (**34**) (120 mg; 482 µmol), and Pd(dppf)Cl_2·DCM (36.9 mg; 45.2 µmol) are suspended in DMF (1.0 mL) under argon. A degassed solution of sodium carbonate (2N, 438 µL; 876 µmol) is added and the resulting mixture is heated at 80 °C for 1 h. After cooling to rt water is added and the mixture is purified by preparative RP-HPLC (column: X-Bridge C-18 30x50 mm) using a MeCN/water gradient under basic conditions. The product containing fractions are freeze dried to give 5-{4-[(dimethylamino)methyl]-2,5-dimethoxyphenyl}-1,3-dimethyl-1,2-dihydropyridin-2-one (**8**) (48.0 mg; 152 µmol; 35 %). ^{1}H NMR (500 MHz, DMSO-d6) δ 7.73 (s, 1H), 7.53 (s, 1H), 7.02 (s, 1H), 6.88 (s, 1H), 3.77 (s, 3H), 3.72 (s, 3H), 3.49 (s, 3H), 3.39 (s, 2H), 2.18 (s, 6H), 2.05 (s, 3H); ^{13}C NMR (125 MHz, DMSO) δ 161.9, 151.8, 150.4, 139.1, 136.6, 127.0, 126.8, 124.9, 115.7, 114.2, 113.1, 57.0, 56.6, 56.5, 45.7 (2C), 37.6, 17.5; HRMS (CI+): calculated for $C_{18}H_{25}N_2O_3$ (MH+) 317.18597, found 317.18577, Δ -0.62 ppm; LC/MS (BAS1): [M+H]+ = 317; t_R = 0.98 min.

Synthesis of compound 9

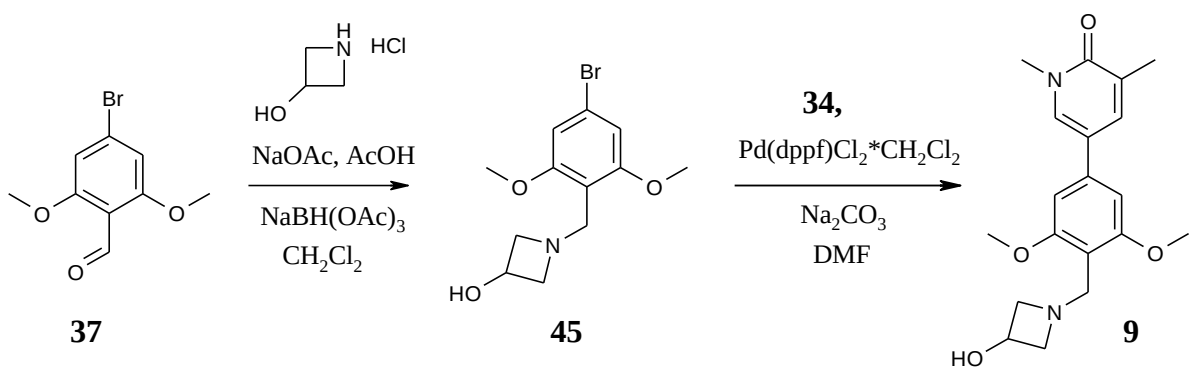

Supplementary Scheme 8: Synthesis of compound (**9**)

1-[(4-bromo-2,6-dimethoxyphenyl)methyl]azetidin-3-ol (45)

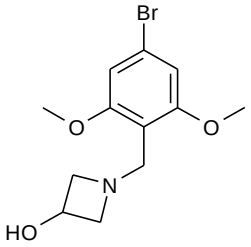

A mixture of NaOAc (95.4 mg; 1.16 mmol), AcOH (46.6 mg; 776 µmol) and azetidin-3-ol (134 mg; 1.22 mmol) in DCM (2.0 mL) is stirred for 10 min at 0 °C. 4-Bromo-2,6-dimethoxybenzaldehyde (**37**) (200 mg; 816 µmol) is added and stirring is continued. After 30 min sodium triacetoxyborohydride (339 mg; 1.60 mmol) is added in one portion and the reaction mixture is stirred at rt for 16 h. Saturated $NaHCO_3$ solution is added and the layers are separated. The aqueous layer is extracted three times with DCM. The combined organic layer is dried over $MgSO_4$, filtered and evaporated to give 1-[(4-bromo-2,6-dimethoxyphenyl)methyl]azetidin-3-ol (**45**) (220 mg; 99.6 mmol; 89 %).

5-{4-[(3-hydroxyazetidin-1-yl)methyl]-3,5-dimethoxyphenyl}-1,3-dimethyl-1,2-dihydropyridin-2-one (9)

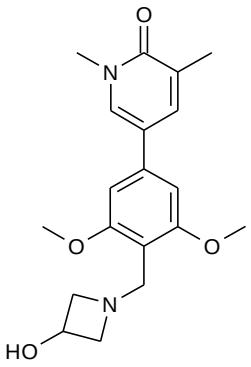

45 (80.0 mg; 264 µmol), 1,3-dimethyl-5-(tetramethyl-1,3,2-dioxaborolan-2-yl)-1,2-dihydropyridin-2-one (**34**) (100 mg; 401 µmol) and Pd(dppf)Cl_2·DCM (21.6 mg; 26.4 µmol) are suspended in DMF (800 µL) under argon. A degassed solution of sodium carbonate (2N; 331 µL; 662 µmol) is added and the resulting mixture is heated to 100 °C for 1 h. After cooling to rt water is added and the mixture is purified by preparative RP-HPLC (column: X-Bridge C-18 30x50 mm) using a MeCN/water gradient under basic conditions. The product containing fractions are freeze dried to give 5-{4-[(3-hydroxyazetidin-1-yl)methyl]-3,5-

dimethoxyphenyl}-1,3-dimethyl-1,2-dihydropyridin-2-one (**9**) (22.7 mg; 65.9 µmol; 25 %). ^{1}H NMR (500 MHz, DMSO-d6) δ 8.04 (d, J = 2.7 Hz, 1H), 7.81 (s, 1H), 6.79 (s, 2H), 5.12 (d, J = 6.4 Hz, 1H), 3.98 – 4.06 (m, 1H), 3.83 (s, 6H), 3.51 – 3.55 (m, 5H), 3.31 (s, 3H), 2.79 (ddd, J = 6.2, 6.2, 2.2 Hz, 2H), 2.10 (s, 3H); ^{13}C NMR (125 MHz, DMSO) δ 162.2, 159.4 (2C), 137.4, 136.5, 135.1, 127.9, 118.0, 112.3, 101.6 (2C), 63.4 (2C), 61.1, 56.2 (2C), 48.2, 37.7, 17.5; HRMS (CI+): calculated for $C_{19}H_{25}N_2O_4$ (MH+) 345.18088, found 345.18048, Δ -1.17 ppm; LC/MS (BAS1): $[M+H]^+$ = 345; t_R = 0.81 min.

Synthesis of compound 10

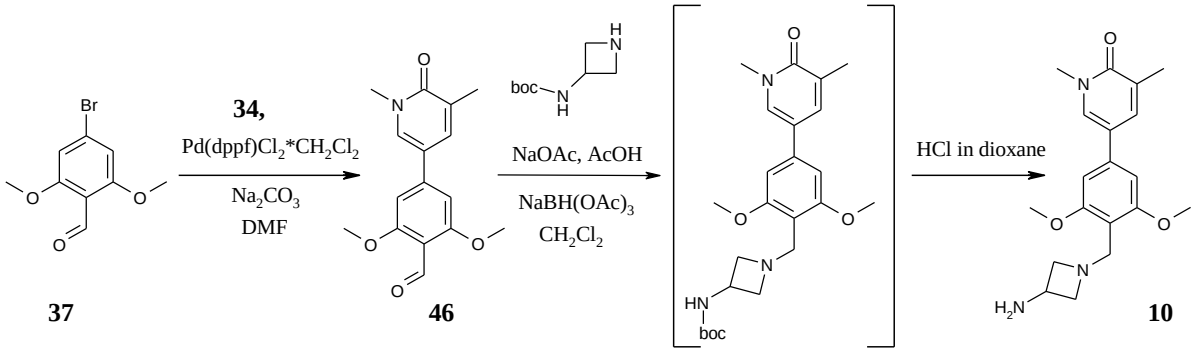

37 **46** **10**

Supplementary Scheme 9: Synthesis of compound (**10**)

4-(1,5-dimethyl-6-oxo-1,6-dihydropyridin-3-yl)-2,6-dimethoxybenzaldehyde (46)

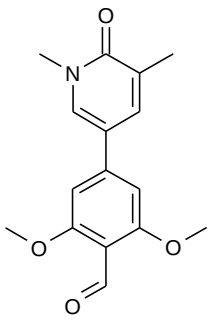

4-bromo-2,6-dimethoxybenzaldehyde (**37**) (518 mg; 2.11 mmol), 1,3-dimethyl-5-(tetramethyl-1,3,2-dioxaborolan-2-yl)-1,2-dihydropyridin-2-one (**34**) (500 mg; 2.01 mmol) and Pd(dppf)Cl_2·DCM (169 mg; 207 µmol) are suspended in DMF (4.0 mL) under argon. A degassed solution of sodium carbonate (2N, 2.51 mL; 5.02 mmol) is added and the resulting mixture is heated at 100 °C for 1 h. After cooling to rt, water is added and the mixture is filtered and purified by by preparative RP-HPLC (column: X-Bridge C-18 30x50 mm) using a

MeCN/water gradient under basic conditions. The product containing fractions are freeze dried to give 4-(1,5-dimethyl-6-oxo-1,6-dihydropyridin-3-yl)-2,6-dimethoxy-benzaldehyde (**46**) (460 mg; 1.60 mmol; 80 %). ^{1}H NMR (400 MHz, DMSO-d6) δ 10.33 (s, 1H), 8.25 (d, J = 2.5 Hz, 1H), 7.95 – 7.90 (m, 1H), 6.91 (s, 2H), 3.92 (s, 6H), 3.56 (s, 3H), 2.11 (s, 3H). LC/MS (BAS1): $[M+H]^+$ = 288; t_R = 0.84 min.

5-{4-[(3-aminoazetidin-1-yl)methyl]-3,5-dimethoxyphenyl}-1,3-dimethyl-1,2-dihydropyridin-2-one (10)

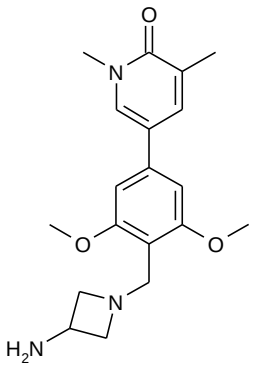

A mixture of NaOAc (40.7 mg; 496 µmol), AcOH (19.9 mg; 331 µmol) and tert-butyl N-(azetidin-3-yl)carbamate (85.4 mg; 496 µmol; commercial from Chontech) in DCM (2.0 mL) is stirred for 10 min at 0 °C. **46** (100 mg; 348 µmol) is added and stirring is continued. After 30 min sodium triacetoxyborohydride (144 mg; 697 µmol) is added in one portion and the reaction mixture is stirred at rt for 16 h. Saturated $NaHCO_3$ solution is added and the layers are separated. The aqueous layer is extracted three times with DCM. The combined organic layer is dried over Na_2SO_4, filtered and evaporated. The crude material is purified by silica gel chromatography (Combiflash; column: Redisep RF, 12g) using a DCM/MeOH gradient as eluent (100:0 --> 90:10). The product containing fractions are evaporated to give tert-butyl N-(1-{[4-(1,5-dimethyl-6-oxo-1,6-dihydropyridin-3-yl)-2,6-dimethoxyphenyl]-methyl}azetidin-3-yl)carbamate (90.0 mg; 203 µmol; 58 %), which is directly dissolved in DCM (10 mL). HCl in 1,4-dioxane (4N solution; 507 µl; 2.03 mmol) is added and the reaction mixture is stirred at rt for 16 h. All volatiles are removed *in vacuo* and the residue is re-dissolved in MeOH. The free base of 5-{4-[(3-aminoazetidin-1-yl)methyl]-3,5-dimethoxyphenyl}-1,3-dimethyl-1,2-dihydropyridin-2-one (**10**) (60.0 mg; 175 µmol; 86 %) is generated using a SPX-cartridge. ^{1}H NMR (400 MHz, DMSO-d6, 1H under DMSO signal) δ 8.07 (d, J = 2.8 Hz, 1H), 7.83 (d, J = 2.6 Hz, 1H), 6.81 (s, 2H), 3.85 (s, 6H), 3.62 (s, 2H), 3.54 (s, 3H), 3.42 – 3.47 (m, 2H), 2.95 (t, J = 6.0 Hz, 2H), 2.10 (s, 3H). HRMS (CI+): calculated for $C_{19}H_{26}N_3O_3$ (MH+) 344.19687, found 344.19660, Δ -0.77 ppm; LC/MS (BAS1): $[M+H]^+$ = 344; t_R = 0.94 min.

Synthesis of compound 11 (BI-7189)[1]

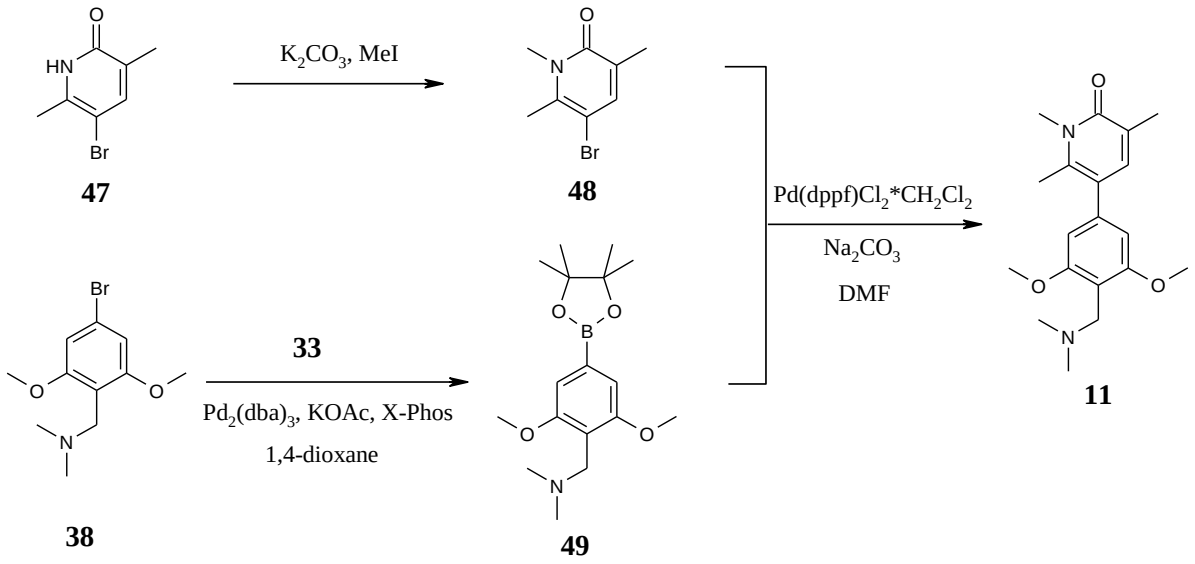

Supplementary Scheme 10: Synthesis of compound (**11**, **BI-7189**)

5-bromo-1,3,6-trimethyl-1,2-dihydropyridin-2-one (48)

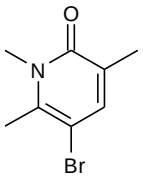

To a suspension of 5-bromo-3,6-dimethyl-1,2-dihydropyridin-2-one (**47**) (2.54 g; 12.6 mmol) and potassium carbonate (4.13 g; 29.9 mmol) in THF (25 mL), iodomethane (811 µL; 13.1 mmol) is added and the resulting mixture is stirred at 80 °C for 16 h. Ammonia (10% aqueous solution; 30 mL) is added followed by water (50 mL). THF is removed under reduced pressure and the aqueous residue is extracted three times with DCM. The combined organic layer is dried over Na_2SO_4 and concentrated *in vacuo* to give crude 5-bromo-1,3,6-trimethyl-1,2-dihydropyridin-2-one (**48**) (2.58 g; 11.9 mmol; 95 %) which is used without further purification. For analytical purposes a small amount was purified by silica gel chromatography. ^{1}H NMR (400 MHz, DMSO-d6) δ 7.47 (s, 1H), 3.51 (s, 3H), 2.47 (s, 3H), 1.98 (s, 3H); LC/MS (BAS1): $[M+H]^+$ = 216/218; t_R = 0.84.

{[2,6-Dimethoxy-4-(tetramethyl-1,3,2-dioxaborolan-2-yl)phenyl]methyl}dimethylamine (49)

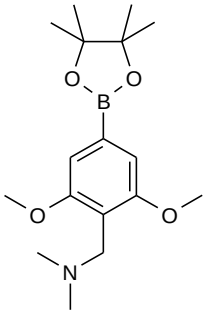

[(4-bromo-2,6-dimethoxyphenyl)methyl]dimethylamine (**38**) (15.7 g; 57.3 mmol) and bis(pinacolato)diboron (**33**) (43.6 g; 1.86 mol) are dissolved/suspended in 1,4-dioxane (300 mL) under N_2. Potassium acetate (17.0 g; 58.8 mmol), Pd_2dba_3 (1.00 g; 1.09 mmol) and 2-dicyclohexyl-phosphino-2′,4′,6′-triisopropylbiphenyl (1.00 g; 2.10 mmol) is added and the mixture is stirred at 90° C for 8 h. After cooling to rt the mixture is concentrated and the residue is taken-up in DCM. Water is added, the layers are separated and the aqueous phase is extracted two times with DCM. The combined organic layer is dried over Na_2SO_4, filtered and evaporated. The crude product is purified by preparative RP-HPLC using a MeCN/water (0.2 % TFA added to the water) gradient as eluent to give the TFA salt of {[2,6-dimethoxy-4-(tetramethyl-1,3,2-dioxaborolan-2-yl)phenyl]methyl}-dimethylamine (**49**) which is transferred into the corresponding hydrochloride by dissolving and stirring in HCl/MeOH for 30 min (5.45 g; 17.0 mmol; 30 %). ^{1}H-NMR (500 MHz, DMSO-d6) δ 9.44 (s, 1H), 6.95 (s, 2H), 4.21 (d, J = 5.3 Hz, 2H), 3.87 (s, 6H), 2.70 (d, J = 5.0 Hz, 6H), 1.32 (s, 12H); LC/MS (BAS1): $[M+H]^+$ = 240 (ester cleaved under basic conditions); t_R = 0.20 min.

5-{4-[(dimethylamino)methyl]-3,5-dimethoxyphenyl}-1,3,6-trimethyl-1,2-dihydro-pyridin-2-one (11)

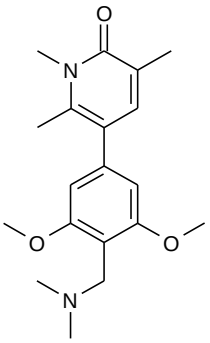

48 (100 mg; 462 µmol), **49** (216 mg; 672 µmol) and Pd(dppf)Cl_2·DCM (38.8 mg; 47.5 µmol) are suspended in DMF (2.0 mL) under argon. A degassed Na_2CO_3-solution (2N; 576 µL; 1.15 mmol) is subsequently added and the resulting mixture is heated to 100 °C for 1 h. After

cooling to rt water is added (several drops) and the mixture is filtered and purified by preparative RP-HPLC (column: X-Bridge C-18 30x50 mm) using a MeCN/water gradient under basic conditions. The product containing fractions are freeze dried. Further purification is achieved by automated silica gel chromatography (Combiflash; column: Redisep RF, 12g) using a DCM/MeOH gradient as eluent (100:0 --> 90:10; MeOH made basic with 0.1% NH_3). The product containing fractions are evaporated, dissolved in MeCN/water and freeze dried to give 5-{4-[(dimethylamino)methyl]-3,5-dimethoxyphenyl}-1,3,6-trimethyl-1,2-dihydro-pyridin-2-one **(11)** (46.0 mg; 139 µmol; 30 %). ^{1}H NMR (500 MHz, DMSO-d6) δ 7.29 (s, 1H), 6.53 (s, 2H), 3.77 (s, 6H), 3.53 (s, 3H), 3.47 (s, 2H), 2.32 (s, 3H), 2.16 (s, 6H), 2.04 (s, 3H); ^{13}C NMR (125 MHz, DMSO, 1 C missing) δ 162.7, 159.0 (2C), 141.9, 140.5, 138.7, 124.2, 118.9, 105.9 (2C), 56.2 (2C), 50.0, 45.3 (2C), 31.9, 18.5, 17.4; HRMS (CI+): calculated for $C_{19}H_{27}N_2O_3$ (MH+) 331.20162, found 331.20123, Δ -1.17 ppm; LC/MS (BAS1): $[M+H]^+$ = 331; t_R = 0.92.

Synthesis of compound 12

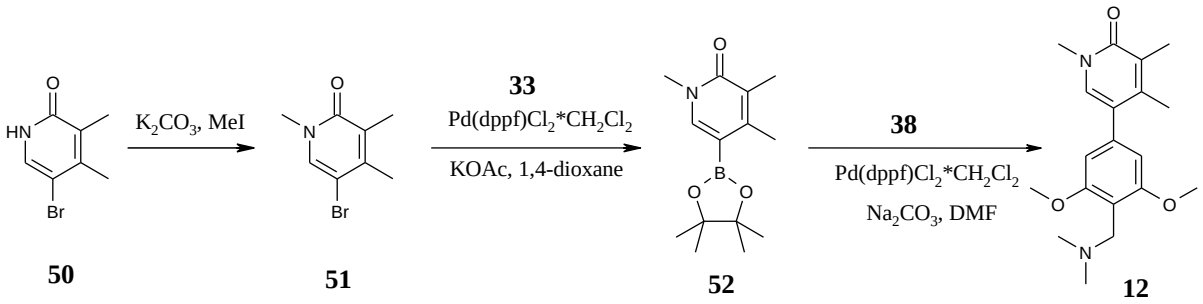

Supplementary Scheme 11: Synthesis of compound (**12**)

5-bromo-1,3,4-trimethyl-1,2-dihydropyridin-2-one (51)

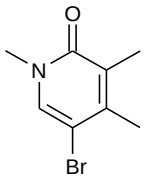

To a suspension of 5-bromo-3,4-dimethyl-1,2-dihydropyridin-2-one **(50)** (2.50 g; 12.4 mmol) and potassium carbonate (4.28 g; 31.0 mmol) in THF (25 mL), iodomethane (840 µL; 13.6 mmol) is added and the resulting mixture is stirred at rt for 16 h. The reaction mixture is evaporated and the crude material is purified by silica gel chromatography (Combiflash;

column: Redisep RF, 40g) using a cHex/EA gradient as eluent (100:0 --> 50:50). Product containing fractions are evaporated to give 5-bromo-1,3,4-trimethyl-1,2-dihydropyridin-2-one (**51**) (2.30 g; 10.6 mmol; 86 %).

1,3,4-trimethyl-5-(tetramethyl-1,3,2-dioxaborolan-2-yl)-1,2-dihydropyridin-2-one (52)

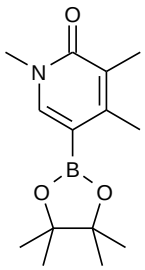

51 (1.00 g; 4.63 mmol), bis(pinacolato)diboron (**33**) (1.76 g; 6.94 mmol), Pd(dppf)Cl_2·DCM (378 mg; 46.3 µmol) and potassium acetate (908 mg; 9.26 mmol) are suspended in 1,4-dioxane (5.0 mL) under argon and the resulting mixture is heated to 80 °C for 16 h. After cooling to rt, the reaction mixture is concentrated under reduced pressure, the residue is taken-up in DCM/MeOH and purified by silica gel chromatography (Combiflash; column: Redisep RF, 40 g) using a chex/EA gradient as eluent (80:20 --> 20:80). The product containing fractions are evaporated to give 1,3,4-trimethyl-5-(tetramethyl-1,3,2-dioxaborolan-2-yl)-1,2-dihydropyridin-2-one (**52**) (1.20 g; 4.56 mmol; 98 %).

5-{4-[(dimethylamino)methyl]-3,5-dimethoxyphenyl}-1,3,4-trimethyl-1,2-dihydro-pyridin-2-one (12)

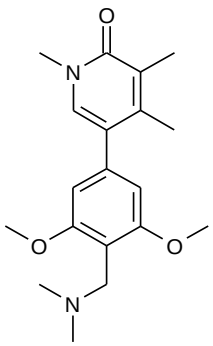

52 (100 mg; 380 µmol), [(4-bromo-2,6-dimethoxyphenyl)methyl]dimethylamine (**38**) (104 mg; 379 µmol) and Pd(dppf)Cl_2·DCM (31.0 mg; 38.0 µmol) are suspended in DMF (800 µL) under argon. A degassed Na_2CO_3-solution (2N; 475 µL; 950 µmol) is subsequently added and the resulting mixture is heated at 100 °C for 1 h. After cooling to rt water is added (several drops) and the mixture is filtered and purified by preparative RP-HPLC (column: X-Bridge C-

18 30x50 mm) using a MeCN/water gradient under basic conditions. The product containing fractions are freeze dried to give 5-{4-[(dimethylamino)methyl]-3,5-dimethoxy-phenyl}-1,3,4-trimethyl-1,2-dihydropyridin-2-one (**12**) (22.8 mg; 69.0 µmol; 18 %). ^{1}H NMR (500 MHz, DMSO-d6) δ 7.52 (s, 1H), 6.53 (d, J = 1.4 Hz, 2H), 3.77 (d, J = 1.4 Hz, 6H), 3.46 (d, J = 1.4 Hz, 3H), 3.41 (s, 2H), 2.12 – 2.04 (m, 12H); ^{13}C NMR (125 MHz, DMSO) δ 161.6, 158.9 (2C), 144.7, 138.4, 135.0, 124.9, 121.6, 113.2, 106.0 (2C), 56.2 (2C), 50.0, 45.5 (2C), 37.3, 18.0, 13.5. HRMS (CI+): calculated for $C_{19}H_{27}N_2O_3$ (MH+) 331.20162, found 331.20101, Δ -1.83 ppm; LC/MS (BAS1): $[M+H]^+$ = 331; t_R = 1.02.

Synthesis of compound 13 (BI-7271)[1]

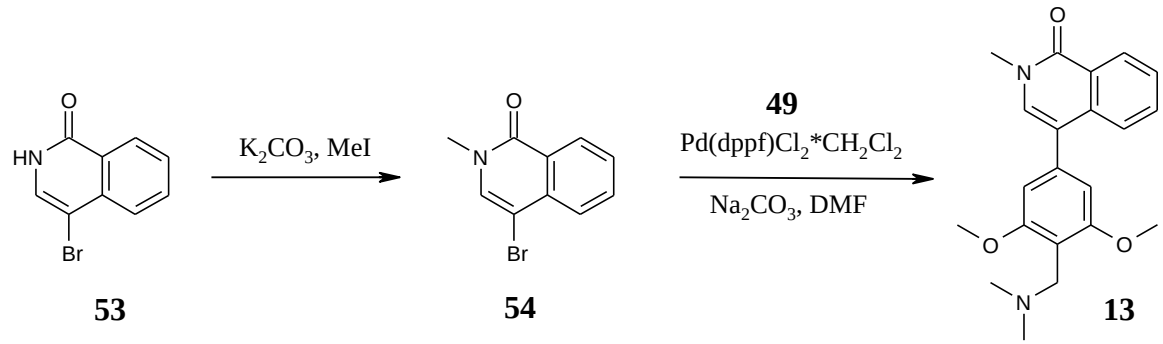

53 **54** **13**

Supplementary Scheme 12: Synthesis of compound (**13, BI-7271**)

4-bromo-2-methyl-1,2-dihydroisoquinolin-1-one (54)

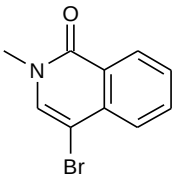

To a suspension of 4-bromo-1,2-dihydroisoquinolin-1-one (**53**) (1.00 g; 4.46 mmol) and potassium carbonate (1.17 g; 8.48 mmol) in THF (10 mL), iodomethane (323 µL; 5.09 mmol) is added and the resulting mixture is stirred at rt for 16 h. Since HPLC-MS of the reaction mixture indicates incomplete conversion, additional iodomethane (100 µl; 1.57 mmol) is added and stirring is continued for 5h. Ammonia (10% aqueous solution; 30 mL) is added followed by water (50 mL). THF is removed under reduced pressure whereupon a precipitation occurs. The solid is collected by filtration, washed with cold water and dried *in vacuo* to give 4-bromo-2-methyl-1,2-dihydroisoquinolin-1-one (**54**) (1.00 g; 4.20 mmol; 94 %) as a yellow solid which is used without further purification. ^{1}H NMR (400 MHz, DMSO-d6)

δ 8.28 (d, J = 8.0 Hz, 1H), 7.98 (s, 1H), 7.86 (t, J = 7.6 Hz, 1H), 7.76 (d, J = 8.1 Hz, 1H), 7.62 (t, J = 7.5 Hz, 1H), 3.52 (s, 3H); LC/MS (BAS1): $[M+H]^+$ = 238/240; t_R = 1.02.

4-{4-[(dimethylamino)methyl]-3,5-dimethoxyphenyl}-2-methyl-1,2-dihydroisoquinolin-1-one (13)

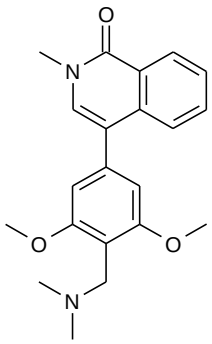

54 (130 mg; 546 µmol), {[2,6-dimethoxy-4-(tetramethyl-1,3,2-dioxaborolan-2-yl)-phenyl]methyl}-dimethylamine (**49**) (284 mg; 884 µmol) and Pd(dppf)Cl_2·DCM (44.6 mg; 54.6 µmol) are suspended in DMF (2.0 mL) under argon. A degassed Na_2CO_3-solution (2N; 683 µL; 1.37 mmol) is subsequently added and the resulting mixture is heated at 100 °C for 1 h. After cooling to rt water is added (several drops) and the mixture is filtered and purified by preparative RP-HPLC (column: X-Bridge C-18 30x50 mm) using a MeCN/water gradient under basic conditions. The product containing fractions are freeze dried. Further purification is achieved by automated silica gel chromatography (Combiflash; column: Redisep RF, 12g) using a DCM/MeOH gradient as eluent (100:0 --> 80:20; MeOH made basic with 0.1% NH_3). The product containing fractions are evaporated, dissolved in MeCN/water and freeze dried to give 4-{4-[(dimethylamino)methyl]-3,5-dimethoxyphenyl}-2-methyl-1,2-dihydroisoquinolin-1-one (**13**) (84.8 mg; 240 µmol; 44 %). ^{1}H NMR (500 MHz, DMSO-d6) δ 8.34 (d, J = 7.1 Hz, 1H), 7.72 (dd, J = 8.3, 7.1, 1H), 7.65 (d, J = 7.9 Hz, 1H), 7.58 – 7.54 (m, 2H), 6.71 (s, 2H), 3.80 (s, 6H), 3.58 (s, 3H), 3.49 (s, 2H), 2.16 (s, 6H); ^{13}C NMR (125 MHz, DMSO) δ 161.3, 159.3 (2C), 137.0, 136.3, 133.3, 132.8, 127.8, 127.1, 125.5, 124.8, 118.2, 113.4, 106.1 (2C), 56.3 (2C), 50.0, 45.4 (2C), 36.8; HRMS (CI+): calculated for $C_{21}H_{25}N_2O_3$ (MH+) 353.18597, found 353.18568, Δ -0.82 ppm; LC/MS (BAS1): $[M+H]^+$ = 353; t_R = 1.05.

Synthesis of compound 14

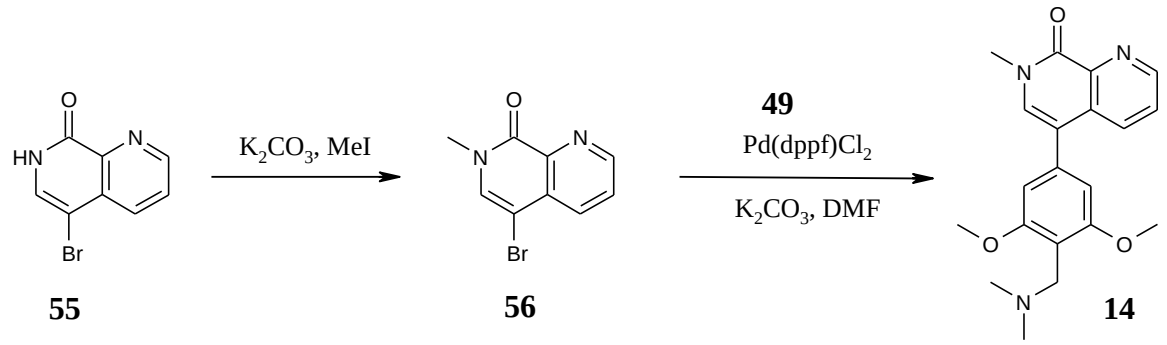

Supplementary Scheme 13: Synthesis of compound (**14**)

4-bromo-2-methyl-1,2-dihydro-2,7-naphthyridin-1-one (56)

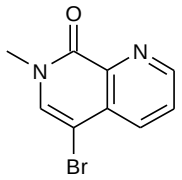

To a suspension of 5-bromo-7,8-dihydro-1,7-naphthyridin-8-one (**55**) (900 mg; 4.00 mmol, commercial from Princeton) and potassium carbonate (1.11 g; 8.03 mmol) in THF (40 mL), iodomethane (430 µL; 6.78 mmol) is carefully added and the resulting mixture is stirred at rt for 16 h. Since HPLC-MS of the reaction mixture indicates incomplete conversion additional iodomethane (400 µl; 6.31 mmol) is added and stirring is continued for 24h. Ammonia (10% aqueous solution; 30 mL) is added followed by water (50 mL). THF is removed under reduced pressure and the aqueous layer is extracted three times with DCM (30 mL each). The combined organic layer is dried over Na_2SO_4, filtered and evaporated to give 4-bromo-2-methyl-1,2-dihydro-2,7-naphthyridin-1-one (**56**) (860 mg; 3.69 mmol; 90 %) which is used without further purification. LC/MS (BAS1): $[M+H]^+$ = 239/241; t_R = 0.87.

5-{4-[(dimethylamino)methyl]-3,5-dimethoxyphenyl}-7-methyl-7,8-dihydro-1,7-naphthyridin-8-one (14)

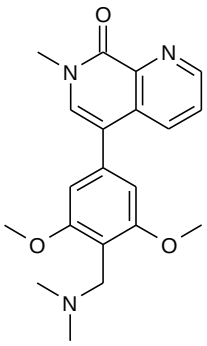

56 (80.0 mg 418 µmol), {[2,6-dimethoxy-4-(tetramethyl-1,3,2-dioxaborolan-2-yl)phenyl]methyl}-dimethylamine (**49**) (134 mg; 418 µmol) and Pd(dppf)Cl_2 (61.0 mg; 83.4 µmol) are suspended in 1,4-dioxane (10 mL) and water (1 mL) under N_2. Potassium carbonate (173 mg; 1.25 mmol) is added and the resulting mixture is heated at 80 °C for 1 h. After cooling to rt water is added and the mixture is extracted three times with EA. The combined organic layer is washed with brine, dried over Na_2SO_4, filtered and evaporated. The residue is purified by preparative RP-HPLC using a MeCN/water gradient under basic conditions. The product containing fractions are freeze dried to give 5-{4-[(dimethylamino)methyl]-3,5-dimethoxyphenyl}-7-methyl-7,8-dihydro-1,7-naphthyridin-8-one (**14**) (33.0 mg; 93.4 µmol; 22 %). ^{1}H NMR (500 MHz, DMSO-d6) δ 8.83 (d, J = 4.2 Hz, 1H), 8.08 (d, J = 8.4 Hz, 1H), 7.74 – 7.65 (m, 2H), 6.74 (s, 2H), 3.81 (s, 6H), 3.59 – 3.65 (m, 5H), 2.28 (s, 6H); ^{13}C NMR (125 MHz, DMSO, 1 C missing) δ 160.2, 159.4 (2C), 149.6, 141.3, 136.6, 134.1, 133.3, 132.6, 127.1, 116.3, 106.0 (2C), 56.4 (2C), 50.0, 45.1 (2C), 37.3; HRMS (CI+): calculated for $C_{20}H_{24}N_3O_3$ (MH+) 354.18122, found 354.18067, Δ -1.55 ppm; LC/MS (BAS1): $[M+H]^+$ = 354; t_R = 0.91.

Synthesis of compound 15 (BI-7273)[1]

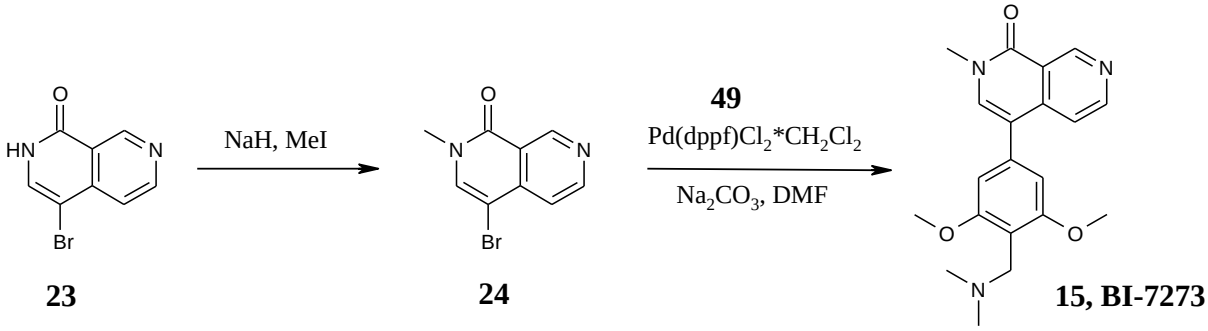

23 **24** **15, BI-7273**

Supplementary Scheme 14: Synthesis of compound (**15, BI-7273**)

4-{4-[(dimethylamino)methyl]-2,6-dimethoxyphenyl}-2-methyl-1,2-dihydro-2,7-naphthyridin-1-one (15)

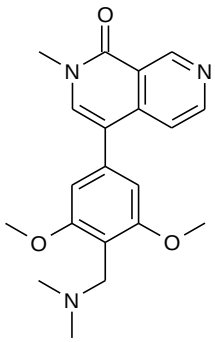

24 (200 mg; 837 µmol) and {[2,6-dimethoxy-4-(tetramethyl-1,3,2-dioxaborolan-2-yl)phenyl]methyl}-dimethylamine (**49**) (375 mg; 1.26 mmol) and Pd(dppf)Cl_2·DCM (70.4 mg; 86.2 µmol) are suspended in DMF (2.0 mL) under argon. A degassed Na_2CO_3-solution (2N; 1.05 mL; 2.10 mmol) is subsequently added and the resulting mixture is heated at 80 °C for 1 h. After cooling to rt, DMF is evaporated and a the residue is purified by flash chromatography on silica gel using a DCM/MeOH gradient as eluent (0:100 --> 90:10; Meoh made basic with 0.1% NH_3) to give pre-purified material. Subsequent preparative RP-HPLC chromatography yields highly pure 4-{4-[(dimethylamino)methyl]-2,6-dimethoxy-phenyl}-2-methyl-1,2-dihydro-2,7-naphthyridin-1-one (**15**) (210 mg; 594 µmol; 71 %). ^{1}H NMR (500 MHz, DMSO-d6) δ 9.44 (s, 1H), 8.72 (d, J = 5.7 Hz, 1H), 7.86 (s, 1H), 7.56 (d, J = 5.7 Hz, 1H), 6.72 (s, 2H), 3.80 (s, 6H), 3.60 (s, 3H), 3.46 (s, 2H), 2.13 (s, 6H); ^{13}C NMR (125 MHz, DMSO) δ 160.9, 159.4 (2C), 151.4, 150.9, 141.5, 138.3, 135.5, 120.2, 117.8, 116.5, 113.9, 105.8 (2C), 56.3 (2C), 50.0, 45.5 (2C), 36.9; HRMS (CI+): calculated for $C_{20}H_{24}N_3O_3$ (MH+) 354.1812, found 354.1808, Δ - 1.1 ppm; LC/MS (BAS1): $[M+H]^+$ = 354; t_R = 0.91 min.

Synthesis of compound 16

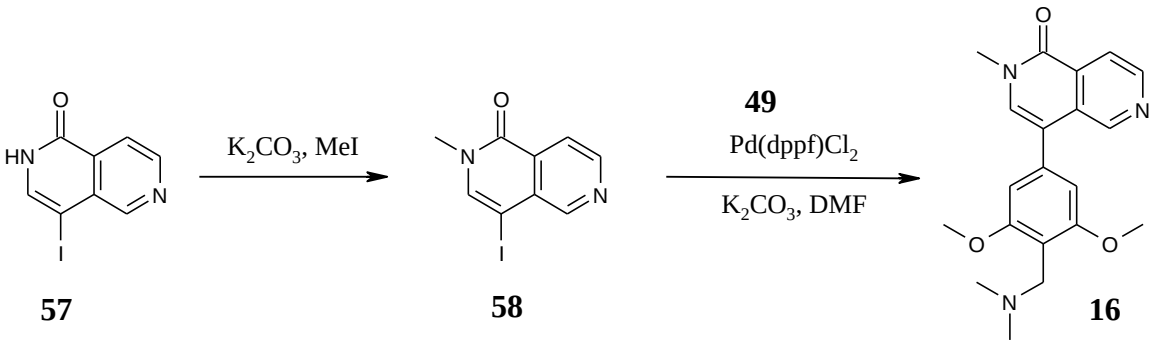

57 **58** **16**

Supplementary Scheme 15: Synthesis of compound (**16**)

4-Iodo-2-methyl-1,2-dihydro-2,6-naphthyridin-1-one (58)

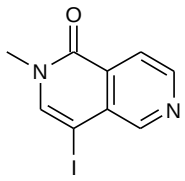

To a suspension of 4-iodo-1,2-dihydro-2,6-naphthyridin-1-one (**57**) (1.00 g; 3.68 mmol, commercial from FCHGroup) and potassium carbonate (1.52 g; 11.0 mmol) in DMF (50 mL), iodomethane (1.04 g; 7.32 mmol) is carefully added and the resulting mixture is stirred at rt for 24 h. Water and EA are added, the layers are separated and the aqueous layer is extracted three times with EA. The combined organic layer is washed with brine, dried over Na_2SO_4, filtered and evaporated to give 4-iodo-2-methyl-1,2-dihydro-2,6-naphthyridin-1-one (**58**) (450 mg; 1.57 mmol; 43 %) which is used without further purification. LC/MS(INT2): (M+H)+ =287; t_R = 0.57 min.

4-{4-[(dimethylamino)methyl]-3,5-dimethoxyphenyl}-2-methyl-1,2-dihydro-2,6-naphthyridin-1-one (16)

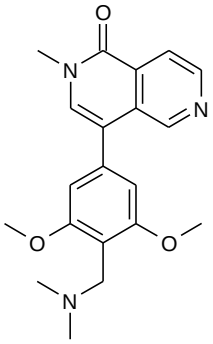

58 (100 mg; 350 µmol), {[2,6-dimethoxy-4-(tetramethyl-1,3,2-dioxaborolan-2-yl)phenyl]methyl}-dimethylamine (**49**) (84.0 mg; 351 µmol) and Pd(dppf)Cl_2 (51.0 mg; 69.8 µmol) are suspended in 1,4-dioxane (10 mL) and water (1 mL) under N_2. Potassium carbonate (145 mg; 1.05 mmol) is added and the resulting mixture is heated at 80 °C for 1 h. After cooling to rt water is added and the mixture is extracted three times with EA. The combined organic layer is washed with brine, dried over Na_2SO_4, filtered and evaporated. The residue is purified by preparative RP-HPLC using a MeCN/water gradient under basic conditions. The product containing fractions are freeze dried to give 4-{4-[(dimethylamino)methyl]-3,5-dimethoxyphenyl}-2-methyl-1,2-dihydro-2,6-naphthyridin-1-one (**16**) (30.0 mg; 84.9 µmol; 24 %). ^{1}H NMR (500 MHz, DMSO-d6) δ 9.02 (s, 1H), 8.71 (d, J = 5.2 Hz, 1H), 8.14 (d, J = 5.2 Hz, 1H), 7.73 (s, 1H), 6.81 (s, 2H), 3.83 (s, 6H), 3.68 (s, 2H), 3.62 (s, 3H), 2.31 (s, 6H); ^{13}C NMR (125 MHz, DMSO, 1 C missing) δ 160.3, 159.4 (2C), 148.3, 146.5, 136.2, 135.2,

130.5, 130.0, 120.0, 116.4, 106.1 (2C), 56.4 (2C), 50.0, 45.0 (2C), 37.1; HRMS (CI+): calculated for $C_{20}H_{24}N_3O_3$ (MH+) 354.18122, found 354.18061, Δ -1.71 ppm; LC/MS (BAS1): $[M+H]^+$ = 354; t_R = 0.96 min.

Synthesis of compound 17

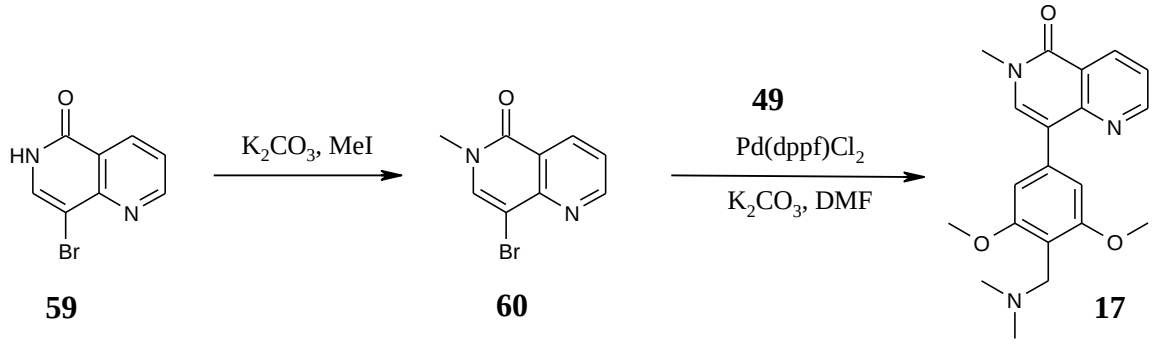

Supplementary Scheme 16: Synthesis of compound (**17**)

8-Bromo-6-methyl-5,6-dihydro-1,6-naphthyridin-5-one (60)

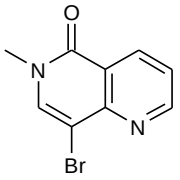

To a suspension of 8-bromo-5,6-dihydro-1,6-naphthyridin-5-one (**59**) (2.00 g; 8.89 mmol, commercial from TCI) and potassium carbonate (3.68 g; 26.6 mmol) in DMF (50 mL), iodomethane (2.52 g; 17.7 mmol) is carefully added and the resulting mixture is stirred at rt for 24 h. Water and EA are added, the layers are separated and the aqueous layer is extracted three times with EA. The combined organic layer is washed with brine, dried over Na_2SO_4, filtered and evaporated to give 8-bromo-6-methyl-5,6-dihydro-1,6-naphthyridin-5-one (**60**) (1.50 g; 6.27 mmol; 71 %) which is used without further purification. ^{1}H NMR (400 MHz, $CDCl_3$) δ 9.06 (d, J = 3.6 Hz, 1H), 8.73 (d, J = 8.0 Hz, 1H), 7.69 (s, 1H), 7.40 – 7.50 (m, 1H), 3.65 (s, 3H); LC/MS(INT2): (M+H)+ =239/241; t_R = 0.52 min.

8-{4-[(dimethylamino)methyl]-3,5-dimethoxyphenyl}-6-methyl-5,6-dihydro-1,6-naphthyridin-5-one (17)

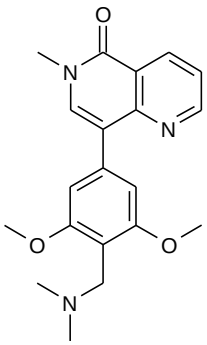

60 (100 mg; 418 µmol), {[2,6-dimethoxy-4-(tetramethyl-1,3,2-dioxaborolan-2-yl)phenyl]methyl}-dimethylamine (**49**) (134 mg; 418 µmol) and Pd(dppf)Cl_2 (61.0 mg; 83.4 µmol) are suspended in 1,4-dioxane (10 mL) and water (1 mL) under N_2. Potassium carbonate (173 mg; 1.25 mmol) is added and the resulting mixture is heated at 80 °C for 1 h. After cooling to rt water is added and the mixture is extracted three times with EA. The combined organic layer is washed with brine, dried over Na_2SO_4, filtered and evaporated. The residue is purified by preparative RP-HPLC using a MeCN/water gradient under basic conditions. The product containing fractions are freeze dried to give 8-{4-[(dimethylamino)methyl]-3,5-dimethoxyphenyl}-6-methyl-5,6-dihydro-1,6-naphthyridin-5-one (**17**) (35.0 mg; 99.0 µmol; 24 %). ^{1}H NMR (500 MHz, DMSO-d6) δ 9.40 (s, 1H, prot. amine), 8.96 (d, J = 4.5 Hz, 1H), 8.65 (d, J = 8.1 Hz, 1H), 8.00 (s, 1H), 7.60 (dd, J = 8.1, 4.5 Hz, 1H), 7.03 (s, 2H), 4.24 (s, 2H), 3.88 (s, 6H), 3.63 (s, 3H), 2.76 (s, 6H); ^{13}C NMR (125 MHz, DMSO) δ 161.6, 158.7 (2C), 154.5, 151.6, 139.7, 137.7, 136.4, 122.5, 121.1, 118.3, 106.5 (2C), 105.2, 56.6 (2C), 49.9, 43.0 (2C), 36.9; HRMS (CI+): calculated for $C_{20}H_{24}N_3O_3$ (MH+) 354.18122, found 354.18067, Δ -1.54 ppm; LC/MS (BAS1): $[M+H]^+$ = 354; t_R = 0.96 min.

Synthesis of compound 18

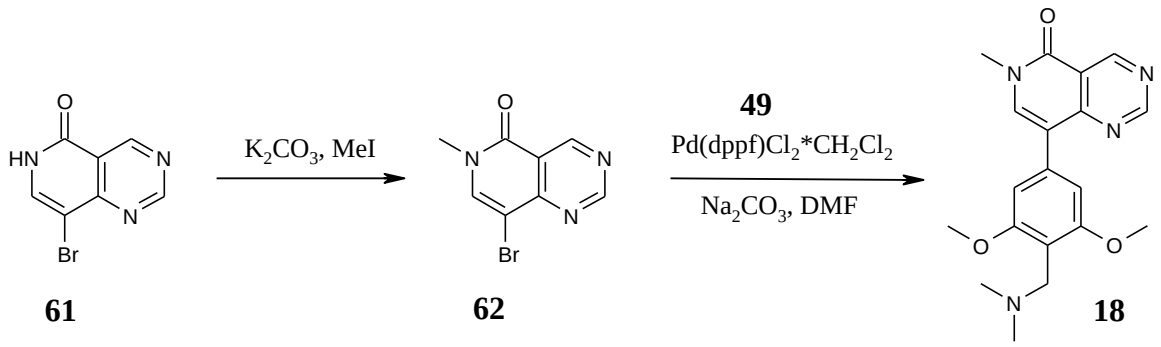

Supplementary Scheme 17: Synthesis of compound (**18**)

8-Bromo-6-methyl-5H,6H-pyrido[4,3-d]pyrimidin-5-one (62)

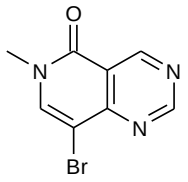

To a suspension of 8-bromo-5H,6H-pyrido[4,3-d]pyrimidin-5-one (**61**) (1.00 g; 4.42 mmol, commercial from FCHGroup) and potassium carbonate (1.19 g; 8.61 mmol) in THF (40 mL), iodomethane (430 µL; 6.78 mmol) is carefully added and the resulting mixture is stirred at rt for 16 h. Since HPLC-MS of the reaction mixture indicates incomplete conversion additional iodomethane (400 µl; 6.31 mmol) is added and stirring is continued for 24h. Ammonia (10% aqueous solution; 30 mL) is added whereupon precipitation occurs. The solid is filtered, washed with water and dried *in vacuo* to give 8-bromo-6-methyl-5H,6H-pyrido[4,3-d]pyrimidin-5-one (**62**) (890 mg; 3.71 mmol; 84 %) which is used without further purification. ^{1}H NMR (400 MHz, DMSO-d6) δ 9.48 (s, 1H), 9.47 (s, 1H), 8.54 (s, 1H), 3.54 (s, 3H); LC/MS (BAS1): $[M+H]^+$ = 240/242; t_R = 0.29 min.

8-{4-[(dimethylamino)methyl]-3,5-dimethoxyphenyl}-6-methyl-5H,6H-pyrido[4,3-d]pyrimidin-5-one (18)

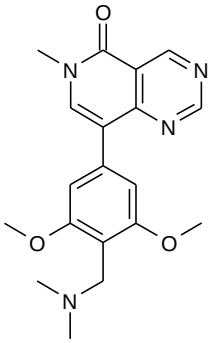

62 (100 mg; 417 µmol), {[2,6-dimethoxy-4-(tetramethyl-1,3,2-dioxaborolan-2-yl)phenyl]methyl}-dimethylamine (**49**) (170 mg; 529 µmol) and Pd(dppf)Cl_2·DCM (34.0 mg; 41.6 µmol) are suspended in DMF (800 µL) under argon. A degassed Na_2CO_3-solution (2N; 521 µL; 1.04 mmol) is subsequently added and the resulting mixture is heated at 100 °C for 1 h. After cooling to rt, water is added (several drops) and the mixture is filtered and purified by preparative RP-HPLC (column: X-Bridge C-18 30x50 mm) using a MeCN/water gradient under basic conditions. The product containing fractions are freeze dried. Further purification is achieved by automated silica gel chromatography (Combiflash; column: Redisep RF, 12g)

using a DCM/MeOH gradient as eluent (100:0 --> 80:20; MeOH made basic with 0.1% NH_3). The product containing fractions are evaporated, dissolved in MeCN/water and freeze dried to give 8-{4-[(dimethylamino)methyl]-3,5-dimethoxyphenyl}-6-methyl-5H,6H-pyrido[4,3-d]pyrimidin-5-one (**18**) (35.4 mg; 99.9 µmol; 24 %). ^{1}H NMR (500 MHz, DMSO-d6) δ 9.55 (s, 1H), 9.39 (s, 1H), 8.24 (s, 1H), 6.91 (s, 2H), 3.80 (s, 6H), 3.63 (s, 3H), 3.46 (s, 2H), 2.14 (s, 6H); ^{13}C NMR (125 MHz, DMSO) δ 160.8, 160.6, 159.0, 158.8 (2C), 156.5, 142.8, 134.8, 117.9, 117.3, 113.5, 106.3 (2C), 56.2 (2C), 50.0, 45.4 (2C), 37.0; HRMS (CI+): calculated for $C_{19}H_{23}N_4O_3$ (MH+) 355.17647, found 355.17598, Δ -1.36 ppm; LC/MS (BAS1): $[M+H]^+$ = 355; t_R = 0.88 min.

Synthesis of compound 19

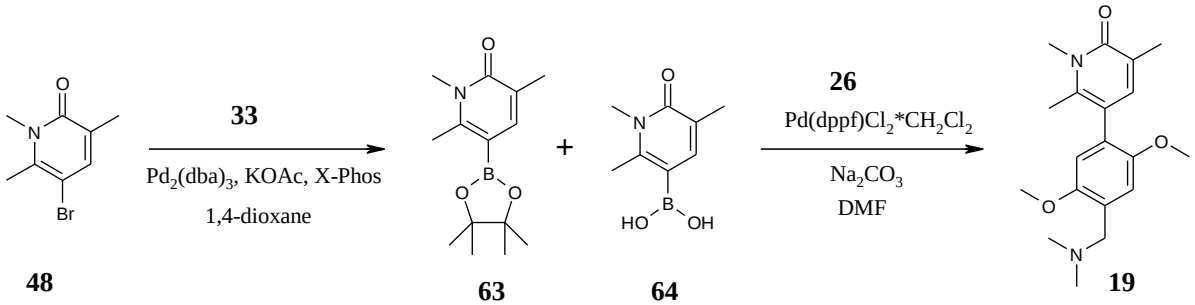

48 **63** **64** **19**

Supplementary Scheme 18: Synthesis of compound (**19**)

1,3,4-Trimethyl-5-(tetramethyl-1,3,2-dioxaborolan-2-yl)-1,2-dihydropyridin-2-one (63) and (1,2,5-trimethyl-6-oxo-1,6-dihydropyridin-3-yl)boronic acid (64)

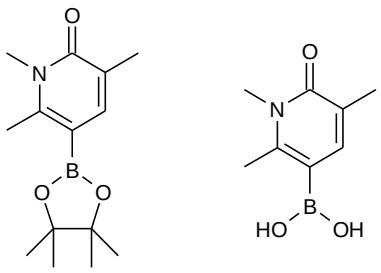

5-Bromo-1,3,6-trimethyl-1,2-dihydropyridin-2-one **(48)** (6.30 g; 29.2 mmol), bis(pinacolato)diboron (**33)** (29.6 g; 117 mmol), $Pd_2(dba)_3$ (0.60 g; 0.66 mmol) and 2-dicyclohexyl-phosphino-2′,4′,6′-triisopropylbiphenyl (0.60 g; 1.26 mmol) (378 mg; 46.3 µmol) and potassium acetate (9.00 g; 91.7 mmol) are suspended in 1,4-dioxane (80 mL) under N_2 and the resulting mixture is heated at 60 °C for 48 h. After cooling to rt the reaction mixture is

concentrated under reduced pressure, the residue is taken-up in EA, water is added and the layers are separated. The aqueous layer is extracted three times with EA. The combined organic layer is dried over Na_2SO_4, filtered and evaporated. The crude material is purified by silica gel chromatography and subsequently by preparative RP-HPLC using a MeCN/water gradient as eluent to give an inseparable mixture of 1,3,4-trimethyl-5-(tetramethyl-1,3,2-dioxaborolan-2-yl)-1,2-dihydropyridin-2-one (**63**) and (1,2,5-trimethyl-6-oxo-1,6-dihydropyridin-3-yl)boronic acid (**64**) (5.40 g; 20.5 mmol; 70 %), which is used for the next step. ^{1}H NMR (500 MHz, DMSO-d6, 3H from **64** covered under DMSO signal) δ 7.88 (s, 2 H, **64**), 7.39 (s, 1H, **63** and **64**), 3.46 (s, 3H, **63** and **64**), 2.57 (s, 3H, **63**), 1.96 (s, 3H, **63** and **64**), 1.27 (s, 12H, **63**); LC/MS (BAS1): $[M+H]^+$ = 264; t_R = 1.16 min (Ester).

5-{4-[(Dimethylamino)methyl]-2,5-dimethoxyphenyl}-1,3,6-trimethyl-1,2-dihydropyridin-2-one (19)

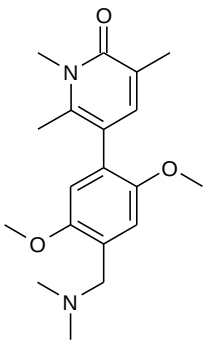

[(4-bromo-2,5-dimethoxyphenyl)methyl]dimethylamine (**26**) (313 mg; 1.14 mmol), inseparable mixture of **63** and **64** (300 mg; 1.14 mmol) and Pd(dppf)Cl_2·DCM (192 mg; 235 µmol) are suspended in DMF (3.0 mL) under argon. A degassed Na_2CO_3-solution (2N; 1.43 mL; 2.86 mmol) is subsequently added and the resulting mixture is heated at 100 °C for 1 h. After cooling to rt, water is added (several drops) and the mixture is filtered and purified by preparative RP-HPLC (column: X-Bridge C-18 30x50 mm) using a MeCN/water gradient under basic conditions. The product containing fractions are freeze dried. Further purification is achieved by automated silica gel chromatography (Combiflash; column: Redisep RF, 12g) using a DCM/MeOH gradient as eluent (100:0 --> 90:10; MeOH made basic with 0.1% NH_3). The product containing fractions are evaporated, dissolved in MeCN/water and freeze dried to give 5-{4-[(dimethylamino)-methyl]-2,5-dimethoxyphenyl}-1,3,6-trimethyl-1,2-dihydro-pyridin-2-one (**19**) (8.30 mg; 25.1 µmol; 2.2 %). ^{1}H NMR (400 MHz, DMSO-d6) δ 7.14 (s, 1H), 7.02 (s, 1H), 6.72 (s, 1H), 3.71 (2, 3H), 3.67 (s, 3H), 3.51 (s, 2H), 2.19 (s, 6H), 2.11 (s, 3H), 2.00 (s, 3H); LC/MS (BAS1): $[M+H]^+$ = 331; t_R = 1.00 min.

Synthesis of compound 20

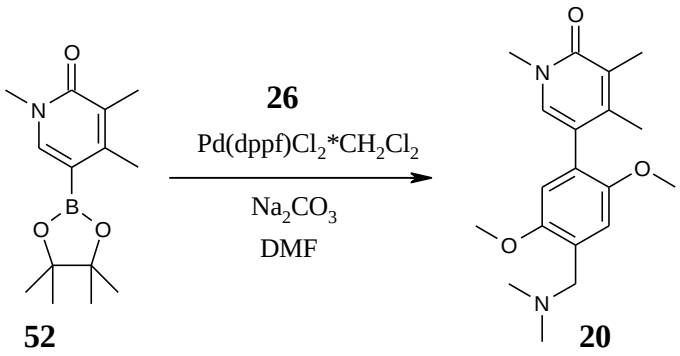

Supplementary Scheme 19: Synthesis of compound (**20**)

5-{4-[(Dimethylamino)methyl]-2,5-dimethoxyphenyl}-1,3,4-trimethyl-1,2-dihydro-pyridin-2-one (20)

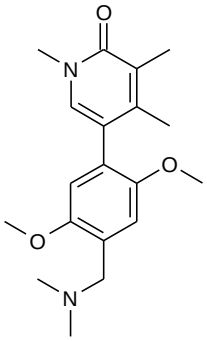

1,3,4-trimethyl-5-(tetramethyl-1,3,2-dioxaborolan-2-yl)-1,2-dihydropyridin-2-one (**52**) (80.0 mg; 304 µmol), [(4-bromo-2,5-dimethoxyphenyl)methyl]dimethylamine (**26**) (83.3 mg; 304 µmol) and Pd(dppf)Cl_2·DCM (24.8 mg; 30.4 µmol) are suspended in DMF (800 µL) under argon. A degassed Na_2CO_3-solution (2N; 380 µL; 760 µmol) is subsequently added and the resulting mixture is heated at 100 °C for 1 h. After cooling to rt, water (several drops) is added, the reaction mixture is filtered and purified by preparative RP-HPLC chromatography (column: X-Bridge C-18 30x50 mm) using a MeCN/water gradient under basic conditions. The product containing fractions are freeze dried to give 5-{4-[(dimethylamino)methyl]-2,5-dimethoxyphenyl}-1,3,4-trimethyl-1,2-dihydropyridin-2-one (**20**) (3.50 mg; 10.6 µmol; 3.5 %). ^{1}H NMR (500 MHz, DMSO-d6) δ 7.38 (s, 1H), 7.01 (s, 1H), 6.75 (d, J = 1.5 Hz, 1H), 3.73 (d, J = 1.5 Hz, 3H), 3.67 (d, J = 1.4 Hz, 3H), 3.39 - 3.44 (m, 5H), 2.19 (d, J = 1.6 Hz, 6H), 2.03 (s, 3H), 1.85 (s, 3H); ^{13}C NMR (125 MHz, DMSO) δ 161.8, 151.4, 151.3, 146.0, 134.9, 127.5, 125.3, 124.1, 118.2, 114.9, 113.0, 57.1, 56.4, 56.1, 45.7 (2C), 37.3, 17.4, 13.4; HRMS

(CI+): calculated for $C_{19}H_{27}N_2O_3$ (MH+) 331.20162, found 331.20108, Δ -1.62 ppm; LC/MS (BAS1): $[M+H]^+$ = 331; t_R = 1.02 min.

Synthesis of compound 22

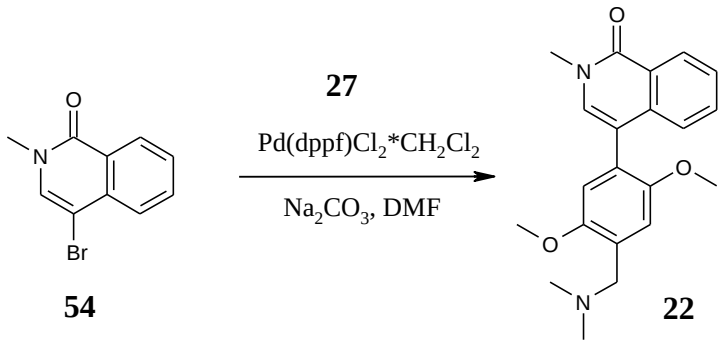

Supplementary Scheme 21: Synthesis of compound (**22**)

4-{4-[(Dimethylamino)methyl]-2,5-dimethoxyphenyl}-2-methyl-1,2-dihydroisoquinolin-1-one (22)

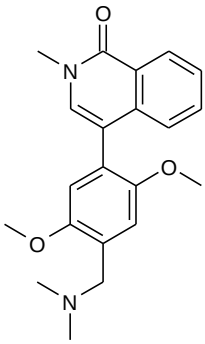

4-bromo-2-methyl-1,2-dihydroisoquinolin-1-one (**54**) (77.8 mg; 327 µmol), {[2,6-dimethoxy-4-(tetramethyl-1,3,2-dioxaborolan-2-yl)phenyl]methyl}-dimethylamine (**27**) (150 mg; 467 µmol) and Pd(dppf)Cl_2·DCM (27.5 mg; 33.7 µmol) are suspended in DMF (1.0 mL) under argon. A degassed Na_2CO_3-solution (2N; 409 µL; 818 µmol) is subsequently added and the resulting mixture is heated at 100 °C for 1 h. After cooling to rt, water is added (several drops) and the mixture is filtered and purified by preparative RP-HPLC (column: X-Bridge C-18 30x50 mm) using a MeCN/water gradient under basic conditions. The product containing fractions are freeze dried. Further purification is achieved by automated silica gel chromatography (Combiflash; column: Redisep RF, 12g) using a DCM/MeOH gradient as eluent (100:0 --> 90:10; MeOH made basic with 0.1% NH_3). The product containing fractions

are evaporated, dissolved in MeCN/water and freeze dried to give 4-{4-[(dimethylamino)-methyl]-2,5-dimethoxyphenyl}-2-methyl-1,2-dihydroiso-quinolin-1-one (**22**) (35.1 mg; 99.6 µmol; 30 %). ^{1}H NMR (500 MHz, DMSO-d6) δ 8.29 (d, J = 7.9 Hz, 1H), 7.63 (t, J = 7.6 Hz, 1H), 7.50 (t, J = 7.6 Hz, 1H), 7.44 (s, 1H), 7.14 (d, J = 8.1 Hz, 1H), 7.11 (s, 1H), 6.90 (s, 1H), 3.74 (s, 3H), 3.61 (s, 3H), 3.56 (s, 3H), 3.47 (s, 2H), 2.23 (s, 6H); ^{13}C NMR (125 MHz, DMSO) δ 161.5, 151.6, 151.6, 136.9, 133.5, 132.3, 127.9, 127.3, 126.8, 125.5, 125.2, 123.7, 115.3, 115.2, 113.4, 57.2, 56.4, 56.2, 45.8 (2C), 36.8; HRMS (CI+): calculated for $C_{21}H_{25}N_2O_3$ (MH+) 353.18597, found 353.18538, Δ -1.68 ppm; LC/MS (BAS1): $[M+H]^+$ = 353; t_R = 1.11 min.

ONLINE METHODS

BRD9 SPR-based fragment screen

The fragment screen was performed on a Biacore T200 instrument (GE Healthcare). His-tagged BRD9 (X-ray crystallography construct with an additional amino-terminal hexahistidine-tag[2]) was immobilized onto a Biacore NTA-chip (GE Healthcare) as described in the literature.[3] Briefly, the BRD9 protein was diluted to a concentration of 0.2 mg/ml in HBS-P+ buffer (10 mM HEPES, pH 7.4, 150 mM NaCl, 0.05 % P20) and injected over flow cell 4 of a Biacore NTA-chip, pre-loaded with Ni^{2+} and activated with EDC/NHS according to the manufacturer's instructions (T = 20°C). A second hexahistidine-tagged bromodomain protein, distantly related to BRD9, was immobilized on flow cell 3 as a control. Carbonic anhydrase II (SIGMA Aldrich) was used as a negative control and immobilized onto flow cell 2 (EDC/NHS activation, but no Ni^{2+}-loading). Buffer was injected over flow cell 1 to generate a blank reference surface. Approximately 8000 RU of each of the three proteins were immobilized. The buffer was then switched to screening buffer (HBS-P+; 1% DMSO).

The chip was equilibrated with running buffer for several hours. After 10 startup cycles (buffer injections) the fragment compounds were injected at a concentration of 100 μM from 384-well plates and the response was recorded for each compound. Positive (a bromodomain binder identified internally in a different bromodomain inhibitor program) and negative (buffer) controls were included at regular intervals to monitor the performance of the assay over the complete screening experiment. It turned out that the proteins on the chip were stable for the time required to analyse 384 compounds. After this a new chip was prepared as described above and the next 384 compounds were analysed. To correct for the excluded volume effect a DMSO calibration series was prepared as detailed in the instrument manufacturer's instructions and the calibration samples were measured at the beginning and end of each run.

The data were evaluated using BiaEvaluation (GE Healthcare) software. Briefly, all SPR responses were corrected for differences in bulk solvent refractive index and contributions from binding of compounds to the blank reference flow cell were subtracted. In this way the response (in response units, RUs) for each compound was determined. Fractional surface occupancy (FSO) normalized to the response for the reference compound was then calculated on a plate basis.[4] Based on our measured FSO the Z' value[5] of our assay over all plates was calculated to be 0.91 which is well above the 0.5 threshold which is considered to be the minimum requirement for a valid screening assay.

Any compounds showing abnormal binding behavior, were identified by visual inspection of the sensorgrams and removed from the list. Equally, any compound which showed binding to the reference protein carbonic anhydrase II was also disqualified. The MEDIAN and the standard deviation (STDEV) over all screened samples were calculated. All compounds showing a FSO $\geq$ MEDIAN + 3 x STDEV were classified as hits and subsequently subjected to SPR Kd measurements as described below.

BRD9 SPR K_D assay

His-tagged BRD9 was immobilized to a density of 2000 - 4000 RUs on flow cells 3 and 4 of a Biacore NTA-chip as described above. Carbonic anhydrase II was immobilized at a similar density on flow cell 2 and a blank reference surface was generated on flow cell 1.

The buffer was then switched to assay buffer (HBS-P+ = 10 mM HEPES, pH 7.4, 150 mM NaCl, 0.05 % P20 + 5 % DMSO) and the chip equilibrated for several hours before use for K_D determinations. To be able to correct for differences in bulk solvent refractive index caused by small variations in the DMSO concentration solvent correction samples were included at the beginning and end of the run as detailed in the instrument manufacturer's instructions.

Compounds were injected in concentration series (1:1 dilutions, 7 different concentrations), starting with a maximum concentration that was approximately 10-20-fold higher than the expected K_D. The concentration series were prepared in 96-well plates. In the case that the dilution window chosen for a particular compound did not appropriately bracket the K_D of the compound the measurement was repeated with an optimized starting concentration. Positive and negative control samples were included at regular intervals to be able to monitor the performance of the assay. CBS was used as a positive control for carbonic anhydrase II to check for integrity of the reference protein at regular intervals. To correct for the excluded volume effect a DMSO calibration series was prepared as detailed in the instrument manufacturer's instructions and the calibration samples were measured at the beginning and end of each run. Kd values were determined using Biaevaluation software by either performing a global fit of the double-referenced association and dissociation data to a 1:1 interaction model or by fitting the steady-state responses at each concentration to a 1:1 interaction model as appropriate. K_Ds from the two flow cells were averaged.

Isothermal Titration Calorimetry (ITC) assay

Protein were cloned, expressed and purified as previously described[6].

Calorimetric experiments were performed on an ITC200 or VP-ITC micro-calorimeter (MicroCalTM, LLC Northampton, MA). Protein solutions were buffer exchanged by dialysis into buffer 20 mM Hepes pH 7.5, 150 mM NaCl, and 0.5 mM TCEP. All measurements were carried out at 293.15 K while stirring at 1000 or 286 rpm. The micro syringe was loaded with protein solutions ranging from 250 to 320 μM, compound solutions were prepared at concentrations between 15 to 30 μM and 200 μl or 2 mL for the cells. All injections were performed using an initial injection of 0.5 μl followed by 30 injections of 1 μl with a duration

of 2 sec per injection and a spacing of 150 sec between injection for the ITC200; for the VP-ITC it was injected 2 µl followed by 34 injections of 8 µl with a duration of 16 sec per injection and a spacing of 240 sec between injections. The data were analysed with the MicroCal ORIGIN software package employing a single binding site model. The first data point was excluded from the analysis. Thermodynamic parameters were calculated ($\Delta G = \Delta H - T\Delta S = -RTlnKB$ where ΔG, ΔH and ΔS are the changes in free energy, enthalpy and entropy of binding, respectively).

Differential Scanning Fluorimetry (DSF)

DSF experiments were carried out in a Bio-Rad CFX384 Real-Time System (C1000Touch Thermal Cycler) in sealed Hard-Shell PCR 384 well plates (#HSP3805; PCR Sealers; #MSB1001; Bio-Rad) and a total volume of 10µl. The assay was optimized regarding protein consumption and SYPRO Orange dye excess (5000x concentration in DMSO, Invitrogen) to obtain a reliable fluorescence signal. Compound dilutions in assay buffer (25 mM HEPES pH 7.5, 150 mM NaCl, 1 mM TCEP) were prepared by a Hamilton Microlab Star pipetting robot. The reaction mixtures contained 8 µl compound dilution and 2µl of the BRD9 SYPRO Orange stock mix to yield final concentrations of 10µM BRD9, 25x SYPRO Orange and 400µM fragment at a DMSO concentration of 2%. Samples were heated at 1°C/min from 25°C to 95°C with fluorescence readings every 0.5°C. The entire BI generic fragment library (1697 compounds) was tested in duplicates. Melting curves were analyzed with the Bio-Rad CFX Manager-Data Analysis software in which T_m values were determined as the minimum of the first derivative of the recorded fluorescence intensity versus temperature plot. The T_m of native BRD9 was determined 200 times (47.2±0.5°C) and an in house positive control 60

times (53.5±0.5°C) from which a Z´ of 0.55 could be calculated. Thermal shifts of $\Delta T_m \geq 1°C$ ($\Delta T_m = T_{m,frag} - T_{m,DMSO}$) were assumed significant and defined as primary FBS hits.

Microscale Thermophoresis (MST)

MST is a fluorescence-based biophysical method which exploits the alteration of the mobility of molecules in a temperature gradient upon binding. The local temperature gradient is induced by an infrared laser and a detailed description of the technique is published elsewhere.[7] Fluorescence labeling of BRD9 with the NT647 dye was performed according to the manufacturer's protocol of the Monolith NT.115 Protein Labeling Kit RED-NHS (NanoTemper Technologies, Munich, Germany). Assay development comprised the optimization of protein concentration, buffer conditions, MST capillaries as well as the strength of the temperature gradient (IR laser power) using an in house positive control to achieve a reliably detectable change in the thermophoretic mobility (ΔF_{norm}) of labeled BRD9. Measurements were carried out in 25mM HEPES pH 7.5, 150 mM NaCl, 1 mM TCEP, 0.05% Tween-20 with 200 nM NT647-labeled BRD9 in the presence of 500 μM compound and 5% (v/v) d6-DMSO at 298K. Monolith NT.115 hydrophilic capillaries, an IR laser power of 40% with a laser on time of 30 seconds and an LED intensity of 60% were used.

For the in house implementation of fully automated sample preparation and MST data acquisition a Monolith NT.015 was modified in collaboration with NanoTemper Technologies and combined with a Hamilton Microlab Star pipetting system equipped with an in house developed tilting station. Individual capillaries were filled by dipping into each well of the vertically tilted 384-well plate (Greiner PP, small volume, deep well from Greiner Bio-One, Frickenhausen, Germany) and transferred in the detection device using a pneumatic gripper (Schunk, Lauffen/Neckar, Germany) attached to a pipetting channel.

Compounds were diluted in 30µl assay buffer with a Hamilton Microlab Star liquid handling system and 10µl of labeled BRD9 was added just-in-time prior to data acquisition to achieve equal incubation times. In one acquisition cycle 16 capillaries could be measured in which capillary 1 and 16 were a DMSO negative control and capillaries 2-14 contained seven fragments in duplicates.

Data was analyzed with the NanoTemper Analysis software version 1.2.205 and exported fluorescence as well as ΔF_{norm} values ($\Delta F_{norm}=F_{hot}/F_{cold}$) further evaluated. All MST traces were inspected manually and irregular traces (e.g. fluorescence quenching, protein aggregation) were discarded. Mean values of the duplicates were calculated and compared to either the mean value of the DMSO negative control in the individual acquisition cycle or the mean value of the DMSO control of the respective 384-well screening plate. An in house positive control was used to monitor integrity of labeled BRD9 throughout screening. Fragments were classified as hits if $\Delta\Delta F_{norm} \geq \Delta F_{norm}$(2sd DMSO) with $\Delta\Delta F_{norm} = \left|\Delta F_{norm}(\text{compound})-\Delta F_{norm}(\text{DMSO})\right|$.

BRD9 NMR spectroscopy

Confirmation of primary FBS hits obtained from DSF, SPR and MST was performed using two-dimensional $^{1}H/^{15}N$ HSQC NMR spectra[8] collected on a Bruker Avance III 600 MHz spectrometer equipped with a 5mm z-gradient TCI cryo-probe and a Bruker Sample Rail. Samples were freshly prepared just-in-time by a Tecan Freedom Evo pipetting robot in house customized for NMR sample tube filling before fully automated data acquisition[9]. Each sample contained 75 µM ^{15}N labeled BRD9 in 20 mM Tris-d11 pH 7.5, 200 mM NaCl, 1 mM TCEP and 8% (v/v) D_2O and was incubated with 500 µM fragment in a 2.5mm NMR tube at 298 K and a d6-DMSO concentration of 1%. Spectra were recorded with 48 transients and 96

data point in the indirect dimension. Identification of BRD9 binders was performed by manual comparison of spectra in the presence of a single fragment and the BRD9 reference spectrum in the presence of 1% (v/v) d6-DMSO using data processed by Bruker Topspin 3.0. For a more quantitative approach chemical shift perturbation was automatically evaluated using the Autoscreen module of Felix 2004 (FelixNMR Inc., San Diego, USA) for which either the entire spectrum or the region of interest (22 cross peaks defined by an in house positive control to identify the preferred binding site) was analyzed[10]. All three analysis methods showed > 90% overlap between confirmed BRD9 binding fragments, which were prioritized for Xray follow-up (see method description "BRD9 X-ray follow-up of confirmed primary FBS hits").

Protein purification and crystallization

The bromodomain of human BRD9 (residues 14-134 of isoform 5, Uniprot identifier Q9H8M2-1) was obtained from the SGC (Structural Genomics Consortium) and has been expressed and purified as previously described[2].

Protein crystallization was done using the hanging drop method by mixing 2.0 µL of apo BRD9 (10 mg/mL in 25 mM HEPES pH 7.5, 300 mM NaCl, 0.5 mM TCEP) with 2 µL of reservoir solution (30 % glycerol ethoxylate, 100 mM Tris pH 8.3) at 4 °C. Crystals grew within a few days to a final size of 150-200 µm). Apo crystals were transferred to a soaking buffer containing 33 % glycerol ethoxylate and soaked overnight by adding 0.1 µL of a 100 mM DMSO stock solution of **BI-7273**. Crystals were frozen in liquid nitrogen and data were collected at the SLS beam line X06SA (Swiss Light Source, Paul Scherrer Institute) at a wavelength of 1 Å using the PILATUS 6M detector. The crystals belonged to space group P21212 and contained 2 monomers per asymmetric unit. Images were processed with

autoPROC.[11] The resolution limits were set using default autoPROC settings. The structures were solved by molecular replacement using the BRD9 structure 3HME as a search model. Subsequent model building and refinement was done using standard protocols using CCP4,[12] COOT [13] and autoBUSTER (Bricogne, G. *et al.* (2011). BUSTER v.2.11.2. http://www.globalphasing.com).

For **BI-7273** (**compound 15**) the unit cell parameters were a = 70.80 Å, b = 125.34 Å, c = 29.92 Å and α, β, γ = 90° data and the structure was refined to Rwork and Rfree values of 17.8 % and 19.2 %, respectively, with 100% of the residues in Ramachandran favoured regions as validated with Molprobity.[14]

Compound 1 (unit cell: a = 70.03 Å, b = 125.41 Å, c = 29.53 Å, α, β, γ = 90°, resolution = 1.80 Å) was refined to R/Rfree = 20.3/22.0% with 100 % of the residues in Ramachandran favoured regions.

Compound 2 (unit cell: a = 71.04 Å, b = 125.02 Å, c= 29.94 Å, α, β, γ = 90°, resolution = 1.68 Å) was refined to R/Rfree = 18.9/20.5 %) with 100 % of the residues in Ramachandran favoured regions.

Compound 9 (unit cell: a = 70.31 Å, b= 125.17 Å, c = 30.02 Å, resolution: 2.3 Å) was refined to R/Rfree = 19.2/20.9 % with 99.55 % of the residues in Ramachandran favoured and 0.45 % in Ramachandran allowed regions.

BI-9564 (**compound 21**) (unit cell: a = 70.03 Å, b = 125.36 Å, c = 29.68 Å, α, β, γ = 90°, resolution = 1.82 Å) was refined to R/Rfree of 19.1/20.2% with 100 % of the residues in Ramachandran favoured regions.

Statistics for data collection and refinement can be found in **Supplementary Table 2**.

Stereo images (wall-eye stereo and cross-exe stereo) can be found in **Supplementary Fig. 5-14**.

The coordinates and structure factors of the structures have been deposited at the Protein Data Bank with the accession codes XXX

BRD9 X-ray follow-up of confirmed primary FBS hits

Protein crystallisation in the FBS setting has been done by the hanging drop method at 20 °C. 1.2 µl of a 14 mg/ml apo protein solution (in 25 mM HEPES pH 7.5, 300 mM NaCl, 0.5 mM TCEP) have been mixed with 1 µl of the reservoir solution (28-33% Glycerol Ethoxylate, 100 mM Tris pH 8.1- 8.7). The resulting crystals were transferred into soaking and cryoprotectant solution (30% Glycerol Ethoxylate, 100 mM Tris pH 8.5) in which compound was dissolved at 100 mM. After overnight incubation crystals were flash frozen in liquid nitrogen. Diffraction data was collected at X06SA and X06DA beamlines of the Swiss Light Source (Paul Scherrer Institute, Switzerland). All following steps have been performed as described in the above section "Protein purification and crystallization".

BRD9 Bromodomain Virtual Screening

Ligand preparation of HiCOS was carried out using Schrodinger's ligprep module. The initial docking was done in Schrodinger's Glide Suite 2012. The standard precision docking mode was employed. The docking protein grid was derived from the in-house X-ray crystal structure of BRD9, including two constraints: one with hydrogen bond donor from the terminal amido_$N^{\delta 2}H$ of Asparigine-100 and the other with the OH of conserved water-106. Follow-up pharmacophore mapping was performed in OpenEye's vROCS 2012. The BRD9

specific pharmacophore model was derived from the binding modes of ligands selected from three in-house X-ray co-crystal structures. ShapeTan and Combifit scoring methods in vROCS were used in combination to select the compounds for further consideration.

BRD9-H3 AlphaScreen assay

This assay is used to identify compounds which inhibit the interaction of the bromodomain of BRD9 with a tetra-acetylated peptide based on the sequence of histone H3 (H3 K9/14/18/23Ac (1-28)). GST-BRD9 protein corresponding to amino acids 130 - 259 that contains the bromodomain of BRD9 (accession number NM_023924.4) was expressed in E. coli with an amino-terminal GST tag. The sequence of the H3 K9/14/18/23Ac(1-28) peptide is Biotin- ARTKQTARK(Ac)STGGK(Ac)APRK(Ac)QLATK(Ac)AARKS, MW: 3392.
Assay concentrations: 4 nM GST-BRD9 protein (aa 130 - 259) and 12 nM biotinylated H3 K9/14/18/23Ac(1-28) peptide are used in the BRD9 H3 AlphaScreen assay.

BRD7 H3 AlphaScreen assay

This assay is used to identify compounds which inhibit the interaction of the bromodomain of BRD7 with a tetra-acetylated peptide based on the sequence of histone H3 (H3 K9/14/18/23Ac (1-28)). GST-BRD7 protein corresponding to amino acids 129 - 236 that contains the bromodomain of BRD7 (accession number NM_013263.4) was expressed in E. coli with an amino-terminal GST tag. The sequence of the H3 K9/14/18/23Ac(1-28) peptide is Biotin- ARTKQTARK(Ac)STGGK(Ac)APRK(Ac)QLATK(Ac)AARKS, MW: 3392.

Assay concentrations: 8 nM GST-BRD7 protein (aa 129 - 236) and 12 nM biotinylated H3 K9/14/18/23Ac(1-28) peptide are used in the BRD7 H3 AlphaScreen assay.

BRD4-BD1 H4 AlphaScreen assay

This assay is used to identify compounds which inhibit the interaction of the bromodomain 1 of BRD4 with a tetra-acetylated peptide based on the sequence of histone H4 (K5/8/12/16(1-18)). GST-BRD4-1 protein corresponding to amino acids 44 - 168 that contains the bromodomain 1 of BRD4 (accession number NP_490597.1) was expressed in E. coli with an amino-terminal GST tag. Tetra-acetylated histone H4 is a synthetic peptide, containing amino acids 1-18 of Histone H4 followed by a GSGS linker and biotinylated lysine (SGRGK(Ac)GGK(Ac)GLGK(Ac)GGAK(Ac)RH-GSGSK-biotin) MW = 2518.7Da.

Assay concentrations: 10 nM GST-BRD4-1 protein (aa 44 - 168) and 5 nM biotinylated H4 (K5/8/12/16(1-18) peptide are used in the BRD4-BD1 H4 AlphaScreen assay.

BRD4-BD2 AlphaScreen assay

This assay is used to identify compounds which inhibit the interaction of the bromodomain 2 of BRD4 with a tetra-acetylated peptide based on the sequence of histone H4 (K5/8/12/16(1-18)). GST-BRD4-2 protein corresponding to amino acids 333 - 460 that contains the bromodomain 2 of BRD4 (accession number NP_490597.1) was expressed in E. coli with an amino-terminal GST tag. Tetra-acetylated histone H4 is a synthetic peptide, containing amino acids 1-18 of Histone H4 followed by a GSGS linker and biotinylated lysine (SGRGK(Ac)GGK(Ac)GLGK(Ac)GGAK(Ac)RH-GSGSK-biotin) MW = 2518.7 Da.

Assay concentrations: 50 nM GST-BRD4-2 protein (aa 333 - 460) and 25 nM biotinylated H4 (K5/8/12/16(1-18) peptide are used in the BRD4-BD2 H4 AlphaScreen assay.

BRD2-BD1 AlphaScreen assay

This assay is used to identify compounds which inhibit the interaction of the bromodomain 1 of BRD2 with a tetra-acetylated peptide based on the sequence of histone H4 (K5/8/12/16(1-18)). GST-BRD2-1 protein corresponding to amino acids 71 - 194 that contains the bromodomain 1 of BRD2 (accession number NP_005095.1) was expressed in E. coli with an amino-terminal GST tag. Tetra-acetylated histone H4 is a synthetic peptide, containing amino acids 1-18 of Histone H4 followed by a GSGS linker and biotinylated lysine (SGRGK(Ac)GGK(Ac)GLGK(Ac)GGAK(Ac)RH-GSGSK-biotin) MW = 2518.7Da.

Assay concentrations: 20 nM GST-BRD2-1 protein (aa 333 - 460) and 10 nM biotinylated H4 (K5/8/12/16(1-18) peptide are used in the BRD4-BD2 H4 AlphaScreen assay.

All AlphaScreen assays are done in a darkened room below 100 Lux. Compounds are dispensed onto assay plates (Proxiplate-384 PLUS, white, PerkinElmer) using an Access Labcyte Workstation with the Labcyte Echo 550 from a DMSO solution. For the chosen highest assay concentration of 100 µM, 150 nL of compound solution are transferred from a 10 mM DMSO compound stock solution. A series of 11 concentrations is transferred for each compound at which each concentration is fivefold lower than the previous one. DMSO is added such that every well has a total of 150 nL compound solution. 10 µL of a mix containing protein and peptide with the assay specific concentrations are prepared in assay buffer (50 mM HEPES pH=7.3; 25 mM NaCl; 0,1% Tween 20; 0.1% bovine serum albumin (BSA); 2 mM dithiothreitol (DTT)) and 5 µL of bead mix (AlphaLISA Glutathione Acceptor Beads and AlphaScreen Streptavidin Donor Beads mixed in assay buffer at a concentration of 10 µg/ml each) are added to the assay plate that contain 150 nL of the compound solution. After 60 minutes at room temperature the signal is measured in a PerkinElmer Envision HTS

Multilabel Reader using the AlphaScreen specifications from PerkinElmer. Each plate contains negative controls where assay specific peptide and protein are left out and replaced by assay buffer. Negative control values are entered as low basis for normalization. IC50 values are calculated using a four parameter non-linear regression model.

BROMOscan

Bromodomain profiling was provided by DiscoveRx Corp. using their BROMOScan platform (http://www.discoverx.com/services/drug-discovery-development-services/epigeneticprofiling/Bromoscan). The BROMOscan screen accounted for the determination of the single concentration binding interaction (percent of control - % ctrl) for compound **BI-7273**, or **BI-9564**, and each of the 32 DNA tagged bromodomains included in the assay by binding competition against a reference immobilized ligand. BromoKdELECT accounted for the determination of the K_D between compound **BI-7273**, or **BI-9564**, and selected DNA tagged bromodomains by binding competition against a reference immobilized ligand.

Fluorescence Recovery After Photobleaching (FRAP)

FRAP studies were performed essentially as described[15] (1). In brief, U2OS cells were transfected (Fugene HD; Roche) with mammalian over-expression constructs encoding GFP fused to the N-terminus of full length BRD9, Brd7 or CECR2, respectively. Mutant proteins mutating the conserved Asn to Phe or Ala were generated as described in (1). The following mutations were introduced: N140A for human CECR2, N211F for mouse Brd7 and N163F for human BRD9. The imaging system consisted of a Zeiss LSM 710 laser-scanning and control system (Zeiss) coupled to an inverted Zeiss Axio Observer.Z1 microscope equipped

with a high-numerical-aperture (N. A. 1.3) 40 x oil immersion objective (Zeiss). Samples were placed in an incubator chamber in order to maintaining temperature and humidity. FRAP and GFP fluorescence imaging were both carried out with an argon-ion laser (488 nm) and with a PMT detector set to detect fluorescence between 500-550 nm. Once an initial scan had been taken, a region of interest corresponding to approximately 50 % of the entire GFP positive nucleus was empirically selected for bleaching. A time lapse series was then taken to record GFP recovery using 1% of the power used for bleaching. The image datasets and fluorescence recovery data were exported from ZEN 2009, the microscope control software, into Origin to determine the average half-time for full recovery for 10-20 cells per treatment point. Data were analysed using one-way ANOVA with Tukey's multiple comparisons test.

Cell lines and proliferation assays

Cells were grown in 50 µl medium as specified by the supplier for 7 days starting with 500 and with 1000 cells per well of a 384 well plate in the presence of varying concentrations of compound before measuring viability via cellular ATP levels using the cell titer glow assay (Promega).

MYC assay

To 750,000 MV-4-11 cells in 250 µl growth medium (in IMDM, 10 % FBS, GlutaMAX, 25 mM HEPES and 0,1% 2-Mercaptoethanol) per well compound was added at the desired concentration from a 10 mM stock solution using the HP D300 Digital Dispenser (Hewlett Packard). After 2 hours of incubation with the compound, cells were collected by centrifugation, washed in ice cold PBS and lysed in 15 µl of cell extraction buffer (Life Technologies #FNN0011 containing 1 mM PMSF and 1x Halt protease inhibitor cocktail

(Thermo)). After 30 minutes on ice, nucleic acids were disrupted by sonication. cMYC levels were measured using the human c-Myc (Total) ELISA Kit (Life Technologies #KHO2041)

Animal handling

Mice were housed under pathogen-free conditions (AAALAC accredited facility) and treated according to the institutional, governmental and European Union guidelines (GV-SOLAS, Felasa, Austrian Animal Protection Laws). All animal studies were reviewed and approved by the internal ethics committee of Boehringer Ingelheim and the local governmental committee (Amt der Wiener Landesregierung, Magistratsabteilung 58, Vienna, Austria).

Pharmacokinetic and efficacy studies in mice

For evaluation of PK properties non-tumor bearing BomTac:NMRI-Foxn1nu mice (Taconic, Ry, Denmark) were treated once with an intravenous bolus dose formulated with 25 % HP-β-CD (dosing volume 5 mL/kg), or orally as a suspension formulated with 0.5% Natrosol^{TM} Hydroxyethylcellulose (dosing volume 10 mL/kg). EDTA-blood was sampled from the *Vena saphena* and plasma was obtained by centrifugation.

Female CIEA-NOG mice (NOD.Cg-*Prkdc*^{scid}*IL2rg*^{tm1Sug}/JicTac; Taconic, Ry, Denmark) were engrafted intravenously with 1×10^7 EOL-1 AML cells stably expressing luciferase and GFP. Following injection of the cells animals were randomized based on body weight (n=10/group). Treatment started on day 5 with either 0.5% Natrosol or **BI-9564** formulated with 0.5% Natrosol. All doses were calculated relative to the mouse body weight on the treatment day. **BI-9564** and the vehicle control were administered orally with a dosing volume of 10 mL/kg body weight. **BI-9564** was administered daily from day 5 until 17 and

from day 20 until 22. Dosing was interrupted on day 18 for two days as one mouse in the treatment group reached -15% body weight loss. Tumour load was measured 2-3 times weekly based on bioluminescence imaging as described previously.[16] The following scoring system was used: score 0, no clinical signs; score 1, tail or hind limb weakness. Animals were sacrificed based on severity criteria including appearance of paralysis score 1 and/or body weight loss exceeding -18%. In this tumor mouse model body weight changes can occur due to increased tumor load or due to intolerability.

Determination of physicochemical and *in vitro* DMPK parameters

Aqueous solubility was determined from 10 mM stock solutions of the compounds in DMSO diluted with aqueous McIlvaine buffer at pH 6.8, or with acetonitrile/water (1:1) as a reference. Samples were shaken for 24 h at room temperature in 96-well plates (Whatman Uniplate® 96 wells, 750 µL, polypropylene, round bottom). The plate was then centrifuged at 3,000 rpm for 2 min. 250 µL of each sample were transferred to a Millipore MultiScreenHTS filter plate with a polycarbonate membrane, pore size 0.45 µm. Filtrates were collected by centrifugation at 3,000 rpm for 2 min. The dissolved concentrations were determined by UPLC/UV on a Waters ACQUITY UPLC® SQD system equipped with a Waters ACQUITY UPLC® BEH 2.1x50 mm C18 column, particle size 1.7 µm, using a short gradient with water/0.1% formic acid as solvent A and acetonitrile/0.1 % formic acid as solvent B (5 to 95 % B with 1.7 min total cycle time). Compound signals were measured with a photodiode array UV detector operated at 254 nm. Solubility was determined with a one point calibration by comparing peak areas relative to the reference standard using Waters Empower software.

In vitro predictions of hepatic metabolic (CL) based on incubations with cryopreserved hepatocytes were carried out with an automated assay in a 24-well plate format on a Tecan

robotic system at a test compound concentration of 1 µM. Cryopreserved hepatocytes (donor pools) were supplied by Celsis IVT. Cryopreserved cells were thawed according to protocols provided by the vendor and suspended in DMEM supplemented with insulin (5 µg/mL), glucagon (7 ng/mL), hydrocortisone (7.5 µg/mL) and serum of the respective species (50% of total volume). Test compounds were added after a 30 min pre-incubation. Suspensions of $1x10^6$ cells/mL were incubated and continuously shaken in a Thermo Scientific Cytomat™ for 4 h at 85-95% relative humidity and 5-10% CO_2 at 37 °C. Aliquots were taken from the medium at 0, 0.5, 1, 1.5, 2.5 und 4 h and concentrations of the test compounds quantified by HPLC/MS/MS on a BIOCIUS Life Sciences RapidFire® system coupled to a Thermo Scientific™ TSQ Vantage™ triple-quadrupole mass spectrometer. Predicted clearances were calculated using the well-stirred model.

In vitro plasma protein binding (PPB) was determined by a semi-automated equilibrium dialysis assay on a Tecan robotic system at a test compound concentration of 3 µM. Dialysis chambers in custom-made Teflon devices for multiple parallel incubations were separated by a 18x18 cm dialysis membrane with molecular weight cut-off of 5,000 Da (Dianorm No. 5214). Plasma of the respective species spiked with test compound was dialyzed against Soerensen buffer (pH 7.4) for 3 h at 37 °C at 12 rpm on an overhead rotator. PPB was calculated based on test compound concentrations in the plasma and buffer compartments quantified by HPLC/MS/MS.

Caco-2 and *in vitro* cytochrome P450 inhibition assays have been carried out as described elsewhere.[17]

Determination of pharmacokinetic properties

Compound concentrations from aliquots of 10 µL plasma were quantified by HPLC-MS/MS at unit mass resolution with ESI+ ionization. The BI proprietary compound BIBI1355BS was added to all samples as internal standard. Calibration and quality control samples were prepared using blank plasma from untreated animals as matrix. Calibration standards were prepared by serial dilutions in twelve steps by manual dilutions or using a Perkin-Elmer Janus automated liquid handling system. Pre-analytical sample preparation was carried out by liquid/liquid extraction in a 96-well plate format with t-butyl methyl ether (TBME) or ethyl acetate under basic conditions, or by acetonitrile precipitation and centrifugation. Extracted plasma samples or supernatants of precipitated samples were evaporated to dryness under N_2, redissolved in 25% methanol/75% water/0.01% formic acid and injected to the HPLC/MS/MS system with a CTC PAL HTS-xt autosampler (injection volume 5 µL for *i.v.* and 1 µL for *p.o.* studies).

Quantitative analyses were performed with Agilent HP1200 analytical HPLC systems equipped with a Waters XBridge BEH C18 reversed phase HPLC column at room temperature (particle size 2.5 µm, column dimension 2.1 x 50 mm), applying a HPLC gradient with 5 mM ammonium acetate (pH 4.0) as solvent A and acetonitrile with 0.1% formic acid as solvent B with a cycle time of 2.0 min per sample. Solvent B was increased from 5 to 95% over 1 min, and then kept constant at 95% B from 1.0 - 1.3 min, before returning to 5% B and column re-equilibration from 1.4 to 2.0 min. The HPLC systems were coupled to SCIEX API5000 triple quadrupole or 4000 QTRAP® hybrid triple quadrupole/linear ion trap mass spectrometers operated in MRM mode with ion transitions of 354.2 to 309.0 for **BI-7273** and **BI-9564**, and 467.3 to 98.1 for BIBI1355BS (dwell times: 70 ms). Declustering potential (DP) and collision energy (CE) settings were automatically optimized using the SCIEX DiscoveryQuantTM 2.1 software. The source temperature of the Turbo Ion Spray source was set to 600°C. Chromatograms were integrated and peak areas were determined with Analyst® 1.5.1 (SCIEX). Pharmacokinetic parameters were calculated

by non-compartmental analysis using the Boehringer Ingelheim proprietary software ATLAS. AUC values were determined by the linear trapezoidal rule and with C(0) = C(t1) for intravascular application and with C(0) = 0 for extravascular application.

Supplementary Figure 1. Screening cascades leading to the identification of compound **1** and **2** as validated hits

Triage Assay	**Prospective Criteria**	**Generic FBS Library***			**Virtual Screening of HiCos compounds****	
Total compounds screened		1697			208	
Screening Assay (fixed conc.)		**DSF** dTm ≥1°C (400 µM)	**SPR** BR ≥20% (100 µM)	**MST** ΔMST (DMSO, Cpd) ≥ MST(2sd DMSO) (500 µM)	**DSF** dTm≥1°C (500 µM)	**SPR** BR ≥8% (100 µM)
		36	45	124	25	23
Orthogonal Assay	Validation	34	38	38	11	23
		77 (^{15}N HSQC NMR)			23 (SPR Kd)	
X ray co-crystal structure		55			11	
Screening Assay SPR	K_D<100µM	12			13	
Resynthesis/ Verification	Activity /Structure confirmation	12			12	
Unwanted Fragment					1	
Validated Hits with K_D(SPR)<100µM		**12**			**11**	

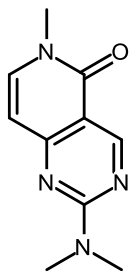

1

K_D(SPR)=37.5 µM

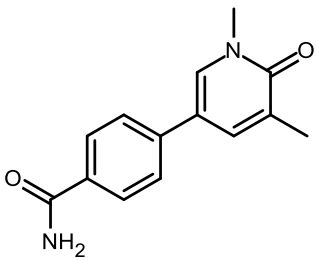

2

K_D(SPR)=9.1 µM

*** Generic FBS library** consists of a diverse set of compounds fulfilling the following constraints: MW 90-270 Da, clogP 0-3, TPSA 20-120, H-bond donors ≤3, H-bond acceptors ≤6, rotatable bonds ≤4, unwanted fragment excluded, DMSO solubility >50mM, solubility buffer pH 7.4 >100µM, LC/MS purity >80%, NMR purity >80%

** **HiCos library** consists of a diverse set of compounds fulfilling the following constraints: MW <300 Da, clogP <6, TPSA <150, H-bond donors + H-bond acceptors >0, rotatable bonds <12, unwanted fragment excluded, stock solution 50mg/mL

Supplementary Figure 2. Overlap analysis of the primary fragment screening as well as follow up results (primary hits / 2D $^{1}H/^{15}N$ NMR confirmed / X-ray co-crystal structure) for the "generic FBS library"

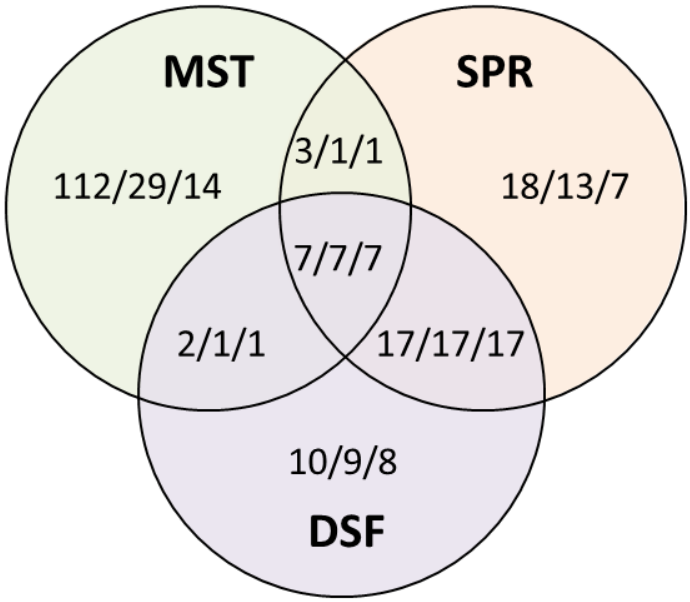

Supplementary Figure 3. Experimental screening data for compound **1**.

a) DSF melting curves (SYPRO Orange fluorescence emission as a function of temperature) of the DMSO negative control (black, T_m=47°C) and compound **1** (red) in duplicates reveals a stabilisation of BRD9 of 2.9°C by compound **1**. 10µM BRD9 was incubated with 400µM compound **1** and 25x SYPRO Orange at a DMSO concentration of 2%; b) SPR primary screen data ([**1**]=100 µM). Compound **1** shows a robust fast on/off response; c) MST screening traces of the DMSO negative control (black) and compound **1** (red). A $\Delta\Delta F_{norm}$ of 22.1 ‰ with a laser power of 40% and a laser on-time of 30s depicts a clear binding signal for compound **1**. 200nM NT647-labeled BRD9 was incubated with 500µM compound **1** at a final DMSO concentration of 5%; d) Confirmation of primary FBS hits bei 2D $^{1}H/^{15}N$ HSQC NMR. Significant chemical shift perturbation observed which is indicative for site specific binding of compound **1** to the bromodomain of BRD9 (75µM ^{15}N labeled protein in the presence of 500µM compound **1** and 1% d6DMSO). Alterations in the complex spectrum are very similar to those obtained for an in-house positive control suggesting that compound **1** binds to the acetyl-lysine binding site; e) SPR Kd data for **1**. The equilibrium binding data can be fitted to a 1:1 binding model, yielding a Kd of 39 µM.

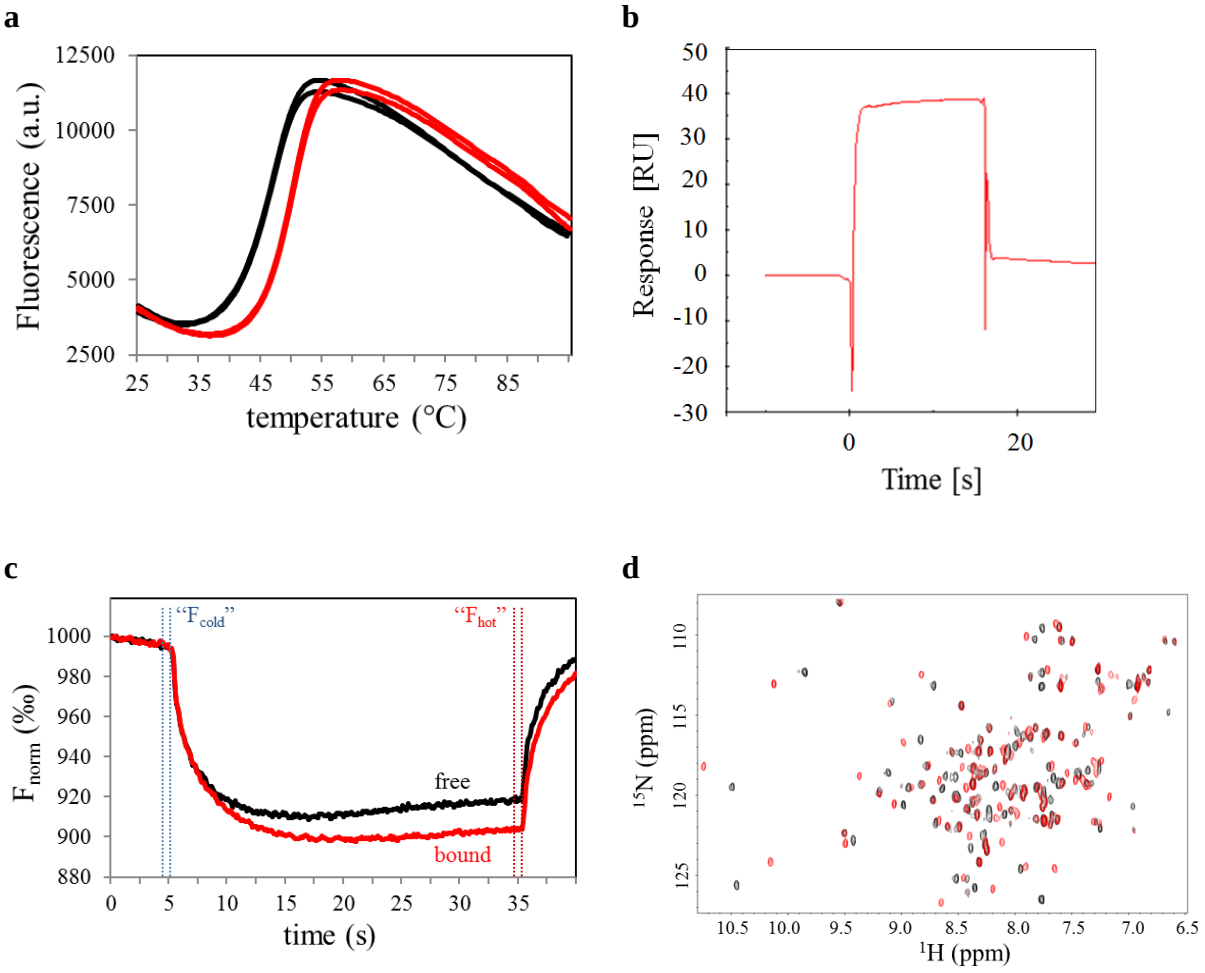

e

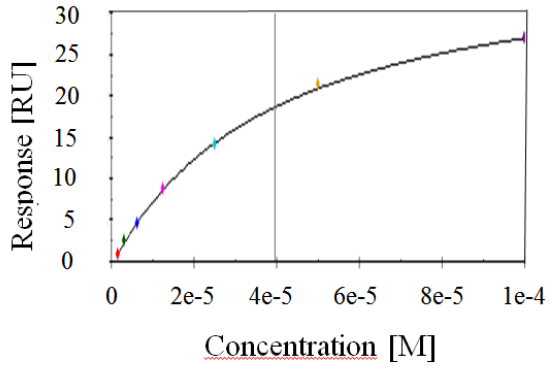

Report | Parameters

KD (M)	Rmax (RU)	offset (RU)	Chi² (RU²)
3.959E-5			0.0806
	38.57	-0.6238	

Supplementary Figure 4. Virtual Screening of HiCoS compounds cascade leading to the selection of 208 molecules: docking in BRD9 BD, followed by pharmacophore shape-based mapping.

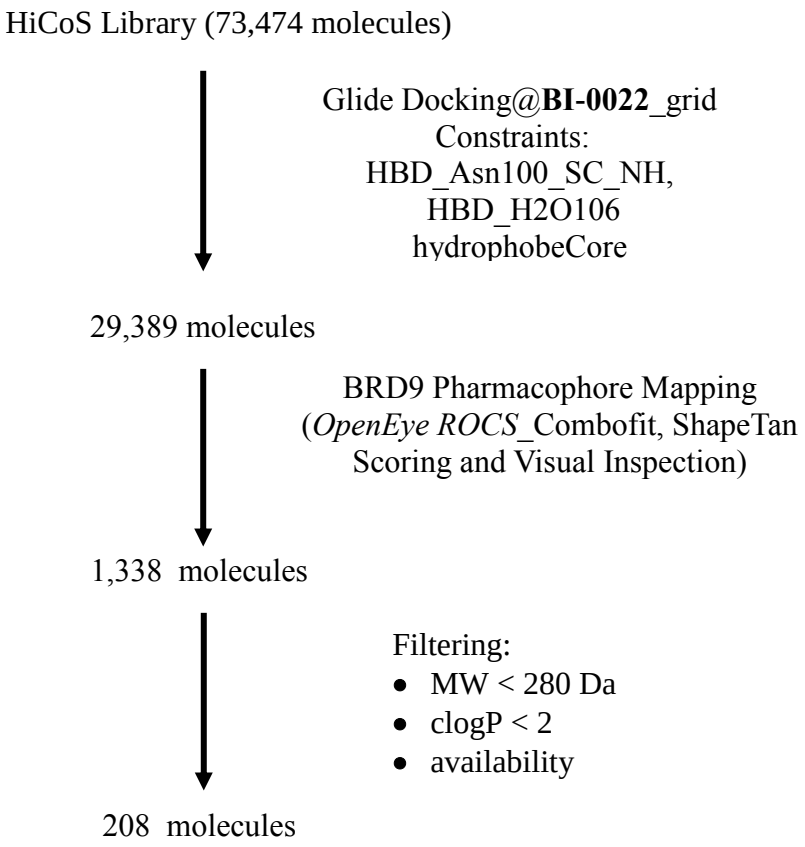

Supplementary Figure 5. Stereo image of **compound 1** bound to BRD9 (wall-eye stereo). The refined $2F_o$-F_c electon density is countoured at 1 σ.

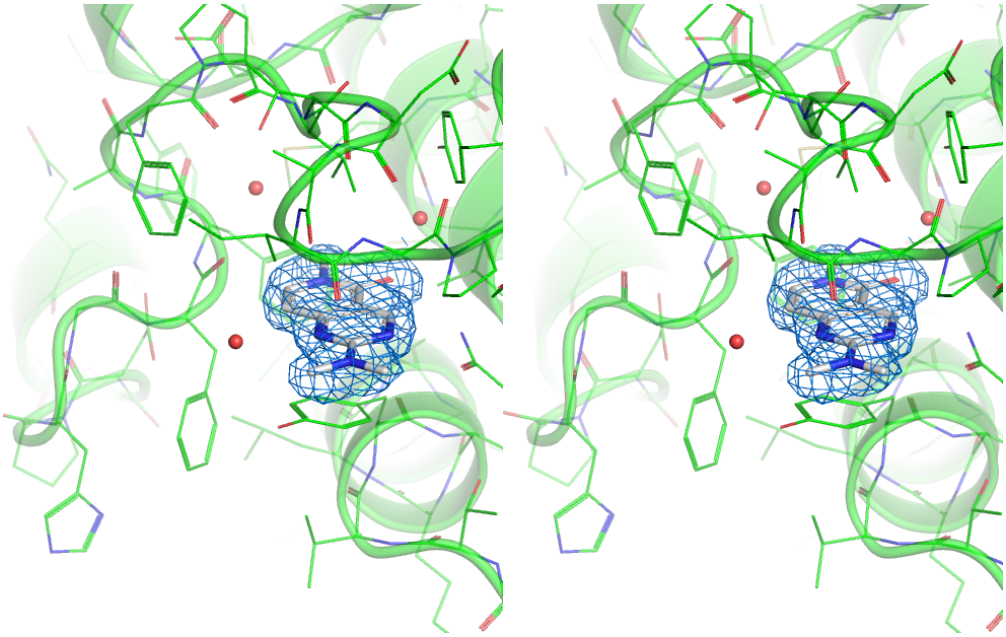

Supplementary Figure 6. Stereo image of **compound 1** bound to BRD9 (cross-eye stereo). The refined $2F_o$-F_c electon density is countoured at 1 σ.

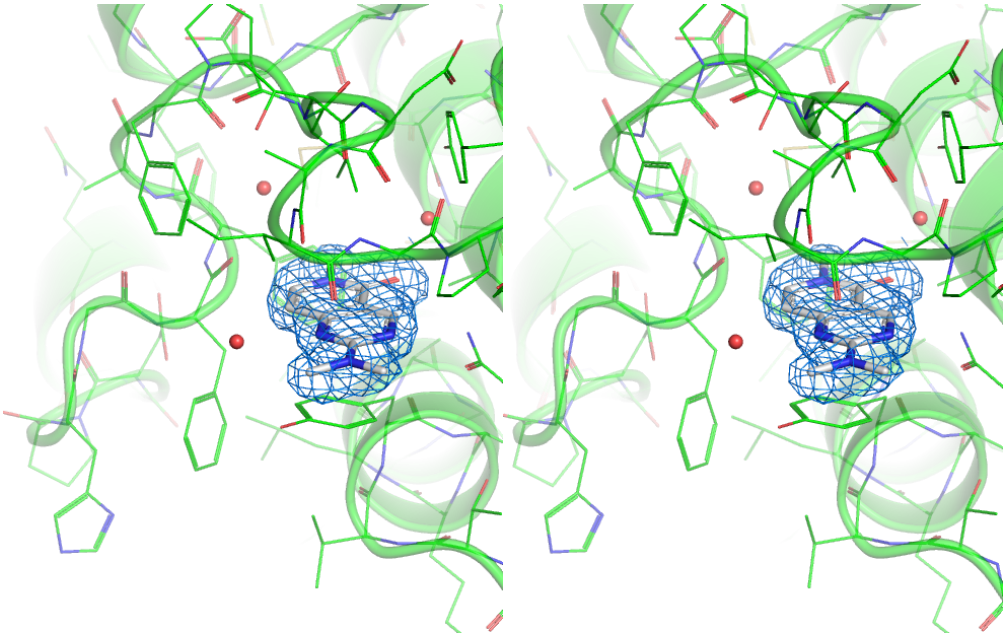

Supplementary Figure 7. Stereo image of **compound 2** bound to BRD9 (wall-eye stereo). The refined $2F_o$-F_c electon density is countoured at 1 σ.

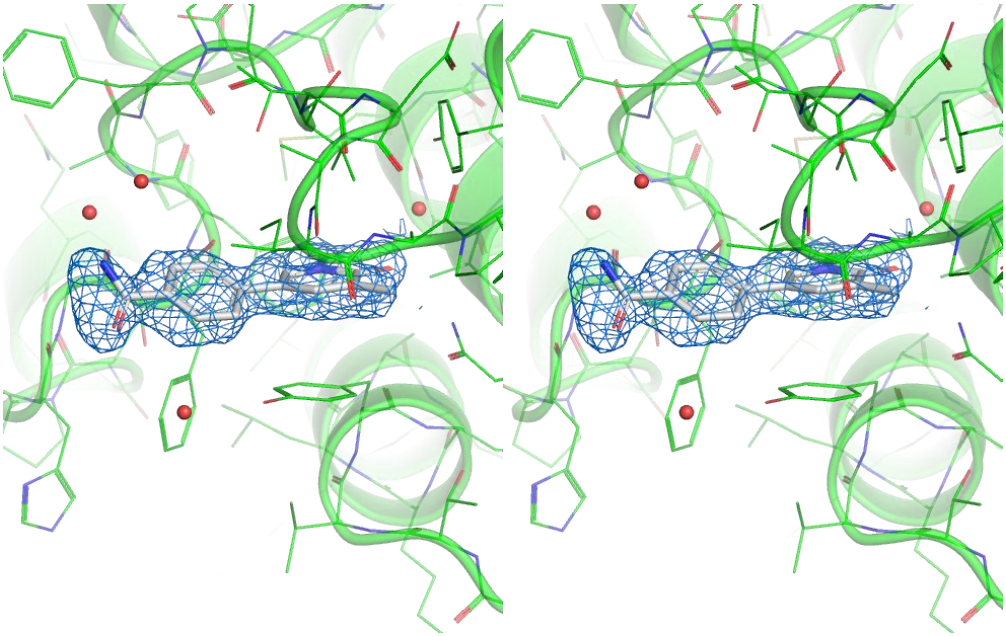

Supplementary Figure 8. Stereo image of **compound 2** bound to BRD9 (cross-eye stereo). The refined $2F_o$-F_c electon density is countoured at 1 σ.

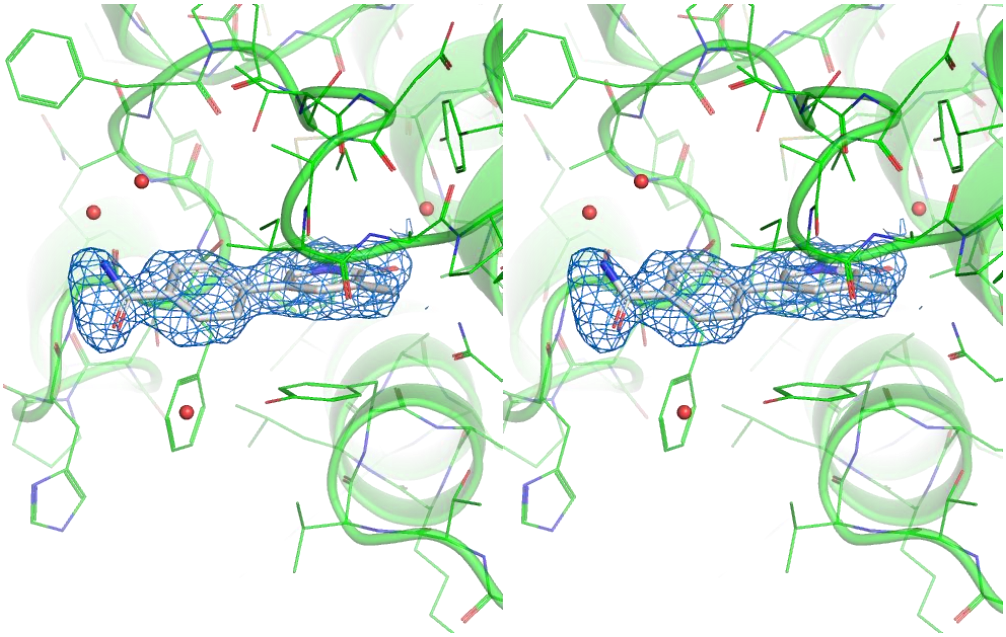

Supplementary Figure 9. Stereo image of **Compound 9** bound to BRD9 (wall-eye stereo). The refined $2F_o$-F_c electon density is countoured at 1 σ.

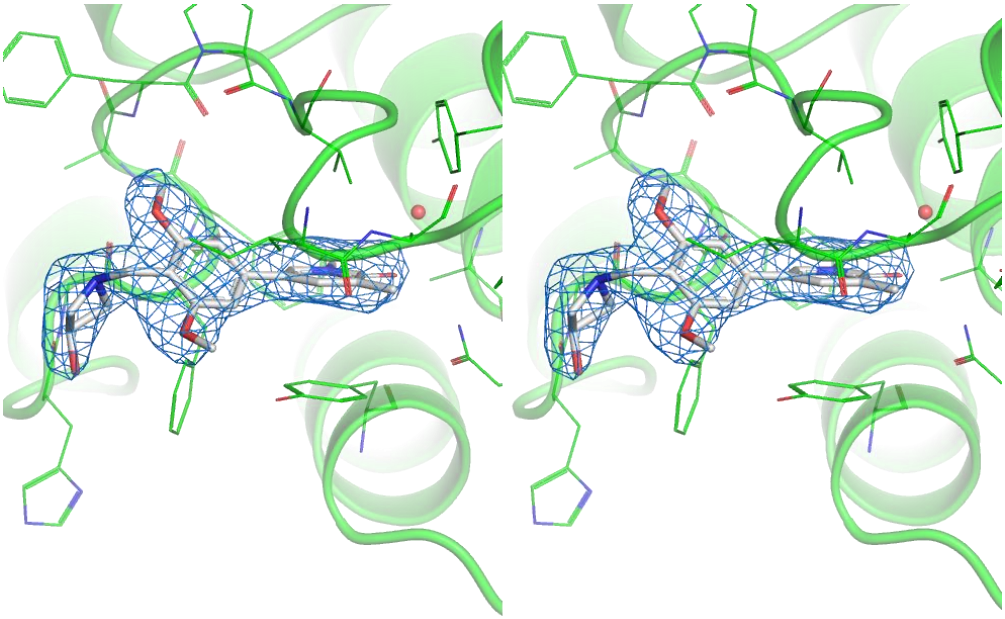

Supplementary Figure 10. Stereo image of **Compound 9** bound to BRD9 (cross-eye stereo). The refined $2F_o$-F_c electon density is countoured at 1 σ

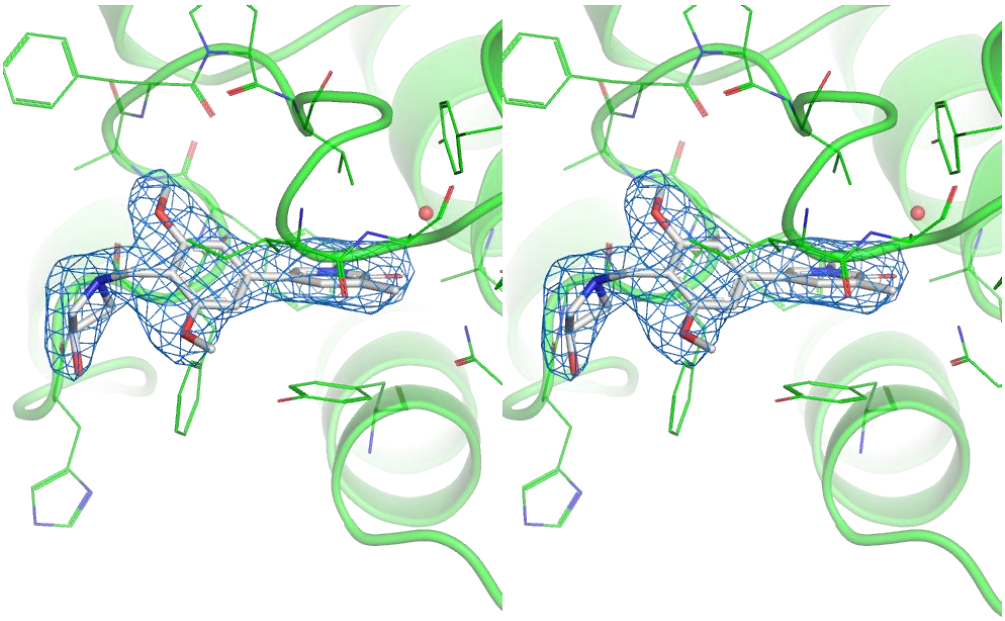

Supplementary Figure 11. Stereo image of **BI-7273** (**compound 15**) bound to BRD9 (wall-eye stereo). The refined $2F_o$-F_c electon density is countoured at 1 σ.

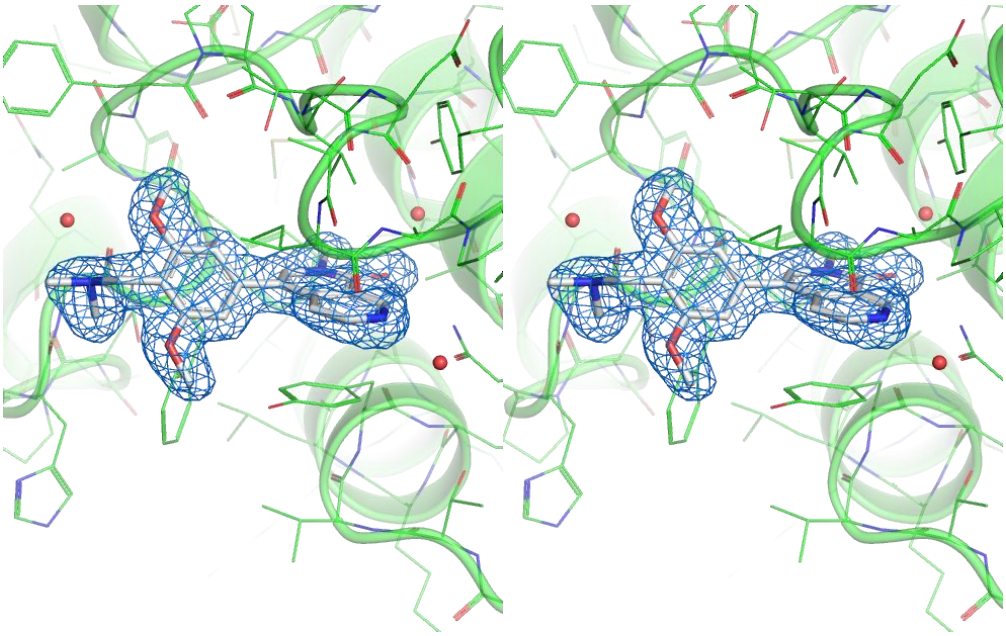

Supplementary Figure 12. Stereo image of **BI-7273** (**compound 15**) bound to BRD9 (cross-eye stereo). The refined $2F_o$-F_c electon density is countoured at 1 σ.

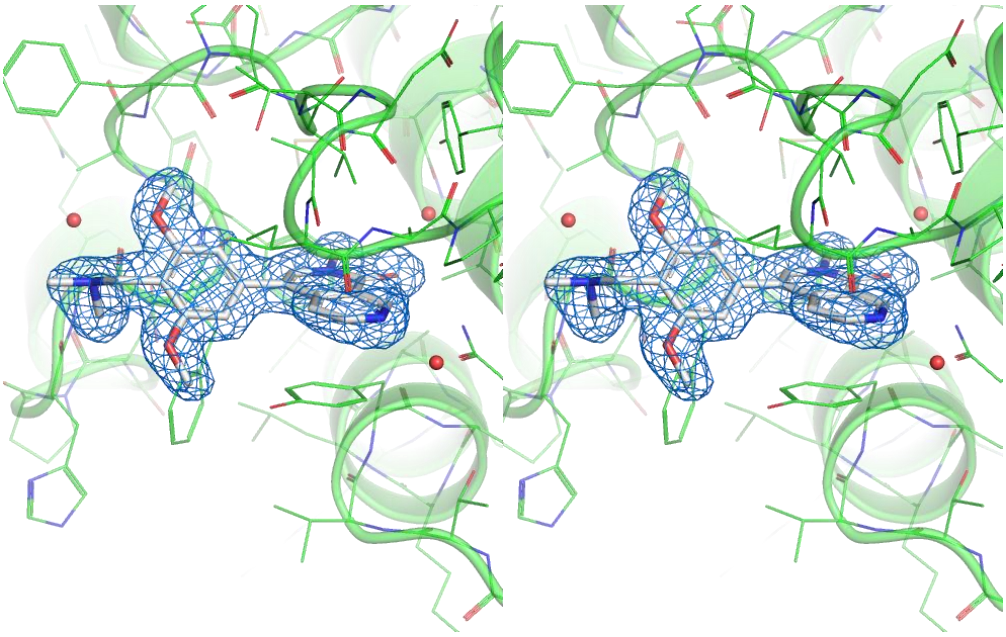

Supplementary Figure 13. Stereo image of **BI-9564** (**compound 21**) bound to BRD9 (wall-eye stereo). The refined $2F_o$-F_c electon density is countoured at 1 σ.

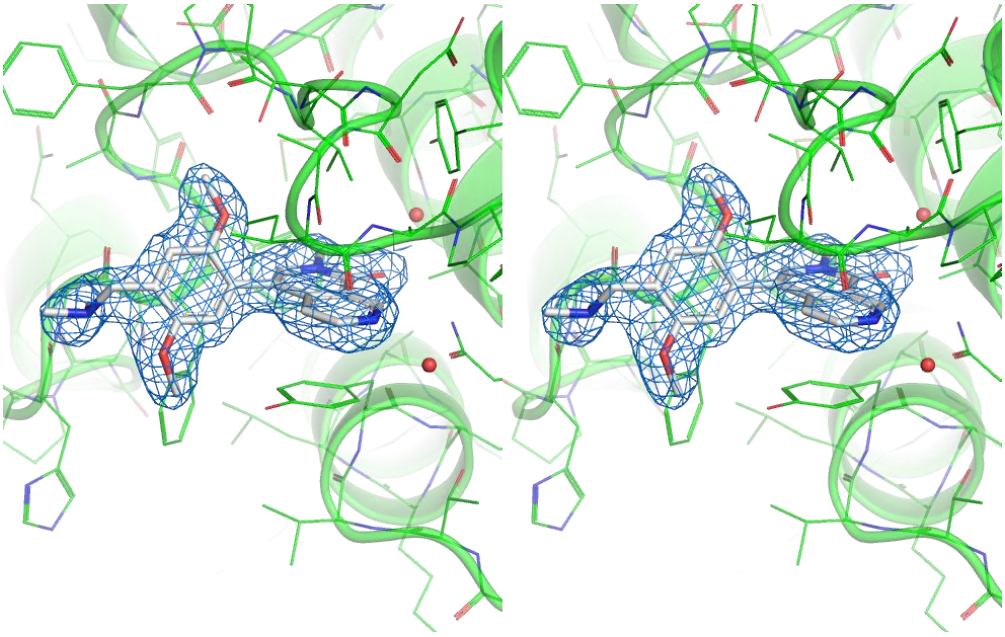

Supplementary Figure 14. Stereo image of **BI-9564** (**compound 21**) bound to BRD9 (cross-eye stereo). The refined $2F_o$-F_c electon density is countoured at 1 σ.

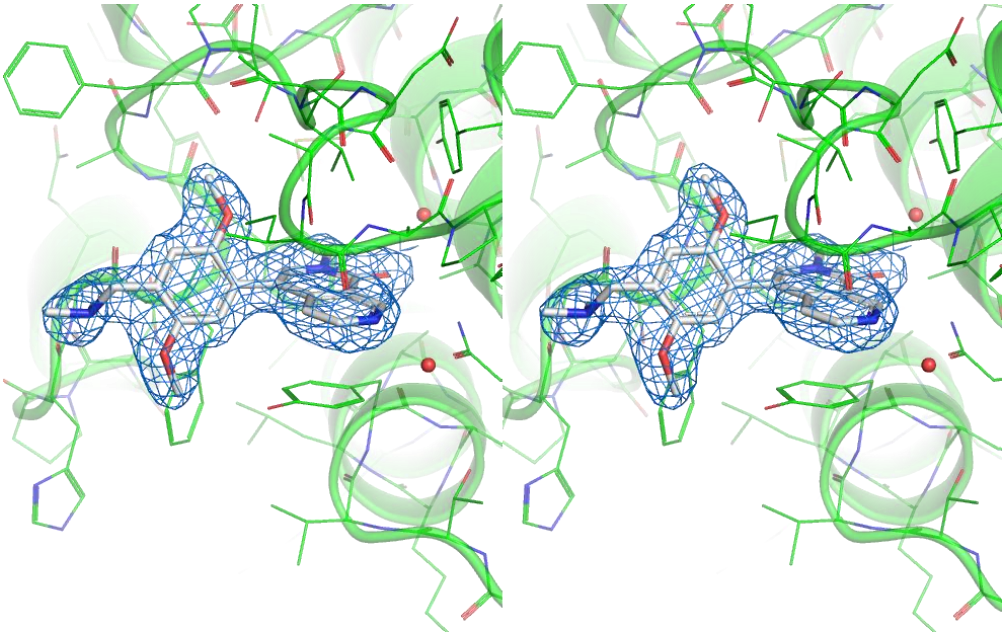

Supplementary Figure 15. Bromodomain selectivity profile for **BI-7273** using differential scanning fluorimetry against 48 bromodomains a) thermal shift difference upon treatment with **BI-7273** (ΔTm °C) **b)** histogram representation of the selectivity pattern using DSF.

BI-7273 showed binding to BRD9, BRD7 and CECR2 bromodomains. **BI-7273** is highly selective towards the BET family members.

a

target	
ASH1L	0.19
ATAD2	-0.04
BAZ1A	-0.3
BAZ1B	-0.57
BAZ2A	-0.14
BAZ2B	-0.38
BRD1	-0.17
BRD2(1)	-0.26
BRD2(2)	-0.6
BRD3(1)	-0.41
BRD3(2)	-0.51
BRD4(1)	-0.4
BRD4(2)	0.23
BRD7	9.74
BRD9	11.38
BRDT(1)	-1.03
BRDT(2)	-0.55
BRPF1A	-0.34
BRPF1B	2.2
BRPF3	-0.26
BRWD3(2)	-1.71
CECR2	8.22
CREBBP	-0.15
EP300	0.95
FALZ	0.33
GCN5L2	-0.48
ATAD2B	0
SP140L	0
MLL	-0.05
PB1(1)	0
PB1(2)	0.23
PB1(3)	0.31
PB1(4)	-0.18
PB1(5)	0.22
PB1(6)	-0.31
PCAF	-0.46
PHIP(2)	-2.05
SMARCA2	0.42
SMARCA4	0.32
SP140	-0.17
TAF1(1)	0.4
TAF1(2)	0.21
TAF1L(1)	0.43
TAF1L(2)	-0.56
TIF1-bromo	0.76
TIF1-phd-bromo	-0.08
TRIM28	0.06
WDR9(2)	-0.1

b

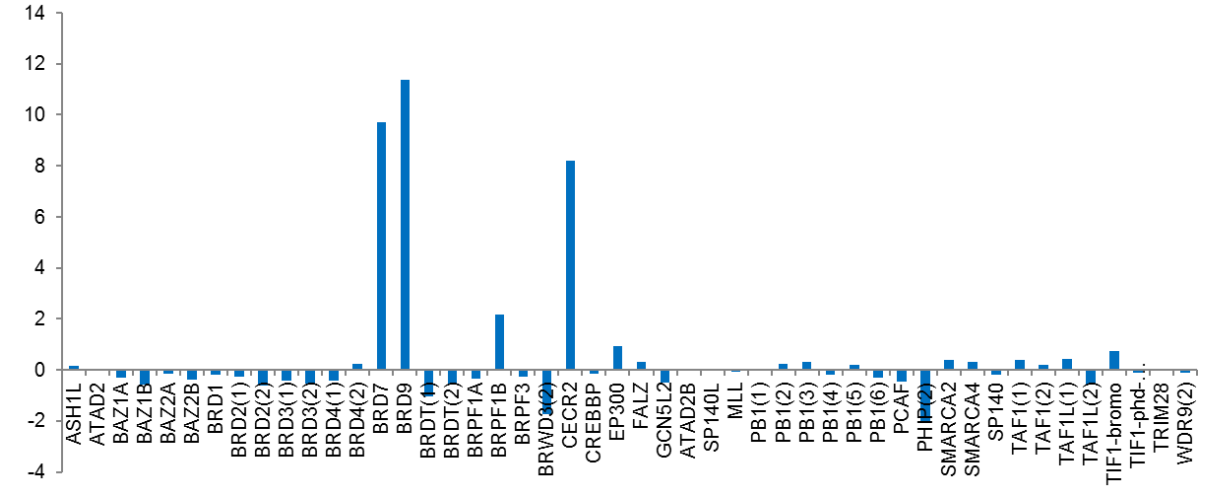
14
12
10
8
6
4
2
0
-2
-4
ASH1L
ATAD2
BAZ1A
BAZ1B
BAZ2A
BAZ2B
BRD1
BRD2(1)
BRD2(2)
BRD3(1)
BRD3(2)
BRD4(1)
BRD4(2)
BRD7
BRD9
BRDT(1)
BRDT(2)
BRPF1A
BRPF1B
BRPF3
CECR2
CREBBP
EP300
FALZ
GCN5L2
ATAD2B
SP140L
MLL
PB1(1)
PB1(2)
PB1(3)
PB1(4)
PB1(5)
PB1(6)
PCAF
SMARCA2
SMARCA4
SP140
TAF1(1)
TAF1(2)
TAF1L(1)
TAF1L(2)
TIF1-bromo
TRIM28
WDR9(2)

Supplementary Figure 16. Bromodomain selectivity profile for **BI-9564** using differential scanning fluorimetry against 48 bromodomains a) thermal shift difference upon treatment with **BI-9564** (ΔTm °C) **b)** histogram representation of the selectivity pattern using DSF**.**

BI-9564 showed binding to BRD9, BRD7 and CECR2 bromodomains. **BI-9564** is highly selective towards the BET family members.

a

Protein	
ASH1LA-p017	-0.23
ATAD2A-p023	0.01
BAZ1AA-p007	-0.34
BAZ1BA-p010	-0.17
BAZ2AA-p006	0.62
BAZ2BA-p028	-0.09
BRD1A-p020	0.43
BRD2A-p052	0.3
BRD2A-p058	0.54
BRD3A-p070	0.47
BRD3A-p071	0.87
BRD4A-p088	0.51
BRD4A-p093	0.23
BRD7A-p009	6.47
BRD9A-p022	9.21
BRDTA-p056	0.07
BRDTA-p057	0.09
BRPF1A-p020	-0.03
BRPF1B-p006	0.89
BRPF3A-p010	-1
BRWD3A-p010	1.4
CECR2A-p021	5.61
CREBBPA-p068	1.82
EP300A-p028	2.07
FALZA-p019	0.1
GCN5L2A-p013	0.45
KIAA1240A-p016	-0.1
LOC93349A-p026	0.28
MLLA-p016	0.07
PB1A-p096	-0.11
PB1A-p101	-0.28
PB1A-p102	-0.08
PB1A-p103	-0.23
PB1A-p104	0.01
PB1A-p106	0.06
PCAFA-p029	-0.06
PHIPA-p020	-1.01
SMARCA2A-p025	0.11
SMARCA4A-p020	-0.25
SP140A-p013	0.02
TAF1A-p023	0.05
TAF1A-p027	-0.03
TAF1LA-p036	-0.48
TAF1LA-p041	-0.11
TIF1A-p039	-0.66
TIF1A-p041	0.36
TRIM28A-p008	-0.24
WDR9A-p015	-0.02

b

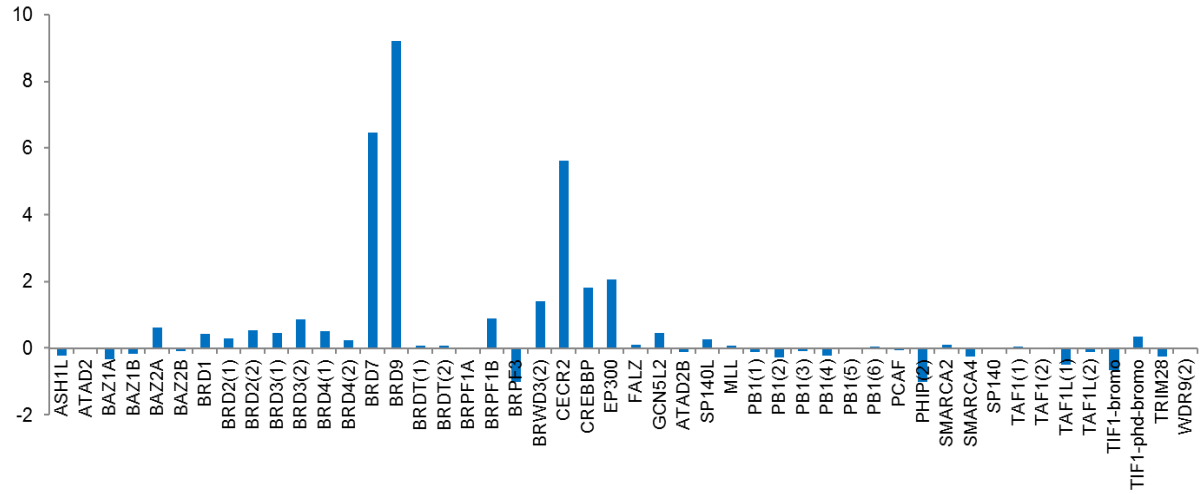
10
8
6
4
2
0
-2
ASH1L
ATAD2
BAZ1A
BAZ1B
BAZ2A
BAZ2B
BRD1
BRD2(1)
BRD2(2)
BRD3(1)
BRD3(2)
BRD4(1)
BRD4(2)
BRD7
BRD9
BRDT(1)
BRDT(2)
BRPF1A
BRPF1B
BRPF3
BRWD3(2)
CECR2
CREBBP
EP300
FALZ
GCN5L2
ATAD2B
SP140L
MLL
PB1(1)
PB1(2)
PB1(3)
PB1(4)
PB1(5)
PB1(6)
PCAF
PHIP(2)
SMARCA2
SMARCA4
SP140
TAF1(1)
TAF1(2)
TAF1L(1)
TAF1L(2)
TIF1-bromo
TIF1-phd-bromo
TRIM28
WDR9(2)

Supplementary Figure 17. DiscoveRx selectivity data for **BI-7273.**[1]
a) % ctrl bromoscan selectivity data at 10 µM (table and phylogenetic tree) ; **b**) BromoMax Kd for selected bromodomains

a

Target	
Gene Symbol	%Ctrl @ 10000nM
ATAD2A	62
ATAD2B	65
BAZ2A	0
BAZ2B	37
BRD1	1.4
BRD2(1)	54
BRD2(2)	55
BRD3(1)	42
BRD3(2)	57
BRD4(1)	59
BRD4(2)	73
BRD7	0.45
BRD9	0
BRDT(1)	62
BRDT(2)	85
BRPF1	3
BRPF3	36
CECR2	0
CREBBP	26
EP300	31
FALZ	0.2
GCN5L2	18
PBRM1(2)	62
PBRM1(5)	90
PCAF	39
SMARCA2	29
SMARCA4	60
TAF1(2)	1.7
TAF1L(2)	12
TRIM24(PHD,Bromo.)	67
TRIM33(PHD,Bromo.)	52
WDR9(2)	80

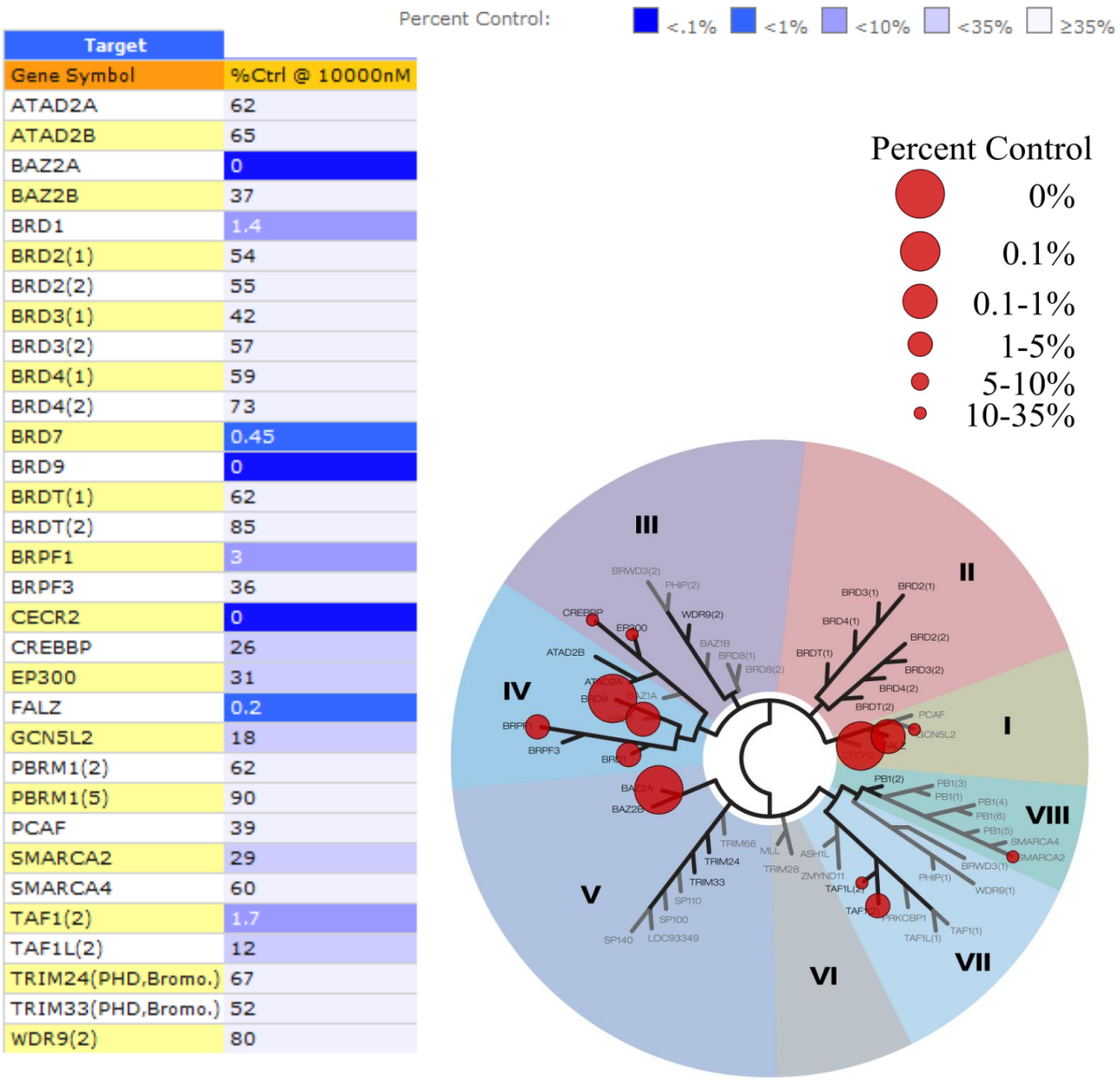

b

Targets	Kd (nM)
BAZ2A	>3,000
BRD1	2,600
BRD4-BD1	> 10,000
BRD7	0
BRD9	**1**
BRPF1	210

Targets	Kd (nM)
CECR2	9
CREBBP	8,600
EP300	10,000
FALZ	850
TAF1(2)	1,000
TAF1L(2)	1,200

Supplementary Figure 18. DiscoveRx selectivity data for **BI-9564.**
a) % ctrl bromoscan selectivity data at 10 µM (table and phylogenetic tree) ; **b**) BromoMax Kd for selected bromodomains

a

Target	
Gene Symbol	%Ctrl @ 10000nM
ATAD2A	81
ATAD2B	60
BAZ2A	20
BAZ2B	74
BRD1	27
BRD2(1)	55
BRD2(2)	85
BRD3(1)	60
BRD3(2)	36
BRD4(1)	61
BRD4(2)	64
BRD7	1.1
BRD9	0
BRDT(1)	82
BRDT(2)	57
BRPF1	31
BRPF3	41
CECR2	0
CREBBP	7.2
EP300	17
FALZ	22
GCN5L2	82
PBRM1(2)	83
PBRM1(5)	64
PCAF	83
SMARCA2	39
SMARCA4	55
TAF1(2)	8.4
TAF1L(2)	18
TRIM24(PHD,Bromo.)	41
TRIM33(PHD,Bromo.)	77
WDR9(2)	83

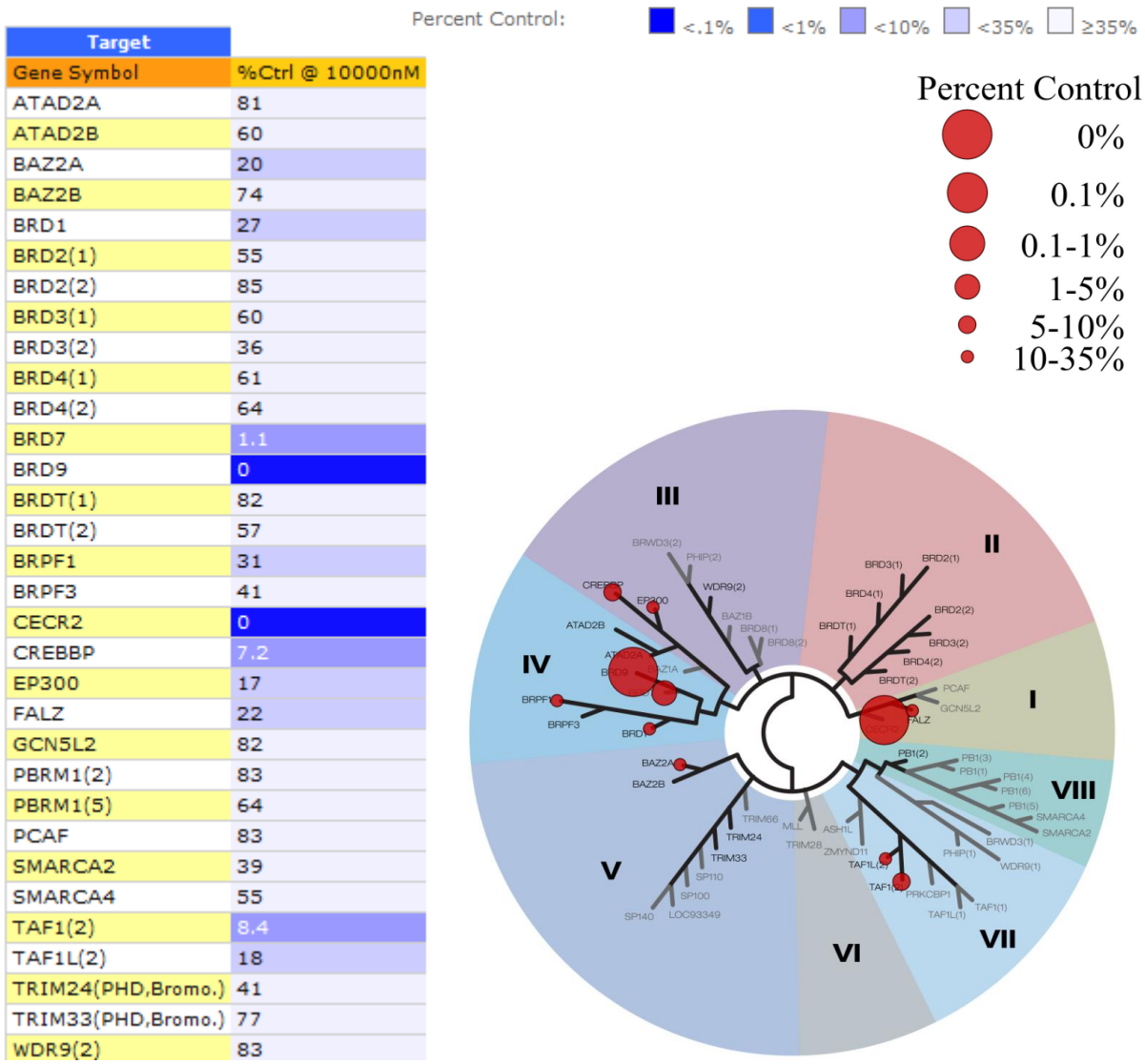

b

Targets	Kd (nM)
BRD4-BD1	> 10,000
BRD7	82
BRD9	**5**
BRPF1	790
CECR2	77

Targets	Kd (nM)
CREBBP	2,700
FALZ	>10,000
GCN5L2	>10,000
TAF1(2)	3,800
TAF1L(2)	4,100

Supplementary Figure 19. ITC analysis of **BI-7273** in CECR2 (T=293.15K)
Compound **BI-7273** binds CECR2 with a K_D value of 187 nM (ΔH = -12.4 kcal/mol)

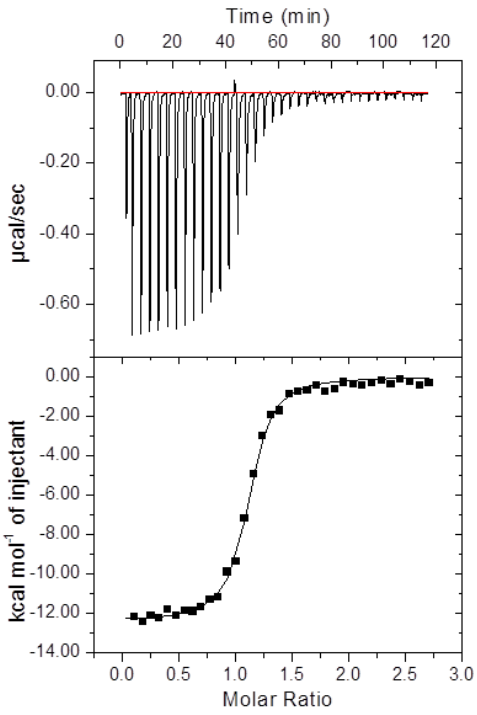

ITC type	Protein	K_A (10^6 M^{-1})	K_D (nM)	N	ΔH (kcal/mol)	TΔS (kcal/mol)	ΔG (kcal/mol)
VP-ITC	CECR2	5.36 ± 0.46	186.57	1.090 ± 0.005	-12.38 ± 0.089	-3.576	-8.804

Supplementary Figure 20. ITC analysis of **BI-9564** in BRD7 and CECR2 (T=293.15 K) a) Compound **BI-9564** binds BRD7 with a K_D value of 239 nM (ΔH = -6.9 kcal/mol); b) Compound **BI-9564** binds CECR2 with a K_D value of 200 nM (ΔH = -11.9 kcal/mol)

a

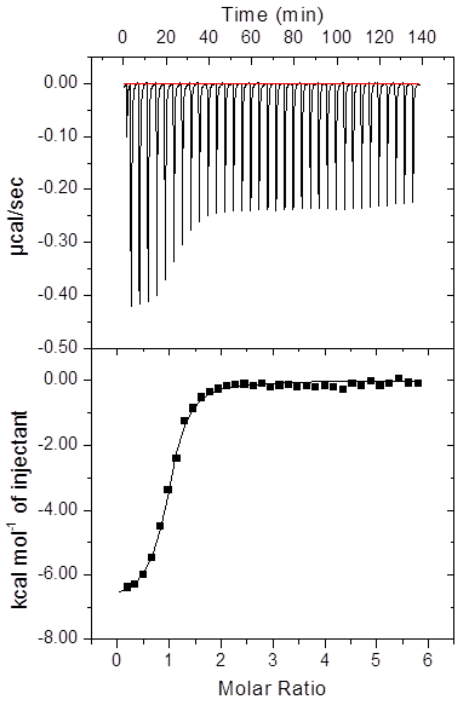

ITC type	Protein	K_A (10^6 M^{-1})	K_D (nM)	N	ΔH (kcal/mol)	TΔS (kcal/mol)	ΔG (kcal/mol)
VP-ITC	BRD7	4.18 ± 0.39	239.23	0.951 ± 0.011	-6.88 ± 0.103	1.879	-8.761

b

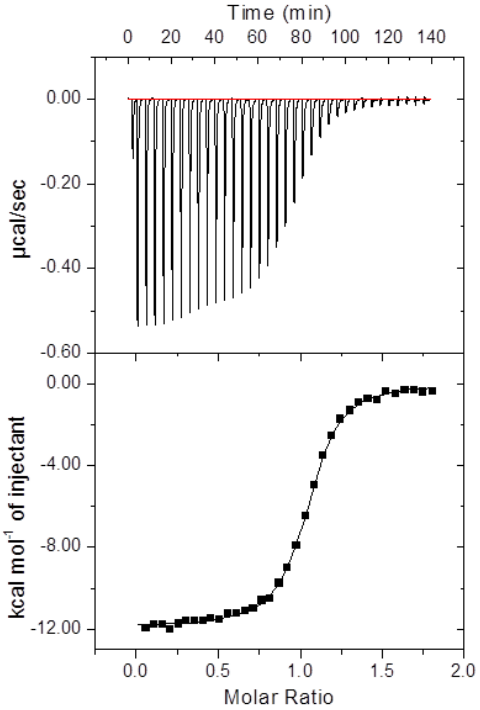

ITC type	Protein	K_A (10^6 M^{-1})	K_D (nM)	N	ΔH (kcal/mol)	TΔS (kcal/mol)	ΔG (kcal/mol)
VP-ITC	CECR2	4.99 ± 0.17	200.40	1.040 ± 0.002	-11.89 ± 0.032	-3.107	-8.783

Supplementary Figure 21. Recovery After Photobleaching (FRAP) assay U2OS cells transfected with GFP-BRD7 for **BI-7273**

(a) Influence of **BI-7273** on half recovery times of U2OS cells transfected with wild-type full-length GFP-BRD7 or the N211F mutant construct. Cells were treated with 2.5 μM SAHA (shown by "#") to increase the assay window. Bars indicate by * indicates $p < 0.05$ significant difference from wt treated with SAHA. (b) Time dependence of fluorescence recovery in the bleached area of cells expressing wt or mutant GFP-BRD9 with the corresponding treatment as in (a).

Curves represent averaged data of at least 20 replicates.

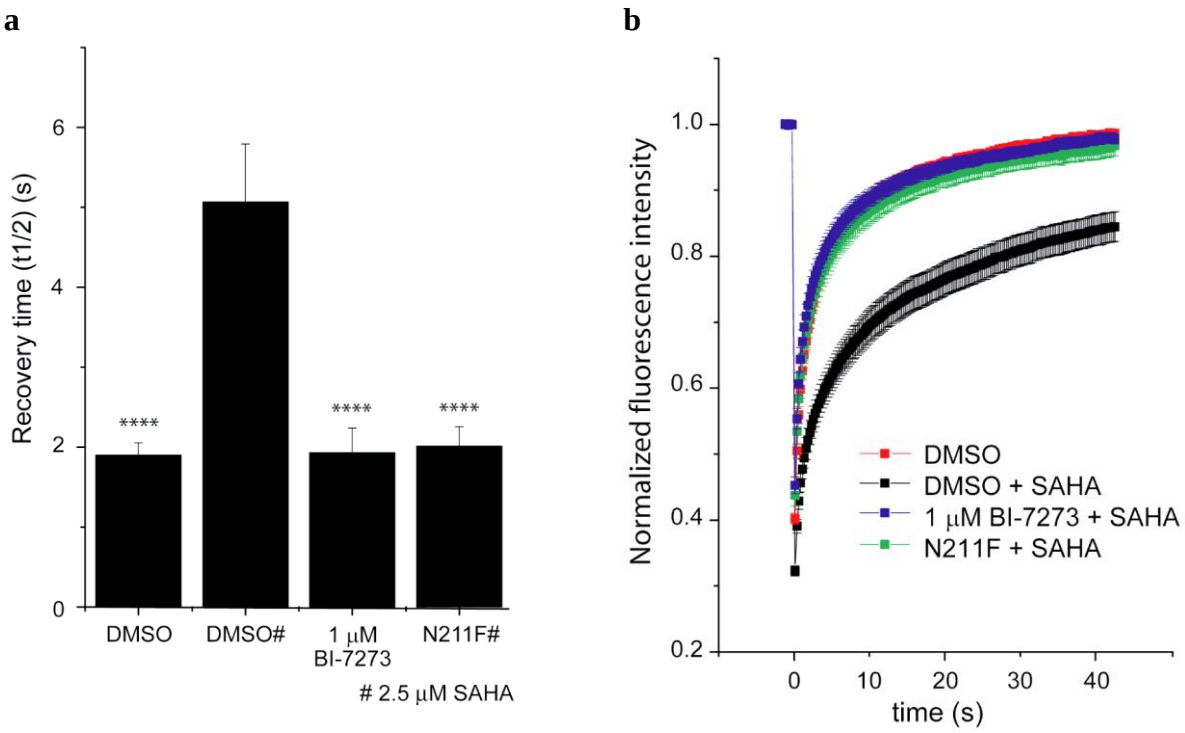

Supplementary Figure 22. Recovery After Photobleaching (FRAP) assay U2OS cells transfected with GFP-BRD7 for **BI-9564**

(a) Influence of **BI-9564** on half recovery times of U2OS cells transfected with wild-type full-length GFP-BRD7 or the N211F mutant construct. Cells were treated with 2.5 μM SAHA (shown by "#") to increase the assay window. Bars indicate by * indicates $p < 0.05$ significant difference from wt treated with SAHA. (b) Time dependence of fluorescence recovery in the bleached area of cells expressing wt or mutant GFP-BRD9 with the corresponding treatment as in (a).

Curves represent averaged data of at least 20 replicates.

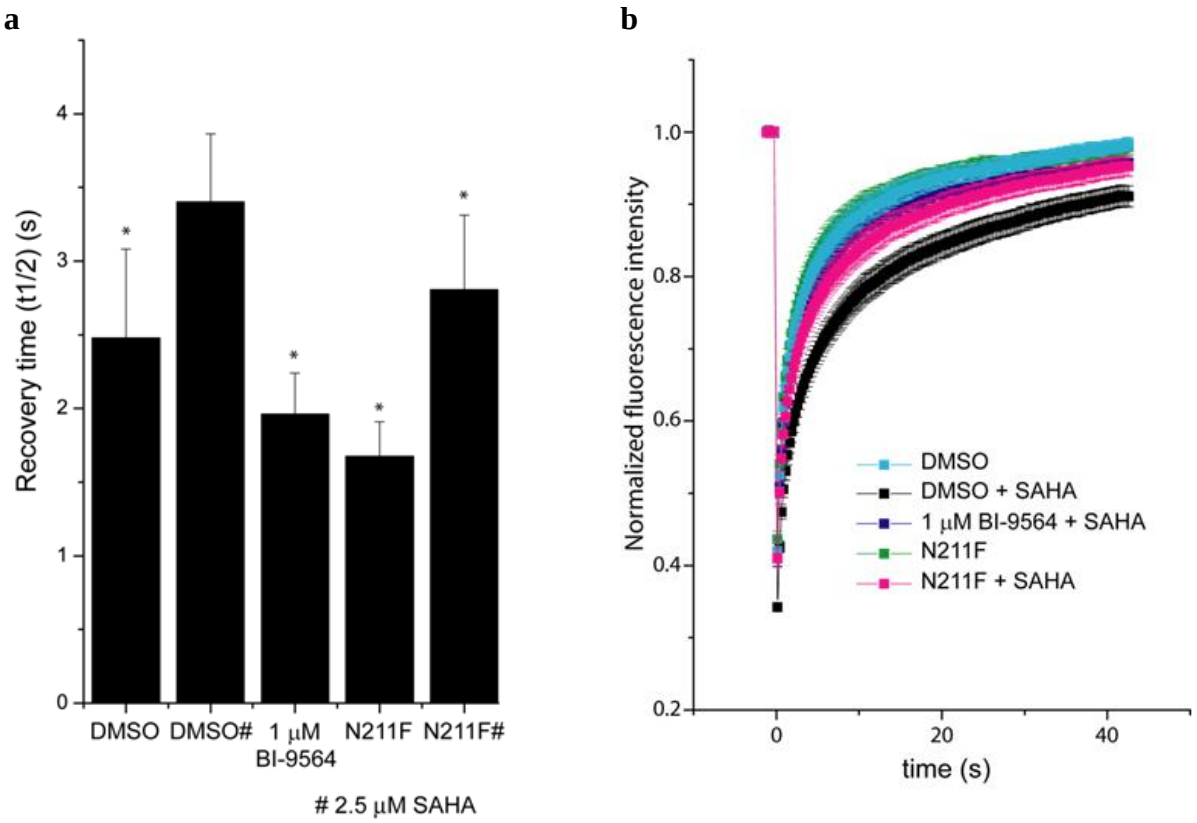

Supplementary Figure 23. Recovery After Photobleaching (FRAP) assay U2OS cells transfected with GFP-CECR2 for **BI-9564**

(a) Influence of **BI-9564** on half recovery times of U2OS cells transfected with wild-type full-length GFP-CECR2 or the N140F mutant construct. Cells were treated with 2.5 μM SAHA (shown by "#") to increase the assay window. Bars indicate by * indicates $p < 0.05$ significant difference from wt treated with SAHA. No cellular inhibition of CECR2 bromodomain was observed with 1μM **BI-9564** (b) Time dependence of fluorescence recovery in the bleached area of cells expressing wt or mutant GFP-CECR2 with the corresponding treatment as in (a).

Curves represent averaged data of at least 20 replicates.

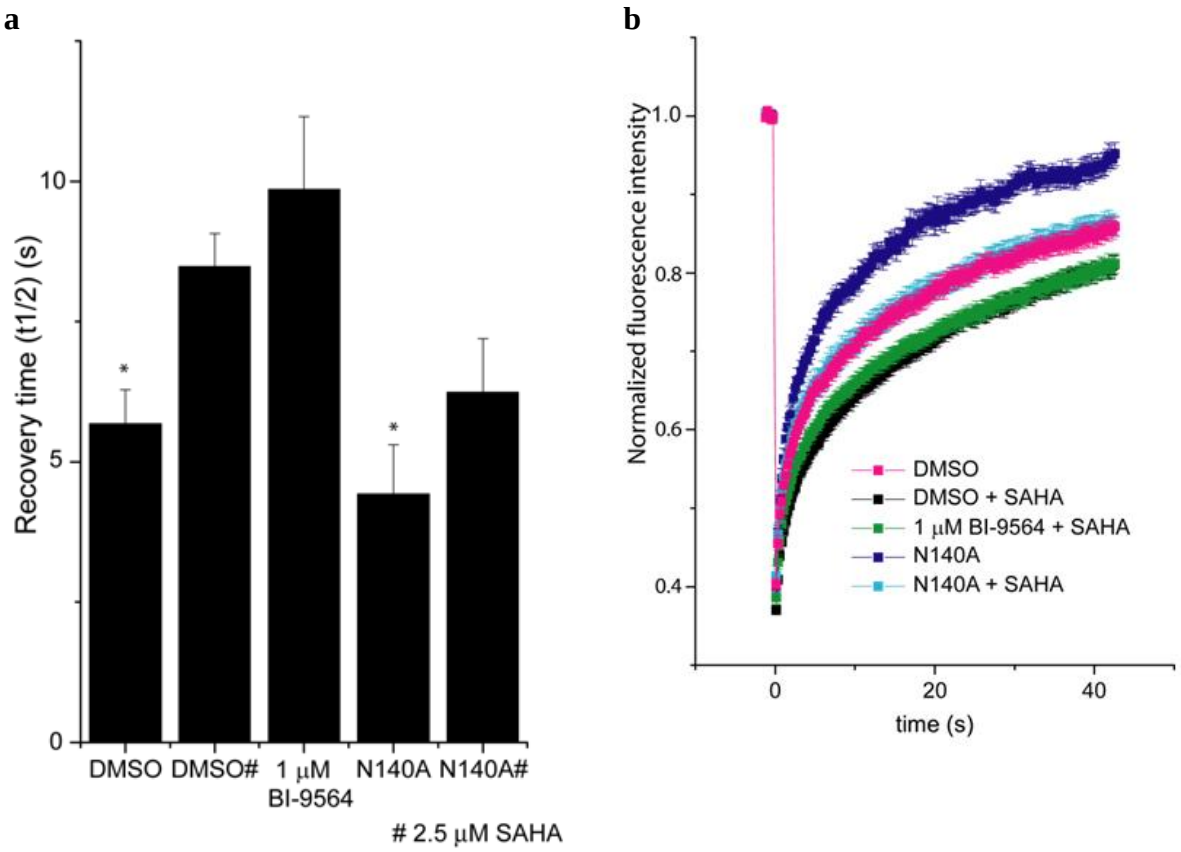

Supplementary Figure 24. Selectivity profile of **BI-9564** towards kinase and GPCR
a) kinase selectivity profile (% inhibition at 10 µM on 324 kinases). 282 kinases showed < 10% inhibition at 10 µM, 3 kinases showed > 40 % inhibition at 10 µM [IC_{50}(**BI-9564**, ACVR1)= 5090 nM, IC_{50}(**BI-9564**, TGFBR1)=5140 nM, IC_{50}(**BI-9564**, ACVR2B)=7680 nM] ; b) GPCR selectivity profile (% inhibition at 10 µM on 55 GPCR). 2 GPCR showed > 40 % Inhibition at 10 µM

a

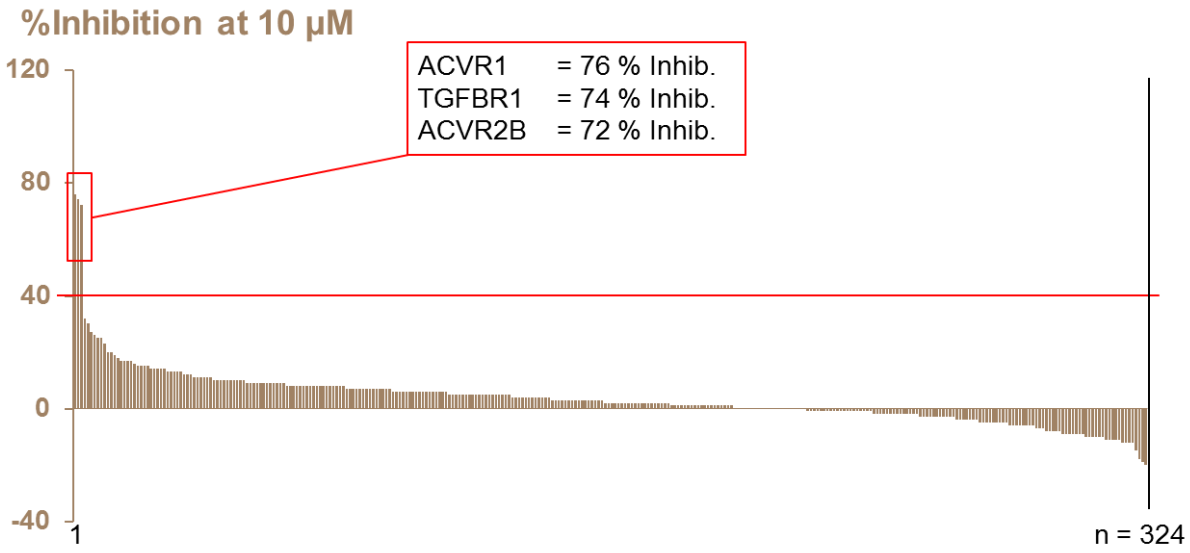

b

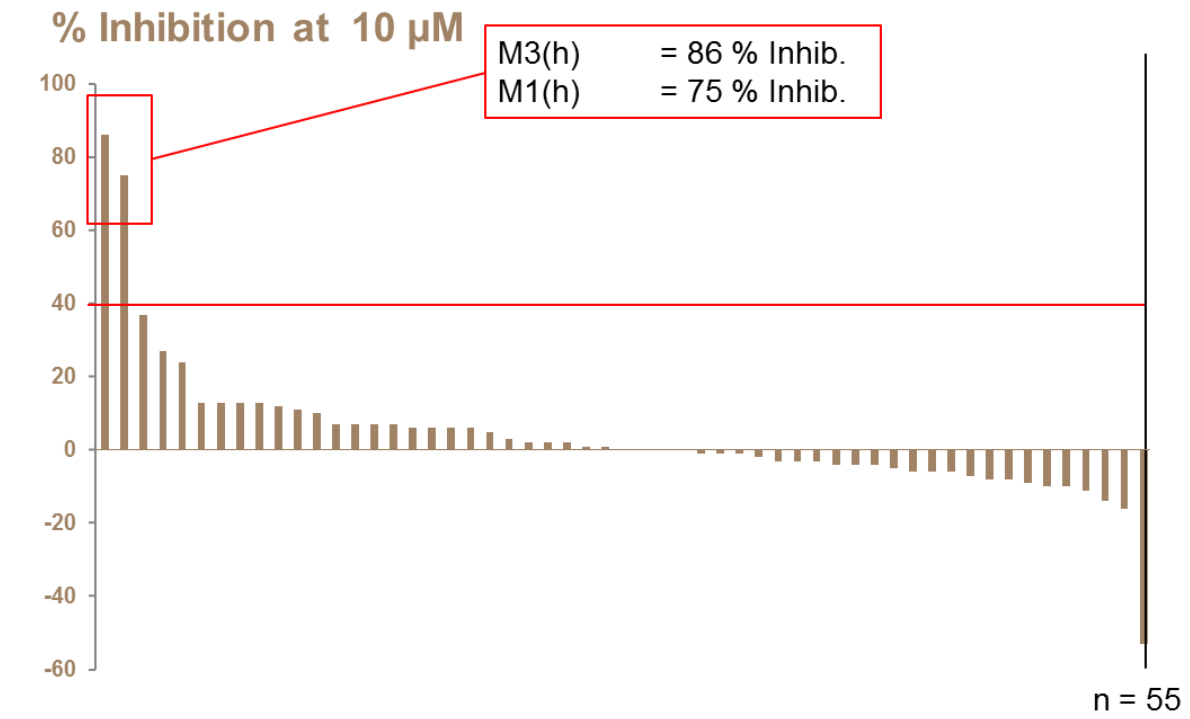

Supplementary Figure 25. PK profile of **BI-7273** in mice upon *i.v.* administration (5 mg/kg)

BI-7273 5 mg/kg INTRAVENOUS BOLUS Mus musculus (house mouse)

BomTac:NMRI-Foxn1nu

1.02 mg BI-7273 + 2 µl HCl 1M + 814 µl HP-ß-CD 25 %

		Blood Plasma Concentration [nM]							
	Time	Animal 1	Animal 2	Animal 3				Mean	Stddev
MW (Salt) 353 g/Mol	0,083	7330	6390	7720				7150	683
MW (Base) 353 g/Mol	0,250	3590	2470	4700				3590	1110
Dose (Base) 5 mg/kg	1,000	1060	456	532				683	330
14,1 µMol/kg	6,000	4,56	3,82	5,23				4,54	0,708
	24,000								
LLOQ 3,8 nM									
QNMR 8 µM									
AUD Range		0h...06h	0h...06h	0h...06h					
AUD [nM*h]		5930	3520	4980				4810	1220
AUC [nM*h]		5930	3520	4990				4810	1220
MRT [h]		0,6	0,5	0,5				0,5	0,1
Clearance [ml/min/kg]		40	67	47				51	14
Vss [l/kg]		1,5	2,0	1,3				1,6	0,4
Clearance [%QH]								57	

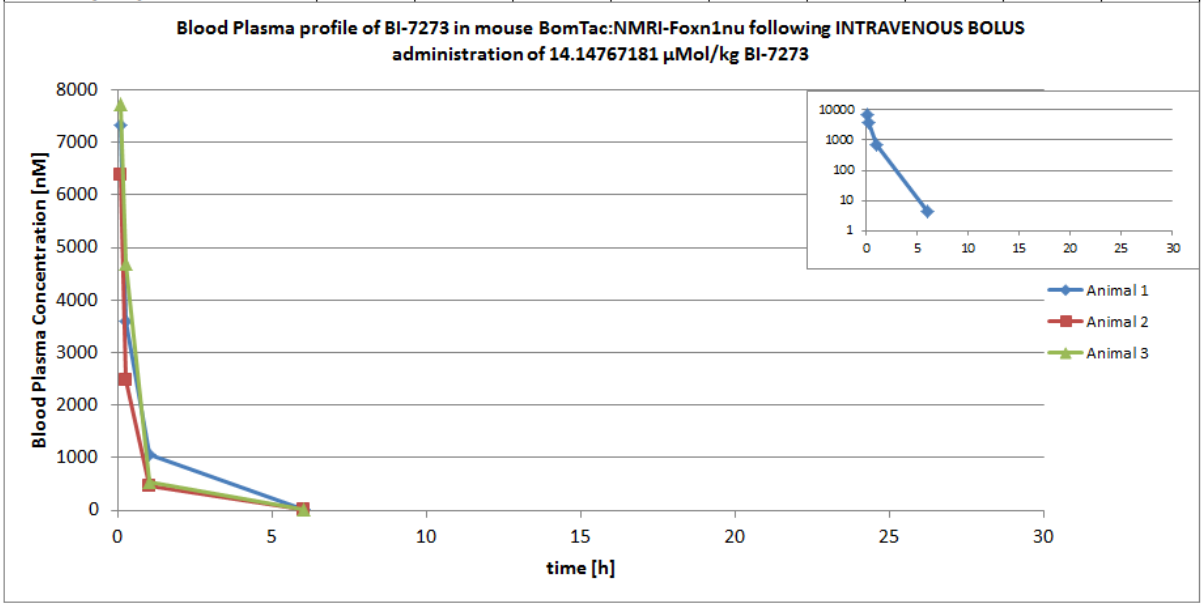

Supplementary Figure 26. PK profile of **BI-7273** in mice upon *p.o.* administration (20 mg/kg)

BI-7273 20 mg/kg per os, fed animal Mus musculus (house mouse)

BomTac:NMRI-Foxn1nu

4.08 mg BI-7273 + 1,632 µl Natrosol 0.5 %

		Time	Blood Plasma Concentration [nM] Animal 1	Animal 2	Animal 3				Mean	Stddev
MW (Salt)	353 g/Mol	0,500	351	263	235				283	60,5
MW (Base)	353 g/Mol	1,000	611	4700	973				2090	2260
Dose (Base)	20 mg/kg	2,000	2730	1830	1490				2010	644
	56,6 µMol/kg	6,000	50,4	80,1	56				62,2	15,8
		24,000	3,59	3,2	7,92				4,9	2,62
LLOQ	2,56 nM									
QNMR	8 µM									
AUD Range			0h...24h	0h...24h	0h...24h					
AUD [nM*h]			8050	9130	5250				7470	2000
Cmax [nM]			2730	4700	1490				2970	1620
Tmax [h]			2,0	1,0	2,0				1,7	0,6

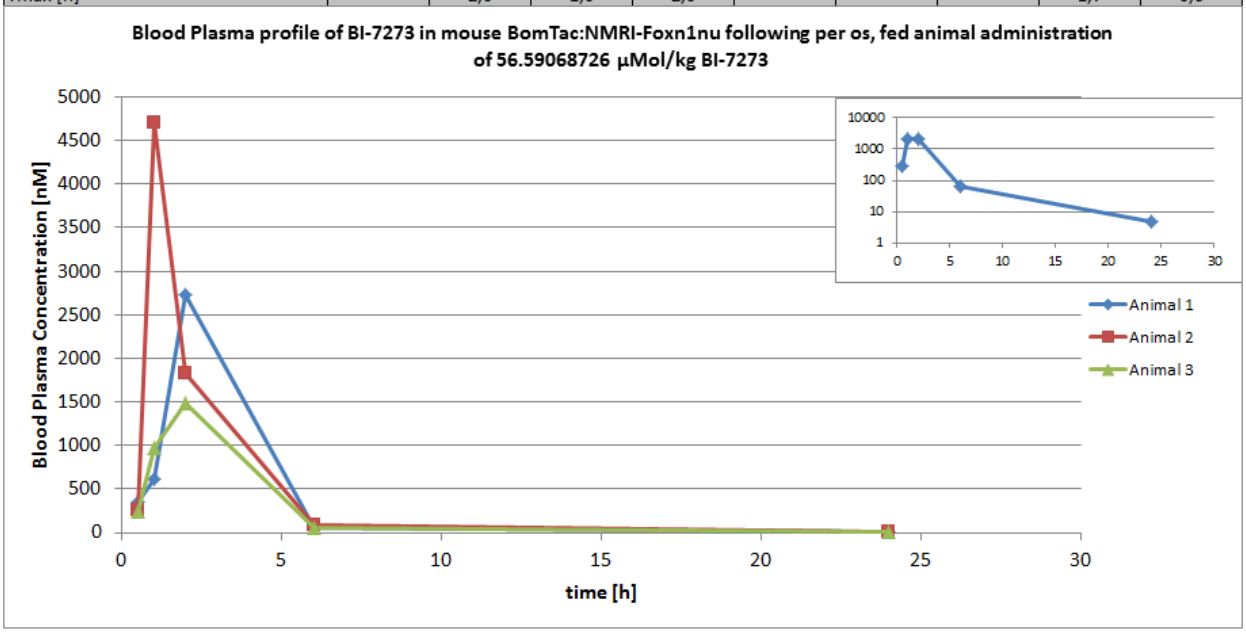

Supplementary Figure 27. PK profile of **BI-7273** in mice upon *p.o.* administration (180 mg/kg)

BI-7273 180 mg/kg per os, fed animal Mus musculus (house mouse)

BomTac:NMRI-Foxn1nu

30.88 mg BI-7273 + 1,680 µl Natrosol 0.5 %

			Blood Plasma Concentration [nM]							
		Time	Animal 1	Animal 2	Animal 3				Mean	Stddev
MW (Salt)	353 g/Mol	0,500	21200	*17900*	20700				21000	340
MW (Base)	353 g/Mol	1,000	21800	*26600*	28100				25000	4440
Dose (Base)	180 mg/kg	2,000	14200	*20900*	26100				20100	8360
	509 µMol/kg	6,000	3760	*1700*	973				2370	1970
		24,000	532		31,4				282	354
LLOQ	19,7 nM									
QNMR	9,79 µM									
AUD Range			0h...24h		0h...24h					
AUD [nM*h]			109000		108000				108000	817
AUC [nM*h]			113000		108000				110000	3480
Cmax [nM]			21800		28100				25000	4440
Tmax [h]			1,0		1,0				1,0	0,0
MRT [h]			5,1		2,1				3,6	2,1
F [%]			65		62				64	2,0

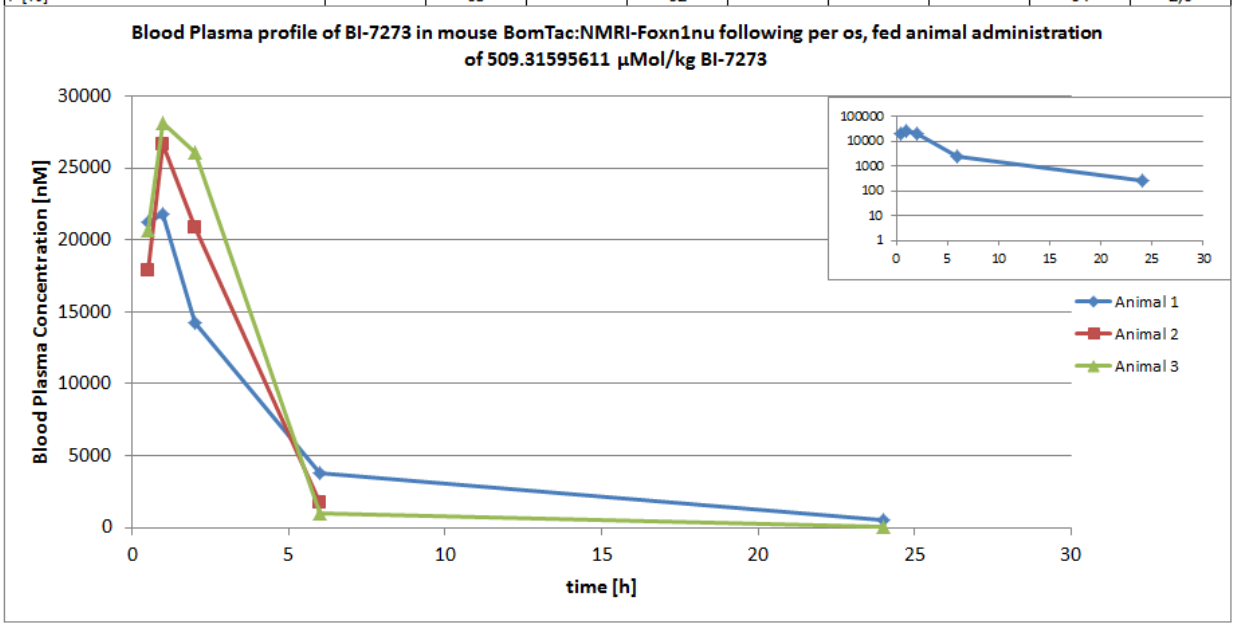

Supplementary Figure 28. PK profile of **BI-9564** in mice upon *i.v.* administration (5 mg/kg)

BI-9564 5 mg/kg INTRAVENOUS BOLUS Mus musculus (house mouse)

BomTac:NMRI-Foxn1nu

1.08 mg BI-9564 + 2 µl HCl 1M + 970 µl HP-ß-CD 25 %

			Blood Plasma Concentration [nM]							
		Time	Animal 1	Animal 2	Animal 3				Mean	Stddev
MW (Salt)	353 g/Mol	0,083	4300	5090	4840				4740	404
MW (Base)	353 g/Mol	0,250	2150	2890	3400				2810	627
Dose (Base)	5 mg/kg	1,000	509	849	789				716	181
	14,1 µMol/kg	6,000	4,53	3,65	7,47				5,22	2
		24,000								
LLOQ	3,6 nM									
QNMR	9 µM									
AUD Range			0h...06h	0h...06h	0h...06h					
AUD [nM*h]			3180	4620	4650				4150	843
AUC [nM*h]			3180	4620	4660				4150	843
MRT [h]			0,6	0,6	0,6				0,6	0,0
Clearance [ml/min/kg]			74	51	51				59	14
Vss [l/kg]			2,6	1,9	1,9				2,1	0,4
Clearance [%QH]									65	

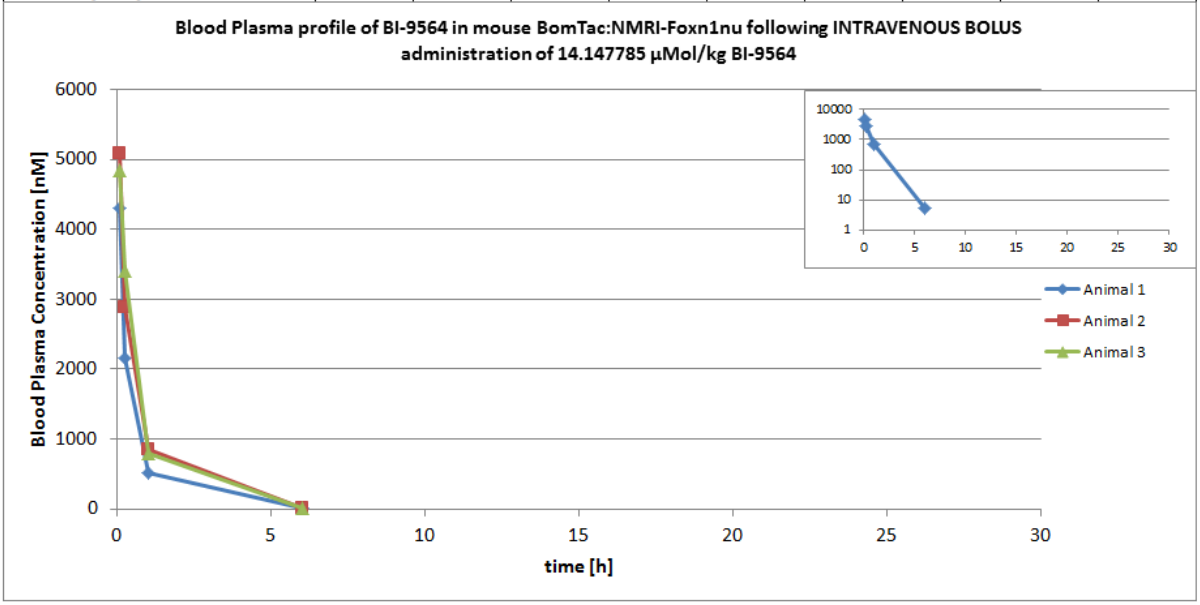

Supplementary Figure 29. PK profile of **BI-9564** in mice upon *p.o.* administration (20 mg/kg)

BI-9564	20 mg/kg	per os, fed animal	Mus musculus (house mouse) BomTac:NMRI-Foxn1nu

4.12 mg BI-9564 + 1,854 µl Natrosol 0.5 %

		Time	Blood Plasma Concentration [nM] Animal 1	Animal 2	Animal 3				Mean	Stddev
MW (Salt)	353 g/Mol	0,500	5550	4440	4220				4730	712
MW (Base)	353 g/Mol	1,000	4130	3480	6170				4590	1400
Dose (Base)	20 mg/kg	2,000	1440	2940	2830				2400	838
	56,6 µMol/kg	6,000	85,7	216	402				234	159
		24,000	5,69	18	8,4				10,7	6,48
LLOQ	5,6 nM									
QNMR	9 µM									
AUD Range			0h...24h	0h...24h	0h...24h					
AUD [nM*h]			10500	14700	18300				14500	3930
AUC [nM*h]			10500	14800	18300				14500	3930
Cmax [nM]			5550	4440	6170				5390	874
Tmax [h]			0,5	0,5	1,0				0,7	0,3
F [%]			63	89	110				88	24

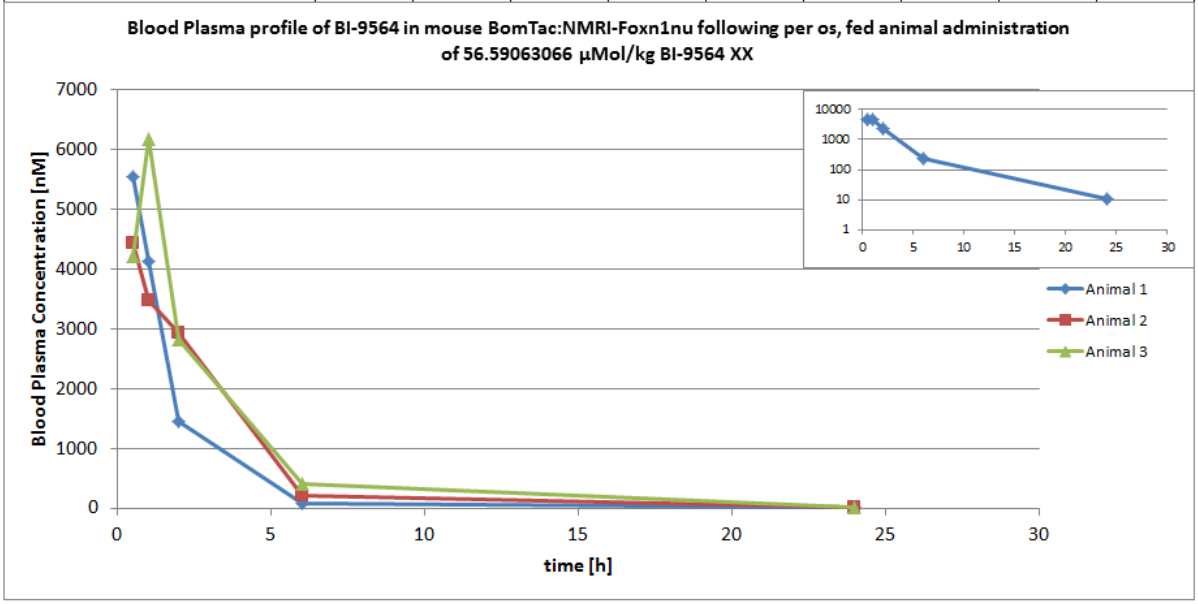

Supplementary Figure 30. PK profile of **BI-9564** in mice upon *p.o.* administration (180 mg/kg)

BI-9564 180 mg/kg per os, fed animal Mus musculus (house mouse)

BomTac:NMRI-Foxn1nu

29.74 mg BI-9564 + 1,591 µl Natrosol 0.5 %

			Blood Plasma Concentration [nM]							
		Time	Animal 1	Animal 2	Animal 3				Mean	Stddev
MW (Salt)	353 g/Mol	0,500	29100	32000	41600				34200	6530
MW (Base)	353 g/Mol	1,000	31400	24300	28300				28000	3560
Dose (Base)	180 mg/kg	2,000	22900	19500	29700				24000	5210
	509 µMol/kg	6,000	10700	9390	14600				11600	2690
		24,000	11,1	14,1	55,5				26,9	24,8
LLOQ	19,8 nM									
QNMR	9,63 µM									
AUD Range			0h...24h	0h...24h	0h...24h					
AUD [nM*h]			213000	186000	277000				226000	46600
AUC [nM*h]			213000	186000	277000				226000	46600
Cmax [nM]			31400	32000	41600				35000	5720
Tmax [h]			1,0	0,5	0,5				0,7	0,3
MRT [h]			4,0	4,0	4,2				4,1	0,1
F [%]			143	125	185				151	31

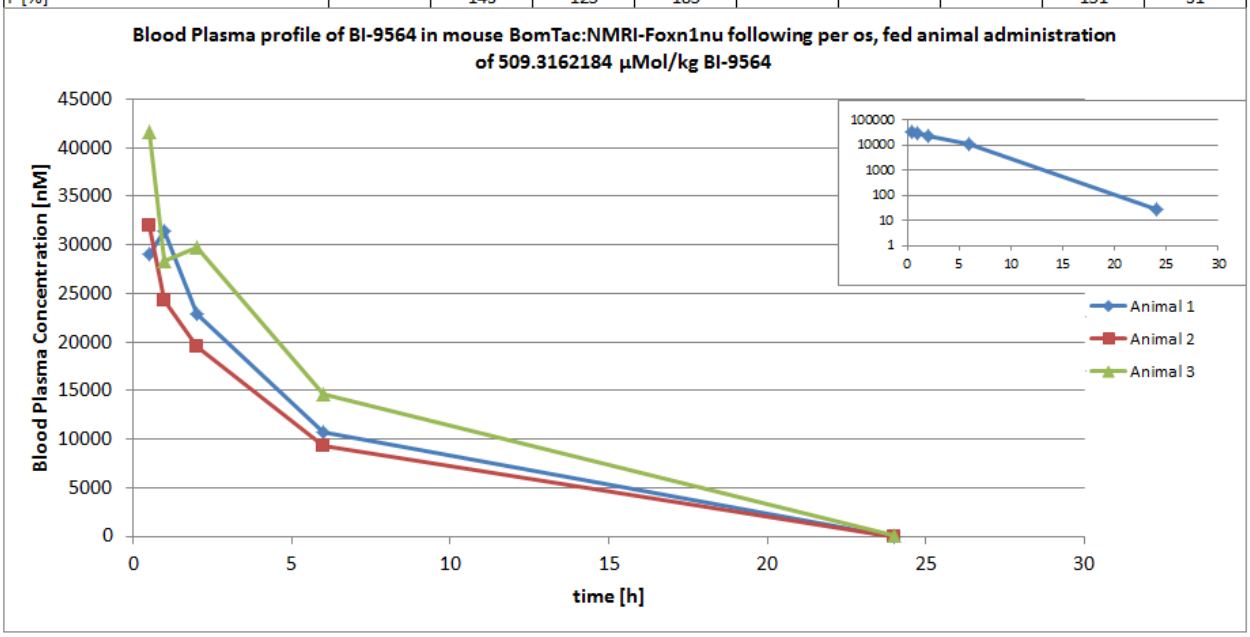

Supplementary Figure 31. Representation of the EC50s of **BI-9564** over various cell lines. (Red bars: AML cell lines).

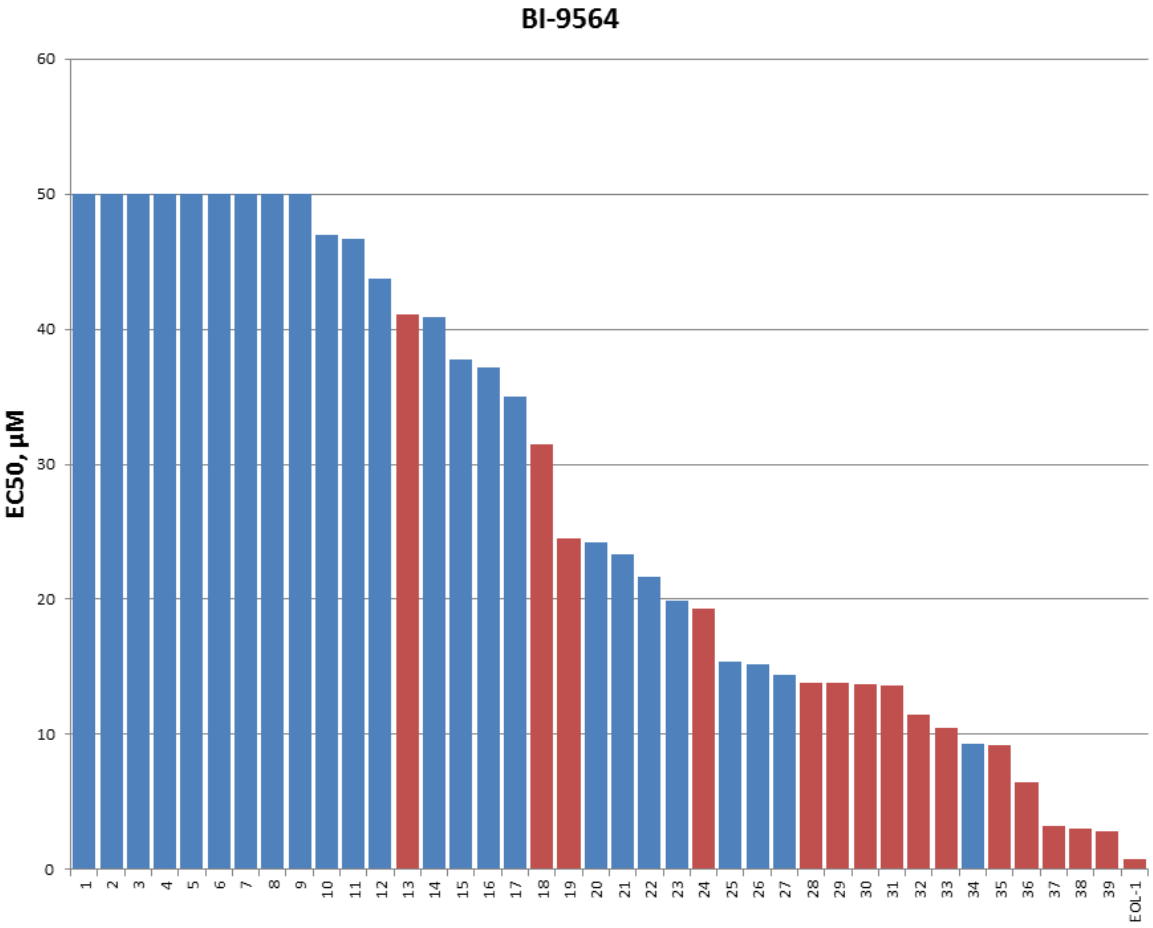

Supplementary Figure 32. Dose dependent partial reduction in MYC levels by BRD9 inhibitors. MV-4-11 cells were treated for 2 hour with BRD9 inhibitors before analysis of MYC protein levels by ELISA

a) MYC reduction levels upon treatment with **BI-7189**, b) MYC reduction levels upon treatment with **BI-7271**, c) MYC reduction levels upon treatment with **BI-7273**, d) MYC reduction levels upon treatment with **BI-9564**.

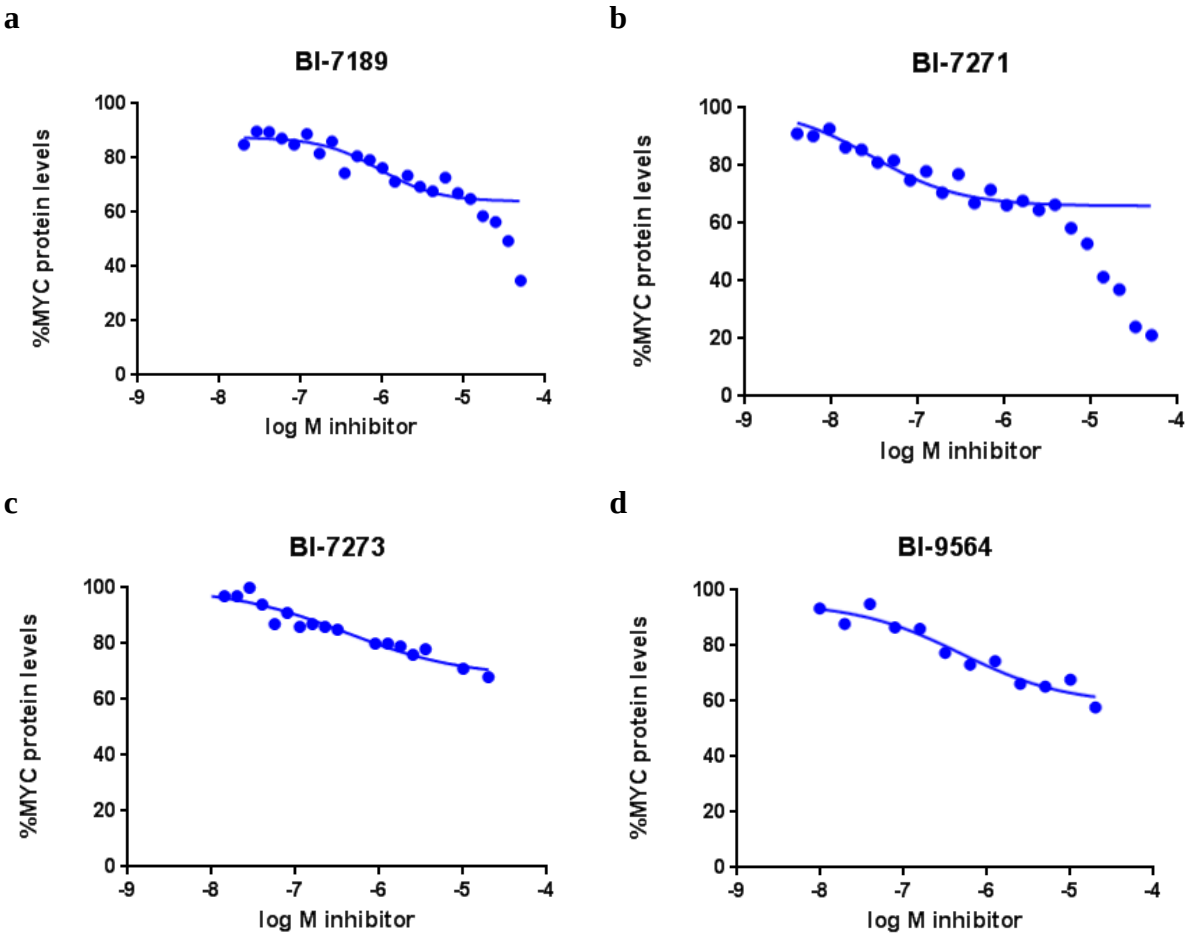

Supplementary Figure 33. Literature BRD9 inhibitors a) **LP-99** binds BRD9 anchor region Asn100 *via* its methyl quinolinone, b) **I-BRD9** binds BRD9 anchor region Asn100 via its ethylthienopyridone, c) **Compound 28** binds BRD9 anchor region Asn100 via the ketone.

a LP99[18]

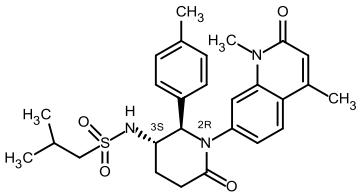

b I-BRD9[19]

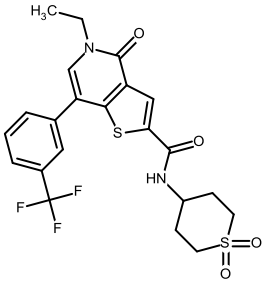

c Compound 28[20]

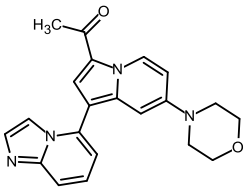

Supplementary Table 1. Small molecules screening data

Category	Parameter	Description	Description	Description
Assay	Type of assay	Thermal Shift Assay (DSF)	Surface Plasmon Resonance	Microscale Thermophoresis
	Target	BRD9	BRD9	BRD9
	Primary measurement	Protein Stability	Mass increase	Protein mobility in temperature gradient
	Key reagents	Fluorescent Dye	His-tagged protein	Fluorescent Dye
	Assay protocol	Anal Biochem. 2004 Sep 1;332(1):153-9.	J.Biomol. Screening 2009 14:337-49	ChemMedChem. 2015 Sep;10(9):1511-21
	Additional comments			
Library	Library size	1.697	1.697	1.697
	Library composition	Generic fragment set	Generic fragment set	Generic fragment set
	Source	BI pool	BI pool	BI pool
	Additional comments			
Screen	Format	384 well	384 well	384 well
	Concentration(s) tested	400 µM, 2% DMSO	100 µM, 1 % DMSO	500 µM, 5% DMSO
	Plate controls	Positive (in-house bromodomain binder) and negative (DMSO) controls	Positive (in-house bromodomain binder) and negative (buffer) controls	Positive (in-house bromodomain binder) and negative (DMSO) controls
	Reagent/ compound dispensing system	Hamilton Star system	CyBio System 6	Hamilton Star system
	Detection instrument and software	Bio-Rad CFX384 Real-Time System (C1000Touch Thermal Cycler;) / Bio-Rad CFX Manager-Data Analysis software	Biacore T200 / BiaEvaluation software	In house implemented automation of Nanotemper NT.015 / Nanotemper Analysis software
	Assay validation/QC	Z' = 0.55	Z' = 0.93	
	Correction factors		DMSO solvent correction	
	Normalization		Normalization to	

			positive control	
	Additional comments			
Post-HTS analysis	Hit criteria	ΔT≥1°C	BR ≥20%	ΔMST(DMSO, Cpd) ≥ MST(2sd DMSO)
	Hit rate	2.1% Hit rate	2.7%	6.6%
	Additional assay(s)			
	Confirmation of hit purity and structure	Entire screening library QC'ed for purity and structural identity	Entire screening library QC'ed for purity and structural identity	Entire screening library QC'ed for purity and structural identity
	Additional comments	94.4% Hit confirmation by ^{15}N HSQC	72.2% Hit confirmation by ^{15}N HSQC	26 % Hit confirmation by ^{15}N HSQC

Supplementary Table 2. Crystallographic data collection and refinement statistics (molecular replacement)

	Compound 1	**Compound 2**	**Compound 9**
Data collection			
Space group	P 2_1 2_1 2	P 2_1 2_1 2	P 2_1 2_1 2
Cell dimensions			
a, *b*, *c* (Å)	70.92, 125.41, 29.53	71.04, 125.02, 29.94	70.31, 125.17, 30.02
α, β, γ (°)	90.00, 90.00, 90.00	90.00, 90.00, 90.00	90.00, 90.00, 90.00
Resolution (Å)	1.803 (1.809-1.803)	1.679 (1.684 – 1.679) *	2.271 (2.279 – 2.271) *
R_{merge}	4.4 (54.9)	3.0 (59.1)	4.6 (123.6)
$I / \sigma I$	20.3 (2.8)	30.9 (3.1)	24.7 (2.3)
Completeness (%)	99.8 (99.2)	100.0 (100.0)	98.5 (98.4)
Redundancy	6.0 (5.8)	6.3 (6.2)	6.3 (6.4)
Refinement			
Resolution (Å)	1.80	1.68	2.30
No. reflections	25074	31312	12218
R_{work} / R_{free}	20.3/22.0	18.9/20.5	19.2/20.9
No. atoms			
Protein	1835	1817	1852
Ligand/ion	30	36	50
Water	235	306	68
B-factors			
Protein	42.56	36.53	70.54
Ligand/ion	35.66	34.64	69.30
Water	48.12	46.45	62.57
R.m.s. deviations			
Bond lengths (Å)	0.008	0.008	0.009
Bond angles (°)	0.80	0.81	0.92

*Values in parentheses are for highest-resolution shell.

	BI-7273[1] (compound 15)	**BI-9564 (compound 21)**
Data collection		
Space group	P 2_1 2_1 2	P 2_1 2_1 2
Cell dimensions		
a, *b*, *c* (Å)	70.80, 125.34, 29.92	70.03, 125.36, 29.68
α, β, γ (°)	90.00, 90.00, 90.00	90.00, 90.00, 90.00
Resolution (Å)	1.605 (1.610 – 1.605) *	1.822 (1.828- 1.822)
R_{merge}	3.2 (101)	4.4 (88.6)
$I / \sigma I$	26.2 (2.2)	19.9 (2.1)
Completeness (%)	99.9 (98.7)	99.8 (100.0)
Redundancy	6.3 (6.4)	6.4 (6.5)
Refinement		
Resolution (Å)	1.60	1.82
No. reflections	35816	24186
R_{work} / R_{free}	17.8/19.2	19.1/20.2
No. atoms		
Protein	1851	1841
Ligand/ion	52	52
Water	352	208
B-factors		
Protein	35.75	49.63
Ligand/ion	32.13	43.47
Water	47.24	53.11
R.m.s. deviations		
Bond lengths (Å)	0.009	0.009
Bond angles (°)	0.81	0.83

*Values in parentheses are for highest-resolution shell.

[1] Hohmann, A. F.; Martin, L. J.; Minder, J.; Roe, J-S.; Shi, J.; Steurer, S.; Bader; G., McConnell, D.; Pearson, M.; Gerstberger, T.; Gottschamel, T.; Thompson, D.; Suzuki, Y.; Koegl, M.; Vakoc, C. R A bromodomain-swap allele demonstrates that on-target chemical inhibition of BRD9 limits the proliferation of acute myeloid leukemia cells, *unpublished results.*

[2] Filippakopoulos, P.; Picaud, S.; Mangos, M.; Keates, T.; Lambert, J. P.; Barsyte-Lovejoy, D.; Felletar, I.; Volkmer, R.; Müller, S.; Pawson, T.; Gingras, A. C.; Arrowsmith, C. H.; Knapp, S. Histone recognition and large-scale structural analysis of the human bromodomain family. *Cell* **2012**, *149*, 214-231.

[3] Kimple, A. J., Muller, R. E.; Siderovski, D. P.; Willard, F. S. A capture coupling method for the covalent immobilization of hexahistidine tagged proteins for surface plasmon resonance *Methods Mol. Biol*. **2010**, *627*, 91-100.

[4] Giannetti, A. M. From experimental design to validated hits: a comprehensive walk-through of fragment lead identification using surface plasmon resonance *Methods in Enzymology* **2011**, *493*, 169-218.

[5] Zhang, J. H., Chung, T. D. Y.; Oldenberg, K. R. A simple statistical parameter for use in evaluation and validation of high throughput screening assays *Journal of Biomolecular Screening* **1999**, *4*, 67-73.

[6] Filippakopoulos, P.; Qi, J.; Picaud, S.; Shen, Y.; Smith, W. B.; Fedorov, O.; Morse, E. M.; Keates, T.; Hickman, T. T.; Felletar, I.; Philpott, M.; Munro, S.; McKeown, M. R.; Wang, Y.; Christie, A. L.; West, N.; Cameron, M. J.; Schwartz, B., Heightman, T. D.; La Thangue, N.; French, C. A.; Wiest, O.; Kung, A. L.; Knapp, S.; Bradner, J. E. Selective inhibition of BET bromodomains. *Nature* **2010**, *468*, 1067-1073.

[7] Jerabek-Willemsen, M., Wienken, C. J., Braun, D. Baaske, P.; Duhr, S. Molecular interaction studies using microscale thermophoresis *Assay Drug Dev Technol.* **2011**, *9*, 342-353.

[8] Mori, S., Abeygunawardana, C., Johnson, M. O.; Vanzijl, P. C. M. Improved sensitivity of HSQC spectra of exchanging protons at short interscan delays using a new fast HSQC (FHSQC) detection scheme that avoids water saturation *J. Magn. Reson. B* **1995**, *108*, 94-98.

[9] Ross, A.; Senn, H. Automation of biomolecular NMR screening *Curr Top Med Chem.* **2003**, *3*, 55-67.

[10] Peng, C.; Unger, S. W.; Filipp, F.V.; Sattler, M. ;Szalma, S. Automated evaluation of chemical shift perturbation spectra: New approaches to quantitative analysis of receptor-ligand interaction NMR spectra *J. Biomol. NMR* **2004**, *29*, 491–504.

[11] Vonrhein, C.; Flensburg, C.; Keller, P.; Sharff , A.; Smart, O.; Paciorek, W.; Womack, T.; Bricogne, G. Data processing and analysis with the autoPROC toolbox. *Acta Cryst*. **2011**, *D67*, 293-302

[12] Collaborative Computational Project, Number 4 The CCP4 Suite: Programs for Protein Crystallography. *Acta Cryst.* **1994**, *D50*, 760-763.

[13] Emsley, P.; Lohkamp, B.; Scott, W. G.; Cowtan K. Features and development of Coot. *Acta Cryst.* **2010**, *D66*,486-501.

[14] Chen, V. B.; Arendall, W. B. 3rd; Headd , J. J.; Keedy, D. A.; Immormino, R. M.; Kapral, G. J.; Murray, L. W.; Richardson, J. S.; Richardson, D. C. MolProbity: all-atom structure validation for macromolecular crystallography. *Acta Crystallogr. D Biol. Crystallogr.* **2010**, *66*, 12–21.

[15] Philpott, M.; Rogers, C. M.; Yapp, C.; Wells, C.; Lambert, J. P.; Strain-Damerell, C.; Burgess-Brown, N. A.; Gingras, A. C.; Knapp, S.; Müller, S. Assessing cellular efficacy of bromodomain inhibitors using fluorescence recovery after photobleaching *Epigenetics Chromatin* **2014**, *7*, 1-12.

[16] Rudolph, D.;, Impagnatiello, M. A.; Blaukopf , C.; Sommer, C.;, Gerlich, D. W.;, Roth, M.; Tontsch-Grunt, U.; Wernitznig, A.; Savarese, F.; Hofmann, M. H.; Albrecht, C.; Geiselmann, L.; Reschke, M.; Garin-Chesa, P.; Zuber, J.;, Moll, J.;, Adolf, G. R.; Kraut, N. Efficacy and mechanism of action of volasertib, a potent and selective inhibitor of Polo-like kinases, in preclinical models of acute myeloid leukemia *J. Pharmacol. Exp.Ther.* **2015**, *352*, 579-589.

[17] Luippold, A. H.; Arnhold, T.; Jörg, W.; Krüger, B.; Süssmuth, R. D. Application of a Rapid and Integrated Analysis System (RIAS) as a High-Throughput Processing Tool for *In Vitro* ADME Samples by Liquid Chromatography/Tandem Mass Spectrometry. *J. Biomol. Screening* **2011**, *16*, 370-377.

[18] Clark, P. G. K.; Vieira, L. C. C.; Tallant, C.; Fedorov, O.; Singleton, D. C.; Rogers, C. M.; Monteiro, O. P.; Bennett, J. M.; Baronio, R.; Müller, S.; Daniels, D. L.; Mendez, J.; Knapp, S.; Brennan, P.; Dixon, D. J. LP99: Discovery and Synthesis of the First Selective BRD7/9 Bromodomain Inhibitor *Angew. Chem. Int. Ed.* **2015**, *54*, 6217-6221.

[19] Theodoulou, N. H.; Bamborough, P.; Bannister, A. J.; Becher, I.; Bit, R. A.; Che, K. H.; Chung, C.-W.; Dittmann, A.; Drewes, G.; Drewry, D. H.; Gordon, L.; Grandi, P.; Leveridge, M.; Lindon, M.; Michon, A.-M.; Molnar, J.; Robson, S. C.; Tomkinson, N. C. O.; Kouzarides, T.; Prinjha, R. K.; Humphreys, P. G. Discovery of I-BRD9, a Selective Cell Active Chemical Probe for Bromodomain Containing Protein 9 Inhibition *J. Med. Chem.* [Online early access]. DOI: 10.1021/acs.jmedchem.5b00256. Published Online: April 9, 2015.

[20] Hay, D. A.; Rogers, C. M.; Fedorov, O.; Tallant, C.; Martin, S.; Monteiro, O. P.; Muller, S.; Knapp, S.; Schofield, C. J.; Brennan, P. E. Design and synthesis of potent and selective inhibitors of BRD7 and BRD9 bromodomains *Med. Chem. Commun.* **2015**, *6*, 1381-1386.